

T 193

50592

CENTRAL LIBRARY	
TEZPUR UNIVERSITY	
Accession No. <u>50592</u>	CENTRAL LIBRARY, T. U.
Date <u>24/11/12</u>	No. CC. NO. <u>T 193</u>

# **Modeling and Simulation of Artificial Synapses**

A thesis submitted in partial fulfillment of the requirements  
for the Degree of Doctor of Philosophy

By

**Mr. Soumik Roy**

Reg. No.: 218/98



School of Engineering  
Department of Electronics and Communication Engineering,  
Tezpur University, Napaam  
Tezpur, Assam  
May 2011

## **Abstract**

This thesis aims at contributing towards development of electronic circuit analog of post synaptic membrane of neuron and relevant biologically motivated models for its simulation to predict the behavior of post synaptic membrane dependent on neurotransmitter-receptor binding activity.

Modeling of neuron has played important roles in the field of network to describe the dynamics of both single neurons and neuronal networks as well as in neuroscience for simulation of receptor function and electrical activity of the postsynaptic neuron. Based on applications, two main classes of models of neurons have been implemented in silicon, namely Integrate-and-Fire (I-F) model and Conductance based model.

The concept of Integrate-and-Fire (I-F) model was first given by Lapique, in the year 1907. Lapique modeled the neuron using an electric circuit consisting of a parallel capacitor and resistor to represent the capacitance and leakage resistance of the cell membrane. This remarkable achievement stresses that, in neural modeling, studies of function do not necessarily require an understanding of mechanism. Significant progress is possible if a phenomenon is adequately described, even if its biophysical basis cannot be modeled. Ever since its inception, its variants have been successfully used in describing the dynamics of both single neurons and neuronal networks. These models have been found to be suitable for many theoretical and computational studies over decades. But one of the main drawback of these type of models that they cannot correctly reproduce the neuronal dynamics close to the firing threshold. What is essential for a neuron to correctly reproduce the neural dynamics that it has to spend a significant amount of time far away from firing threshold.

In 1952, Hodgkin and Huxley published a paper on membrane current and its applications to conduction and excitation in nerves that is cited by many authors in the context of conductance based neuron models. They have conducted a series of experiments to study in great detail the properties of postsynaptic membrane. On the basis of these experiments, they have given a quantitative description of membrane current and its application to conduction and excitation in nerve. From these experimental results, they have proposed an equivalent circuit to account for the resistive and capacitive properties of a patch of membrane. This circuit is known as Hodgkin and Huxley (H-H) model. Since 1952, led by Hodgkin and Huxley, many electronic circuits have been developed to reproduce the behavior of nerve axons. Due to the inclusion of many biological phenomena of postsynaptic membrane through conductances, this model can reproduce electrophysiological measurements to a high degree of accuracy. H-H model is, therefore, considered as one of the most basic models in neuroscience and still widely used today. But these models have not explained the function of synapses on which the variable permeability of postsynaptic membrane arises.

In this research work attempts have been made in a very modest way to contribute the following:-

- (1) Analog integrated circuit models of neuron are developed to emulate the behavior of real neuron and simulated in ORCAD. Simple neuron models have been developed and simulated by considering each dendrite as one spiking source. The model has been developed by considering (i) Dendrite is supposed to be consisting of three regions; each receives three inputs from three nearby neurons. Each input to a specific dendritic region is connected with the synaptic weight values to

represent the synaptic action. Effect of all these three inputs is then spatially integrated and brought to a single point value. It is assumed that this integration process takes place separately inside the soma. Each integrated output generates an action potential if it crosses a threshold value, which is required for impulse to be transmitted through the axon to the postsynaptic neuron via synapse, and (ii) the three outputs through the axon are again connected with the synaptic weight values before reaching postsynaptic neuron. This is done to emulate the synaptic mechanism of real biological neuron. A comparator integrates these outputs and generates a voltage i.e. membrane voltage. Action potential is triggered when the membrane voltages reaches a specific threshold value.

- (2) Simple integrate-and-fire based model both for excitatory and inhibitory synapses has been developed by considering a synapse to be made of presynaptic terminals, cleft and postsynaptic membrane. The overall effect of all presynaptic terminals is integrated and then reduced to a single point. The single point value is compared with threshold to produce an output. Simulation of the model yields an output representing the overall membrane potential of the postsynaptic region. Simulation is performed in ORCAD both for normal (excitatory) and unhealthy (inhibitory) states and results are compared with the previously obtained data and a good agreement is obtained.
- (3) The variable conductance of ion channels of post synaptic neuron, dependence on the transmitters diffused through the synaptic cleft and bind with the receptor sites of the post synaptic membrane of neuron, is represented by metal-oxide semiconductor field effect transistor

(MOSFET). MOSFET is chosen because it functions as a voltage controlled conductance in the linear region, analogous to the variable conductance of the transmitter gated ion channels of post synaptic region of neuron. This analog is incorporated into the famous Hodgkin-Huxley (H-H) model of neuron at the synaptic cleft. Postsynaptic membrane is divided into three patches to represent spatial summation of gated currents. Temporal integration of the currents is achieved by modeling exponentially varying time dependent gate voltage applied to MOSFET. Simulation is performed in MATLAB environment both for excitatory and inhibitory actions of synapses and the results are presented. These results are analyzed and compared with the previously obtained data and a good agreement is obtained.

- (4) ISFET based electrical models both for excitatory and inhibitory actions of neurons have been developed. Similarity between MOSFET and ISFET indicates that like MOSFET, ISFET can also function as a voltage controlled conductance. But since ISFET can be converted into an enzyme modified field effect transistor (ENFET) and therefore can provide a means of measurement of specific neurotransmitters that bind with the receptor sites of postsynaptic membrane. This ISFET based analog is incorporated into the Hodgkin-Huxley (H-H) model of neuron to substitute the variable  $\text{Na}^+$  and  $\text{Cl}^+$  conductances. Postsynaptic membrane is divided into three patches to represent spatial summation of gated currents. Temporal integration of the currents is achieved by modeling exponentially varying time dependent threshold voltage applied to ISFET. The aim of this work is to show that ISFET can be used as circuit analog to simulate the excitatory and inhibitory

postsynaptic potentials with an additional advantage: possibility of measurement of neurotransmitters diffused through the synaptic cleft by converting the ISFET into neurotransmitter sensitive ENFET. Simulation results are presented and compared with the results obtained by previous researchers.


- (5) The variable conductance of postsynaptic membrane of neuron dependence on the acetylcholine-receptor binding activity is represented by enzyme modified field effect transistor (ENFET) sensitive to acetylcholine. Acetylcholine sensitive ENFET functions not only as a voltage controlled conductance but can also provide a means of measurement of acetylcholine neurotransmitters that bind with the receptor sites of postsynaptic membrane. This analog is incorporated into the Hodgkin-Huxley (H-H) model of neuron to substitute the variable  $\text{Na}^+$  conductance. Simulation is performed in MATLAB environment both for normal (excitatory) and pathologic states and results are presented.

The results obtained from simulation leads to the conclusion that ISFET based model is more advantageous because it can be modified into specific neurotransmitter sensitive ENFET leading to the simultaneous measurement of neurotransmitter that binds with the receptor sites of the postsynaptic membrane. Measurement of neurotransmitter plays an important role in the field of neurology. ISFET based approach may also make the research area more wide in near future.

## DECLARATION

I hereby declare that the thesis entitled “**Modeling and Simulation of Artificial Synapses**” is an outcome of my research carried out at the Department of Electronics & Communication Engineering, School of Engineering, Tezpur University, Assam, India. The work is original and has not been submitted in part or full, for any degree or diploma of any other University or Institute.

Date: 16-11-11

  
(Soumik Roy)



*Dedicated to*

*My Parents and Family Members*



## TEZPUR UNIVERSITY

This is to certify that the thesis entitled “**Modeling and Simulation of Artificial Synapses**” submitted to the Tezpur University in the Department of Electronics and Communication Engineering under the School of Engineering in partial fulfillment for the award of the degree of Doctor of Philosophy in Electronics and Communication Engineering is a record of research work carried out by Mr. Soumik Roy under my supervision and guidance.

All help received by him/her from various sources have been duly acknowledged.

No part of this thesis has been submitted elsewhere for award of any other degree.

Date: 16/03/11

Place: Tezpur

(Dr. Jiten Ch. Dutta)  
Supervisor,  
Associate Professor,  
Department of Electronics and  
Communication Engineering,  
Tezpur University, Napaam,  
Tezpur, Assam, India  
PIN- 784 028.



## TEZPUR UNIVERSITY

This is to certify that the thesis entitled “**Modeling and Simulation of Artificial Synapses**” submitted by Mr. Soumik Roy to the Tezpur University in the Department of Electronics and Communication Engineering under the School of Engineering in partial fulfillment for the award of the degree of Doctor of Philosophy in Electronics and Communication Engineering has been examined by us and found to be satisfactory.

The committee recommends for the award of the degree of Doctor of Philosophy.

Supervisor

  
External Examiner

Date: 5.12.2011.

<b><u>Contents</u></b>	<b><u>Page</u></b>
<b>Abstract</b>	<b>i</b>
<b>Declaration</b>	<b>vi</b>
<b>Dedication</b>	<b>vii</b>
<b>Certificate of Supervisor</b>	<b>viii</b>
<b>Certificate of Examiner</b>	<b>ix</b>
<b>Table of contents</b>	<b>x</b>
<b>List of Figures</b>	<b>xv</b>
<b>Acknowledgement</b>	<b>xx</b>
<b>List of author's publications</b>	<b>xxi</b>
<b>Chapter 1: Introduction</b>	<b>1</b>
<b>1.1</b> Neuron Modeling	<b>2</b>
<b>1.2</b> Research Problems	<b>4</b>
<b>1.3</b> Research Objective	<b>5</b>
<b>1.4</b> Scope of the work	<b>6</b>
<b>1.5</b> Thesis Outline	<b>6</b>
<b>1.6</b> References	<b>7</b>
<b>Chapter 2: Introduction to Neuron and Synapse: Physiology</b>	<b>10</b>
<b>2.1</b> Introduction	<b>11</b>
<b>2.2</b> Biological Neuron: Overview	<b>11</b>
<b>2.2.1</b> Structure of neuron or neuron morphology	<b>13</b>
<b>2.2.1.1</b> Cell Body	<b>14</b>
<b>2.2.1.2</b> Dendrites or nerve ending	<b>14</b>
<b>2.2.1.3</b> Axon	<b>14</b>
<b>2.2.2</b> Types of neuron	<b>15</b>
<b>2.2.2.1</b> Multipolar neurons	<b>15</b>
<b>2.2.2.2</b> Unipolar neurons	<b>16</b>
<b>2.2.2.3</b> Bipolar neurons	<b>17</b>
	<b>x</b>

2.2.3	An outline of real neuron	18
2.2.4	Resting potential of Neuron	19
2.2.5	Action potential	21
2.2.6	All or None principle	26
2.2.7	Refractory period	26
2.2.8	Impulse conduction	28
2.3	Introduction to Synapse	29
2.3.1	Types of Synapse	31
2.3.2	Synaptic Communication	33
2.4	References	37
<b>Chapter 3: General Overview of Neuron Modeling</b>		<b>39</b>
3.1	Introduction	40
3.2	Conductance based model	41
3.2.1	Hodgkin-Huxley Membrane Model	42
3.2.2	Lewis Membrane Model	47
3.2.2.1	Potassium Conductance of Lewis Membrane model	49
3.2.2.2	Sodium Conductance of Lewis Membrane model	50
3.2.2.3	Simulated Action Pulse of Lewis Membrane model	51
3.2.3	Roy Membrane Model	52
3.2.4	Farquhar and Hasler Membrane Model	55
3.3	Integrate and Fire (I-F) model	59
3.3.1	I & F model of Mead	60
3.3.2	Leaky integrate and fire model	62
3.4	References	65

<b>Chapter 4: General Overview of Synapse Modeling</b>	<b>67</b>
4.1 Introduction	68
4.2 Synaptic Neuron Models	71
4.2.1 Theory of Metal-oxide Semiconductor Field-Effect Transistor (MOSFET)	71
4.2.1.1 Drain Characteristics for the Enhancement-Mode MOSFET	77
4.2.2 Neuron Model for Excitation and Inhibition of Postsynaptic Membrane of Levine, Marvin et al.	88
4.2.3 Synaptic Neuron Model of Levine, Marvin et al.	92
4.3 References	96
<b>Chapter 5: Study on the development of Neuron Model: Integrate-and-Fire Based Models</b>	<b>97</b>
5.1 Introduction	98
5.2 Integrate-and-Fire Based Model 1	100
5.2.1 Results	104
5.3 Integrate-and-Fire Based Model 2	107
5.3.1 Results	109
5.4 References	113
<b>Chapter 6: Study on the Development of Synapse Model: Integrate-and-Fire Based Model</b>	<b>114</b>
6.1 Introduction	115
6.2 A Simple Integrate-and-Fire Based Circuit Model for Excitatory and Inhibitory Synapse	116
6.2.1 Results	121
6.3 References	124

<b>Chapter 7: Some Aspects of Development of Biologically Motivated Circuit Models of Synapses</b>	<b>126</b>
7.1 Introduction	127
7.2 Biologically Motivated Circuit Model of Neuron for Simulation of Excitatory and Inhibitory Actions of Synapses	128
7.2.1 Modeling Neuron for Excitatory Synapse	131
7.2.2 Modeling Neuron for Inhibitory Synapse	133
7.2.3 Results	135
7.3 Modeling Neuron for Simulation of Transmitter Gated Ion Channels of Postsynaptic Membrane at Synaptic Cleft	137
7.3.1 Ion Sensitive Field-Effect Transistor (ISFET)	137
7.3.1.1 Theory of ISFET	139
7.3.1.2 ISFET Operational Principle	145
7.3.1.3 ISFET Modeling	149
7.3.1.4 ISFET Technology	155
7.3.2 ISFET Based Modified H-H Model	158
7.3.2.1 Modeling Neuron for Excitatory Synapse	160
7.3.2.2 Modeling Neuron for Inhibitory Synapse	162
7.3.2.3 Results	164
7.4 Biologically Inspired Circuit Model for Simulation of Acetylcholine Gated Ion Channels of the Postsynaptic Membrane at Synaptic Cleft	167
7.4.1 Acetylcholine (ACh)	167
7.4.2 Acetylcholine-sensitive ENFET	170
7.4.3 Circuit Model based on Acetylcholine Sensitive ENFET	175
7.4.4 The Result	180
7.5 References	181

<b>Chapter 8: Conclusion and Future Research</b>	<b>187</b>
<b>8.1 Conclusion and Future Research</b>	<b>188</b>



## **List of Figures**

### **Chapter – 2**

- Fig. 2.1: Basic block diagram of Neuron
- Fig. 2.2: Multipolar neuron
- Fig. 2.3 : Unipolar neuron
- Fig. 2.4 : Bipolar neuron
- Fig. 2.5: Patch of cell neuron membrane
- Fig. 2.6: The active transport mechanism
- Fig. 2.7: Measurement of action potentials in a neuron
- Fig. 2.8: Ion flow in action potential
- Fig. 2.9: The absolute and relative refractory period
- Fig. 2.10: Anatomy of Chemical Synapses
- Fig. 2.11: Types of synapses according to site
- Fig. 2.12: Excitatory Post Synaptic Potential (EPSP)
- Fig. 2.13: Inhibitory Post Synaptic Potential (IPSP)

### **Chapter – 3**

- Fig. 3.1: Electrical circuit representing membrane
- Fig. 3.2: The simulated output of H-H model
- Fig. 3.3: The block diagram of Lewis Membrane Model
- Fig. 3.4: The circuit simulating the potassium conductance of the Lewis membrane model
- Fig. 3.5: The circuit simulating the sodium conductance of the Lewis membrane model
- Fig. 3.6: The complete Lewis membrane model

- Fig. 3.7: Single action potential pulse generated by Lewis Membrane Model
- Fig. 3.8: The circuits simulating (A) sodium and (B) potassium conductances in the Roy Membrane Model
- Fig. 3.9: Steady-state values of the (A)  $G_K$  and (B)  $G'_{Na}$  as a function of membrane voltage clamp in the Roy model (solid lines), compared to the measurements of Hodgkin and Huxley (dots).  $V_m$ , the transmembrane voltage, is related to the resting value of the applied voltage clamp.
- Fig. 3.10: Voltage-clamp measurements made for (A) potassium and (B) sodium conductances in the Roy model. The voltage steps are 20, 40, 60, 80, and 100 mV. (C) The action pulse simulated with the Roy model.
- Fig. 3.11: The figure shows the model proposed by E. Farquhar and P. Hasler
- Fig. 3.12: The sodium channel circuit model of E. Farquhar and P. Hasler
- Fig. 3.13: The potassium channel circuit model of E. Farquhar and P. Hasler
- Fig. 3.14: The neuron circuit model using both sodium and potassium channel circuit of E. Farquhar and P. Hasler
- Fig. 3.15: The action potential generated by the neuron circuit model of E. Farquhar and P. Hasler
- Fig. 3.16: The Axon Hillock Integrate and Fire circuit of C. Mead
- Fig. 3.17: Basic Integrate and Fire circuit
- Fig. 3.18: The leaky integrate and fire model

#### **Chapter – 4**

- Fig. 4.1(a): Electrical mechanism of synapse
- Fig. 4.1(b): Equivalent circuit of a presynaptic neuron
- Fig. 4.1(c): Electrical equivalent circuit of synapse
- Fig. 4.2: Structure of an  $n$ -channel enhancement-mode MOSFET

- Fig. 4.3(a)(i): Enhancement mode MOSFET structure and Circuit symbol (n-channel)
- Fig. 4.3(a)(ii): Enhancement mode MOSFET structure and Circuit symbol (p-channel)
- Fig. 4.3(b)(i): Depletion mode MOSFET structure and Circuit symbol (n-channel)
- Fig. 4.3(b)(ii): Depletion mode MOSFET structure and Circuit symbol (p-channel)
- Fig. 4.4(a): Output Characteristics of an  $n$ -channel enhancement mode MOSFET
- Fig. 4.4(b): Input Characteristics of an  $n$ -channel enhancement mode MOSFET
- Fig. 4.5: Shape of the channel width of an  $n$ -channel enhancement mode MOSFET, caused by the applications of a large drain-source voltage  $V_D$
- Fig. 4.6(a): Shape of the channel width of an  $n$ -channel enhancement mode MOSFET for  $V_{DS}=(V_{GS}-V_{TH})$
- Fig. 4.6(b): Shape of the channel width of an  $n$ -channel enhancement mode MOSFET for  $V_{DS}>(V_{GS}-V_{TH})$
- Fig. 4.7: Excitatory and inhibitory postsynaptic circuit model of Levine, Marvin et al.
- Fig. 4.8: Simulated result of the excitatory and inhibitory postsynaptic circuit model of Levine, Marvin et al.
- Fig. 4.9: Circuit model of Levine, Eisenberg, and Fare for the membrane of the postsynaptic region
- Fig. 4.10: Simulated Postsynaptic Membrane Potential of Model of Levine, Eisenberg, and Fare

**Chapter – 5**

- Fig. 5.1: Basic Silicon Neuron model
- Fig. 5.2: Proposed electrical model of neuron (Excitation)
- Fig. 5.3: Proposed electrical neuron model at rest
- Fig. 5.4: The simulation result of excitable neuron model of Fig. 4.2
- Fig. 5.5: The simulation result of proposed model electrical neuron at rest
- Fig. 5.6: Proposed electrical model of neuron
- Fig. 5.7: The simulation output of dendritic regions
- Fig. 5.8: The simulation result of neuron model of Fig. 4.6

**Chapter – 6**

- Fig. 6.1: Electrical circuit model of excitatory synapse
- Fig. 6.2: Electrical circuit model of inhibitory synapse
- Fig. 6.3: The output profile of excitatory synapse
- Fig. 6.4: The output profile of Inhibitory synapse

**Chapter – 7**

- Fig. 7.1: Biologically motivated model of postsynaptic membrane
- Fig. 7.2: Circuit model for excitatory action of synapse
- Fig. 7.3: Circuit model for inhibitory action of synapse
- Fig. 7.4: Simulation results of excitatory and inhibitory actions of postsynaptic membrane. Top waveform represents the EPSP and bottom waveform represents the IPSP
- Fig. 7.5(a): Structure of MOSFET
- Fig. 7.5(b): Schematic of ISFET
- Fig. 7.5(c): Electronic Diagram of ISFET
- Fig. 7.6(a): Drain current vs. drain to source voltage at various Gate voltage of

## a MOSFET

- Fig. 7.6(b): Drain current vs. drain to source voltage at various pH of an ISFET
- Fig. 7.7(a): Site binding theory of electrical double layer
- Fig. 7.7(b) Charge and potential distribution of an ISFET for  $\text{pH} < \text{pH}_{\text{pzc}}$
- Fig. 7.7(c): Charge and potential distribution of an ISFET for  $\text{pH} > \text{pH}_{\text{pzc}}$
- Fig. 7.8: Modified H-H model of Postsynaptic membrane
- Fig. 7.9: ISFET based Circuit model for excitatory action of synapse
- Fig. 7.10: ISFET based Circuit model for inhibitory action of synapse
- Fig. 7.11: Simulation results of excitatory and inhibitory actions of postsynaptic membrane. Top waveform represents the EPSP and bottom waveform represents the IPSP
- Fig. 7.12: General configuration of ENFET
- Fig. 7.13: Acetylcholine ENFET (a) Schematic diagram (b) Electronic diagram
- Fig. 7.14: Calibration plot of the AChE-modified ENFET in the presence of different concentrations of acetylcholine. Inset: time-dependent response of the AChE-modified ENFET upon interaction with a acetylcholine solution
- Fig. 7.15: Circuit model for Postsynaptic membrane
- Fig. 7.16: Simulated result of postsynaptic membrane potential

## **Acknowledgement**

I would like to thank all those people whose help and support has made this work possible.

At the onset, I am indebted to Dr. Jiten Ch. Dutta, Associate Professor, Dept. of Electronics & Communication Engineering, Tezpur University for giving me the opportunity to do my research work under his supervision. I would like to express my sincere gratitude to him, for his thought provoking talks with me during my research work. His enlighten suggestions and constructive criticize has gone a long way in the successful completion of research work including the thesis writing.

I would like to thank P P Sahu, Professor & HoD, Dept. of Electronics & Communication Engineering, Tezpur University for his constant encouragement and timely support.

I would also like to thank all the members of the Dept. of Electronics & Communication Engineering, Tezpur University, who have helped me at various junctures in making my research work a successful one.

My research work has involved many people at different stages. I would like to thank all those who have directly or indirectly helped me.

Soumik Roy

## List of Author's Publications

### Journal:

- [1] Dutta, J. C. Roy, S. Modeling Neuron for Simulation of Transmitter Gated Ion Channels of Postsynaptic Membrane at Synaptic Cleft, *Am. J. Biomed. Sci.* 2011, ISSN: 1937-9080, doi: 10.5099/aj110300176.
- [2] Dutta, J. C. Roy, S. Biologically Motivated Circuit Model of Neuron for Simulation of Excitatory and Inhibitory Actions of Synapses, *Canadian Journal on Biomedical Engineering & Technology.*, Vol. 1, No. 3, June 2010, ISSN: 1923-1644.
- [3] Roy, S. Dutta, J. C. Phukan, S. Integrate-and-Fire Based Circuit Model for Simulation of Excitatory and Inhibitory Synapses, *Canadian Journal on Biomedical Engineering & Technology* Vol. 1, No. 2 March 2010, ISSN: 1923-1644.
- [4] Roy, S Dutta, J. C. Silicon Neuron Model : A Review, *Journal of the Assam Science Society*, Vol. 50, No. 1,2, pp 01-172, December 2009, 10-19, ISSN: 0587-1921.
- [5] Dutta, J. C. Sharma, S. Roy, S. Ion Sensitive Field Effect Transistors (ISFETs): Transducers for Biosensors, *IE(I) Journal-ET*, Vol. 88, July 2007, ISSN: 0251-1096.

### Conference Proceedings:

- [1] Dutta, J. C. Roy, S. An Electronic Circuit Model for simulation of Synaptic Communication: The NEUROISFET for Wireless Biotelemetry, *IEEE International Conference on Devices & Communication (ICDeCom-11)*, Feb'

24-25, 2011, Birla Institute of Technology, Mesra, Ranchi, Print ISBN: 978-1-4244-9189-6, DOI: 10.1109/ICDECOM.2011.5738455

- [2] Dutta, J. C. Roy, S. Biologically Inspired Circuit Model for Simulation of Acetylcholine Gated Ion Channels of the Postsynaptic Membrane at Synaptic Cleft, *Proc. 2010 IEEE EMBS Conference on Biomedical Engineering & Sciences*, University of Malaya, Kuala Lumpur, 30<sup>th</sup> Nov – 2<sup>nd</sup> Dec' 2010, Print ISBN: 978-1-4244-7599-5 . DOI: 10.1109/IECBES.2010.5742191
  
- [3] Roy, S. Dutta, J. C. Phukan, S. An Analog Circuit Model and Simulation of Excitatory Synapse, *National Conference on New Approaches of Basic Sciences Towards the Development of Engineering and Technology*, 12<sup>th</sup>-13<sup>th</sup> March '10, DBCET, Guwahati, Assam.
  
- [4] Roy, S. Dutta, J. C. Phukan, S. An Analog Circuit Model and Simulation of Synapse, *55<sup>th</sup> Annual Technical Session of Assam Science Society*, 15<sup>th</sup> Feb '10, Gauhati University, Assam.
  
- [5] Roy, S. Dutta, J. C. Analog Circuit Model & Simulation of Neurons, *National Conference on Emerging Trends in Engg. Technology & Applications (NCETETA-2009)*, Organized by Sirdi Sai Engg. College, Bangalore, in association with Computer Society of India, IETE, ISTE, SAEINDIA, 29-30<sup>th</sup> April '09.
  
- [6] Roy, S. Synaptic Communication: A Review, *Proc. of Seminar on Bioelectronics*, pp. 26-29, 27th March, 2006.



# **Chapter 1**

## **Introduction**

## Introduction

### 1.1 Neuron Modeling:

Over past hundred years, many different variations of neurons have been implemented in silicon. Two main classes of models of spiking neurons that have been implemented in silicon are Integrate-and-Fire (I&F) model and conductance based models. Both models have their own merits and demerits and consequently they are application specific.

In 1907, long before the mechanisms responsible for the generation of neuronal action potentials were known, Lapicque developed a neuron model that is still widely used [1]-[2]. This memorable achievement stresses that, in neural modeling, studies of function do not necessarily require an understanding of mechanism. Significant progress is possible if a phenomenon is adequately described, even if its biological basis cannot be modeled. It is important to note that Lapicque's study is actually not about integrate-and-fire models but has given the concept that even if the biophysical basis of neuron cannot be modeled, significant progress is possible if a phenomenon is adequately described. Based on this, Richard Stein introduced in 1965 a leaky integrate-and-fire model with random Poisson excitatory and inhibitory inputs [3]. However, it was Bruce Knight that introduced the term "integrate-and-fire" neuron in the sixties, and the first paper where the name appears seems to be his seminal 1972 paper on the dynamics of the firing rate of this model neuron [4], together with a companion experimental paper on visual cells of the Limulus [5]. Bruce Knight introduced the term 'forgetful integrate-and-

fire' neuron, but the term 'leaky integrate-and-fire' (LIF) neuron, coined by Rick Purple (a student of Hartline) soon became more popular. This integrate-and-fire neuron with no leak had been analyzed earlier by Gerstein and Mandelbrot. From the nineties onwards the leaky integrate-and-fire model and its variants became very popular when theorists started to study the dynamics of networks of spiking neurons. The LIF is easy and efficient to implement, and its behavior can in some cases be analyzed mathematically [6]-[8]. Integrate-and-fire models have been used in a wide variety of studies ranging from investigations of synaptic integration by single neurons to simulations of networks containing hundreds of thousands of neurons. The integrate-and-fire model has proven particularly useful in elucidating the properties of large neural networks and the implications of large numbers of synaptic connections in such networks [9]. Quite frequently, especially in well-conceived, parsimonious, large-scale neuronal network models and also direct numerical simulation using such models, the simplicity of the I&F model becomes a major advantage in efficiently and effectively uncovering robust network mechanisms governing the model dynamics [10]. As a consequence, the I&F model has been the focus of many theoretical and computational studies over decades. Here a humble attempt has been made to develop a new simple variant of I&F model that can reproduce the voltage dynamics of neuron as close as to Hodgkin-Huxley (H-H) type models

As far as H-H models concerned, due to introduction of voltage dependent membrane conductances and most of experimentally found as parameters, this model can reproduce electrophysiological measurements to a high degree of accuracy. H-H equations are simple and elegant tool, capable of explaining the activity of neuron with the help of variable permeability of membrane from

different ions. H-H model is, therefore, considered as one of the most basic models in neuroscience. Since many conductances namely  $\text{Na}^+$  and  $\text{Cl}^-$  conductances are voltage and time dependent, effort has been made to represent these conductances with various types of field effect transistors (FET) namely MOSFET, ISFET and ENFETs. The threshold voltages of these FETs are mathematically modeled capable of describing transmitter-receptor activities upon which conductances of different ion channels depend.

## 1.2 Research Problems:

(i) Though the Hodgkin-Huxley (H-H) type models can reproduce electrophysiological measurements to a high degree of accuracy, its intrinsic complexity restricts its use in describing neural network dynamics. For this reason, many phenomenological spiking neuron models such as Integrate-and-Fire (I&F) models have been developed in the past to discuss aspects of neuronal coding, memory or network dynamics. Due to replacement of the rich dynamics of H-H type models, I&F models cannot correctly reproduce the neuronal dynamics close to the firing threshold. Due to this reason, many details of electrophysiology of neurons are missed in I&F models. As a consequence, the utility of I&F models in neuroscience has been contrasted with more detailed H-H model. But the simplicity of I&F models become a major advantage in describing network mechanism efficiently and effectively. Here, therefore attempt has been made to develop a simple variant of I&F model that can approximately reproduce the voltage dynamics of neuron as close as to H-H type models.

(ii) Since 1952, led by Hodgkin-Huxley, many electronic circuits have been developed to reproduce the behavior of nerve axons [11]-[15]. A very good

account of this type of modeling is reviewed by Harmon et al [16] and Lewis [17]. But among these models, scientists have so far utilized Hodgkin-Huxley (H-H) model as a circuit analog of the axonal membrane. It is because the H-H equations are simple and elegant tool, capable of explaining the activity of neuron with the help of variable permeability of membrane for different ions, e.g., sodium, potassium, chloride etc. Due to the inclusion of many biological phenomena of postsynaptic membrane through conductances, H-H model can reproduce electrophysiological measurements to a high degree of accuracy. H-H model is, therefore, considered as one of the most basic models in neuroscience and is still widely used today. The experiments conducted by Hodgkin-Huxley upon which the H-H model is based were confined only to postsynaptic membrane. As a result, these models could not explain the function of synapses on which the variable permeability of postsynaptic membrane arises. It is, therefore, proposed to develop biologically motivated neuron models that include the action of synapse on the transmitter gated ion channels of postsynaptic membrane. It is expected that these models will play important role in neurobiology for simulation of receptor function and electrical activity of the postsynaptic cell.

### **1.3 Research Objectives:**

- (i) To develop a simple variant of Integrate-and-Fire model that can approximately reproduce the voltage dynamics of neuron analogous to H-H model, so that the same can be used both in neural field and neurology area.

- (ii) To develop excitatory and inhibitory actions of synapse models using various types of field effect transistors namely MOSFET, ISFET and ENFET.
- (iii) To compare the performance characteristics of the models developed in (ii) with the existing models.

### **1.4 Scope of the work:**

The models developed in this work will provide important tools for prediction of function of neurons at excitatory and inhibitory states. Such models have important applications in the field of neurology for simulation of receptor function and electrical activity of the postsynaptic cell.

The simulation results indicate that the behaviour of the conductance before and after applying voltage to the cell may provide a path to future research to investigate other techniques to improve the models. It is expected that the techniques used in the development of models, analysis and the findings will be very useful for any research in the same or other fields.

In future, the characteristics obtained from simulation results may be explored by introducing feed back circuit in the gate of ISFET/ENFET. The time dependence of conductances can be simulated by introducing RC circuit in the feed back path. Such circuit, that can accurately simulate the action of the chemical transmitters, will have importance in building complex neuron networks.

### **1.6 Thesis Outline:**

Chapter 2 describes the physiological structure of nerve membrane and the principle of generation & conduction of nerve impulses. Chapter 3 presents the

literature review of neuron modeling. It starts with the conductance based model to integrate-&-fire model proposed by different scientists. Chapter 4 describes the general overview of synapse starting with the literature review of different models of synapse proposed by different neurologists. In chapter 5, simple silicon neuron models have been proposed based on Lapique's philosophy. The simulation results indicate that this I&F model can reproduce the neural dynamics as close as to H-H type models. In Chapter 6, a simple integrate-and-fire based circuit model for excitatory and inhibitory synapse has been developed and simulated. The results are presented and analyzed.

In chapter 7, biologically motivated circuit models of synapse have been proposed and simulated. It starts with the biologically inspired circuit model for excitatory and inhibitory actions of synapse using both MOSFET and ISFET and then expanded to ENFET with special emphasis to acetylcholine gated ion channels of the postsynaptic membrane at synaptic cleft. Conclusion & discussion of the research and future research options are presented in Chapter 8.

### **1.7 References:**

- [1] Bugmann, G.; Cristodoulou, C.; Taylor, J. G. Role of temporal integration and fluctuation detection in the highly irregular firing of a leaky integrator neuron model with partial reset, *Neural Comput.*, 1997; 9:985-1000.
- [2] Tuckwell, H. C. *Introduction to theoretical neurobiology*, Cambridge, UK; Cambridge University Press; 1988.
- [3] Stein, R. A theoretical analysis of neuronal variability, *Biophys J.*, 1965, 5:173-194.

- 
- [4] Knight, B. W. Dynamics of encoding in a population of neurons, *J. Gen Physiol*, 1972a, 59:734-766.
- [5] Knight, B. W. The relationship between the firing rate of a single neuron and the level of activity in a population of neurons, *J. Gen Physiol*, 1972b, 59:767-778.
- [6] Burkit, A. N. A review of the integrate-and-fire neuron model: I. Homogeneous synaptic input, *Biol Cybern*, 2006a, 95(1):1-19.
- [7] Burkit, A. N. A review of the integrate-and-fire neuron model: II. Inhomogeneous synaptic input and network properties, *Biol Cybern*, 2006b, 95(2):97-112.
- [8] Brunel, N.; Rossum, M. C. V. Lapicque's 1907 paper: from frogs to integrate-and-fire, *Biol Cybern*, 2007, 97:337-339.
- [9] Abbott, L. F. Lapicque's Introduction of the integrate-and-fire model neuron (1907), *Brain Research Bulletin*, 1999, Vol. 50, nos 5/6 pp. 303-304.
- [10] Katherine, A. Newhall et. al. Dynamics of current-based, Poisson driven, integrate-and-fire neuronal networks, *Commun. Math. Sci.*, 2010, Vol. 8, No. 2, pp. 541-600.
- [11] Hodgkin, A. L. Huxley, A. F. A quantitative description of membrane current and its application to conduction and excitation in nerve, *J. Physiol*, 1952, 117. 500-544.
- [12] Hodgkin, A. L. Ionic movements and electrical activity in giant nerve fibers, *Proceedings of the Royal Society of London. Series B, Biological Sciences*, 1957, Vol. 148, 1-38.



- 
- [13] Fitzhugh, R. Threshold and plateaus in the Hodgkin-Huxley nerve equations, *J. Gen. Physiology*, 1960, 43, 867.
- [14] Johnson, and Hanna, Membrane model: A single transistor analog of excitable membrane, *J. Theoret. Bio*, 1969, 22, 401-411.
- [15] Lewis, E. R. Neuroelectric potentials derived from an extended version of the Hodgkin and Huxley model, *J. Theor. Biol.*, 1965 Vol.10,125-158.
- [16] Harmon, L.D. Lewis, E. R. Neural modeling, *Physiol. Rev.*, 1966, Vol, 48, 513-591.
- [17] Lewis, E. R. Using electronic circuits to model simple neuroelectric interactions, *Proc. IEEE*, 1968, vol 56, 931-949.

## **Chapter 2**

### **Introduction to Neuron and Synapse: Physiology**

---

## Introduction to Neuron and Synapse: Physiology

### 2.1 Introduction:

The nerve cell (or Neurons) is the basic functional unit of communication in the vertebrate nervous system, which transmits nerve messages. Indeed communication between two neurons takes place through synapse. Synapse is essentially a connection between two neurons namely presynaptic and postsynaptic neurons. Synaptic communication is the inseparable part of neuro-bio-engineering having the common goal of analyzing the function of the neuron and nervous system, developing methods to restore damaged neurological function & creating artificial neuronal systems by integrating physical, chemical, mathematical & engineering tools. Major thrusts in neuro-bio-engineering include new technology & approaches to advanced basic research on the nervous system, including signal processing, modeling & simulation of neural systems & their functions; development & application of specialized technology for medical diagnosis, monitoring & treatment of nervous system disorders; & bio-neuro technology applications such as enhanced-performance systems designed on the basis of fundamental principles of nervous systems structure & function.

### 2.2 Biological Neuron: Overview

The central nervous system (CNS) is composed of two kinds of specialized cells; Neurons and glial or neuroglial cells, which are the basic unit of communication in vertebrate nervous system. Every information

processing system in the CNS is composed of Neuron and glial cell. Without this two types of cells, the CNS would not be able to do what it does. The nerve cells can respond to stimuli, conduct impulses and communicate with each other. It can respond to stimulus and conduct impulses because a membrane potential is established across the cell membrane. In other words there is an unequal distribution of ions (charge atoms) on the two sides of a nerve cell membrane, because carriers actively transport these two ions; sodium from the inside to the outside and potassium from the outside to the inside. As a result of this active transport mechanism (commonly referred to as the Sodium Potassium pump), there is a higher concentration of sodium on the outside than the inside and a higher concentration of potassium on the inside than the outside. The Glial cells provide structural support to the neuron for information processing. Each neuron receives electrochemical inputs from other neurons. Impulses arriving simultaneously are added together and, if sufficiently strong, lead to the generation of an electrochemical discharge, known as an action potential (a 'nerve impulse'). The action potential then forms the input to the next neuron in the network i.e., neuron conduct electrochemical impulses [1]. The basic block diagram of neuron is shown in Fig. 2.1.

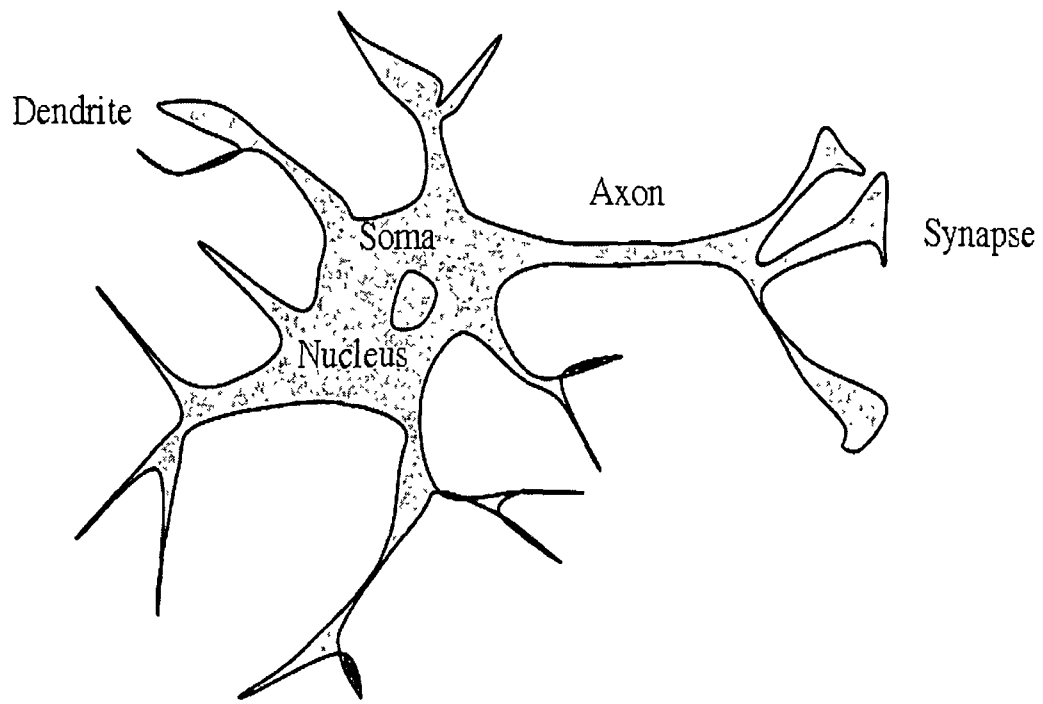


Fig. 2.1: Basic block diagram of Neuron.

### 2.2.1 Structure of neuron or neuron morphology:

The neuron is the cell that animals use to detect the outside environment, the internal environment of their own bodies, to formulate behavioral responses to those signals, and to control their bodies based on the chosen responses. While there are as many as 10,000 specific types of neurons in the human brain, generally speaking, there are three kinds of neurons: *motor neurons* (for conveying motor information), *sensory neurons* (for conveying sensory information), and *interneurons* (which convey information between different types of neurons) [2]. A Neuron have three distinct parts, they are-

2.2.1.1 Cell body or soma.

2.2.1.2 Dendrites, and

2.2.1.3 Axon

### **2.2.1.1 Cell body:**

The main central portion of the cell is called the soma or cell body. This is not only the metabolic center of neuron, it is also its manufacturing and recycling plant. For instance, it is within the cell body that neuronal proteins are synthesized. It contains the nucleus, which in turn contains the genetic material in the form of chromosomes. If the cell body dies, the neuron also dies. The soma and the nucleus do not play an active role in the transmission of the neural signal.

### **2.2.1.2 Dendrites or nerve ending:**

Neuron has a large number of extensions called, dendrites. Dendrites receive impulses and conduct them towards the cell body. Most Neurons have multiple dendrites, which extend outward from the cell body and are specialized to receive chemical signals from the axonal terminals of other neurons. Dendrites convert this signal to small electrochemical impulses and transmit them inward in the direction of cell body.

### **2.2.1.3 Axon:**

The axon is a single, long thin extension that sends impulses towards another neuron. Axons are specialized for the conduction of electrical impulses called action potentials. Axons are surrounded by a many-layered

lipid and protein covering called the myeline sheath, produced by the schwann cells. This myeline acts as an insulator. Thus myelinated axon transmit information much faster than other neuron, which is known as saltatory conduction.

Another distinct part of the neuron is Axon hillock or Axon terminal, which is located at the end of the soma and controls the firing of a neuron, also contains neurotransmitters. Neurotransmitters are the chemical medium through which the signal flow from one neuron to another at chemical synapses. It fires an action potential. The morphology of dendritic tree plays an important role in the integration of synaptic inputs and it influences the way the neuron processes and computers.

### **2.2.2 Types of neuron:**

The three main types of neurons are basically multipolar neuron, unipolar neuron and biopolar neuron.

#### **2.2.2.1 Multipolar neurons:**

They are so-named because they have many (multi) processes that extend from the cell body, lots of dendrites plus a single axon. Functionally, these neurons are either motor (conducting impulses that will cause activity such as the contraction of muscles) or association (conducting impulses and permitting 'communication' between neurons within the central nervous system (CNS)). The schematic of multipolar neuron is shown in Fig. 2.2.

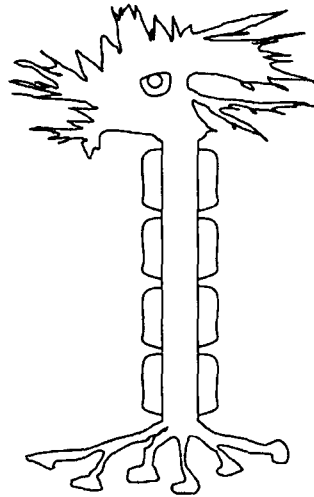


Fig. 2.2 : Multipolar neuron.

### 2.2.2.2 Unipolar neurons:

It has one process from the cell body. However, that single, very short, process splits into longer processes (a dendrite plus an axon). Unipolar neurons are sensory neurons - conducting impulses into the central nervous system. The schematic of unipolar neuron is shown in Fig. 2.3.

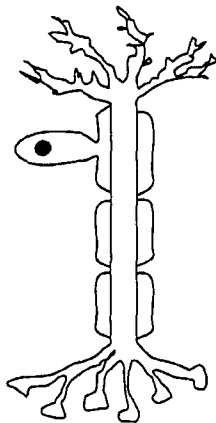


Fig. 2.3: Unipolar neuron



### 2.2.2.3 Bipolar neurons:

It has two processes - one axon & one dendrite. These neurons are also sensory. For example, bipolar neurons can be found in the retina of the eye. The schematic of bipolar neuron is shown in Fig. 2.4.



Fig. 2.4: Bipolar neuron

While there are three types of other neurons based on their function:

#### **Motor neuron:**

Motor Neuron have a long axon & short dendrites & transmit signals from the CNS to the other parts (skin, glands, muscles) of the body.

#### **Sensory neuron:**

Sensory neuron have a long dendrites and short axon, and it carry signals from the outer part of the body to CNS.

#### **Interneuron:**

An interneuron (also called relay neuron or association neuron or bipolar neuron) is a neuron that communicates only to other neurons. Interneurons are

found only in the CNS where they connect neuron to neuron, so, it acts as a link between sensory neurons and motor neurons.

### 2.2.3 An outline of real neuron:

To support the general function of the nervous system, neurons have evolved unique capabilities for *intracellular signaling* (communication within the cell) and *intercellular* signaling (communication between the cells). To achieve long distance, for rapid communication, neurons have evolved special abilities for sending electrical signals (action potential) along axons. This mechanism is called conduction. In order for neurons to communicate, they need to transmit information both within the neuron and from one neuron to the next. This process utilizes both electrical signals as well as chemical messengers. The operation of neuron relies on the neuron excitable membrane. In neuron, this membrane is a bilipid membrane which contains ionic channels and this bilipid part of a membrane is essentially a very thin insulator, separating the relatively conducting electrolytes inside and outside the cell. The ionic channels (there are many different types of ionic channels) embedded in this membrane allow selected (charged) ions to cross the membrane. The ions of particular significance here are potassium ( $K^+$ ), sodium ( $Na^+$ ), Calcium ( $Ca^+$ ), and chloride ( $Cl^-$ ). In the absence of any input to the neuron, the excitable membrane will maintain the inside of the neuron at a particular potential relative to the outside of the neuron. This resting membrane potential is usually of the order of -70 mV (millivolts) (though this does vary across different populations of neurons). This resting potential results from movement of ions primarily due to the different ionic

concentrations inside and outside of the neurons, and this is maintained by the  $\text{Na}^+$ - $\text{K}^+$  pump which keeps the  $\text{Na}^+$  concentration inside the cell low, and the  $\text{K}^+$  concentration inside the cell high. External inputs to the neuron result in the increase of this potential (known as depolarization in the neurophysiology community) or decrease of this potential (hyperpolarisation) [3]. The schematic of patch of cell neuron membrane is shown in Fig. 2.5.

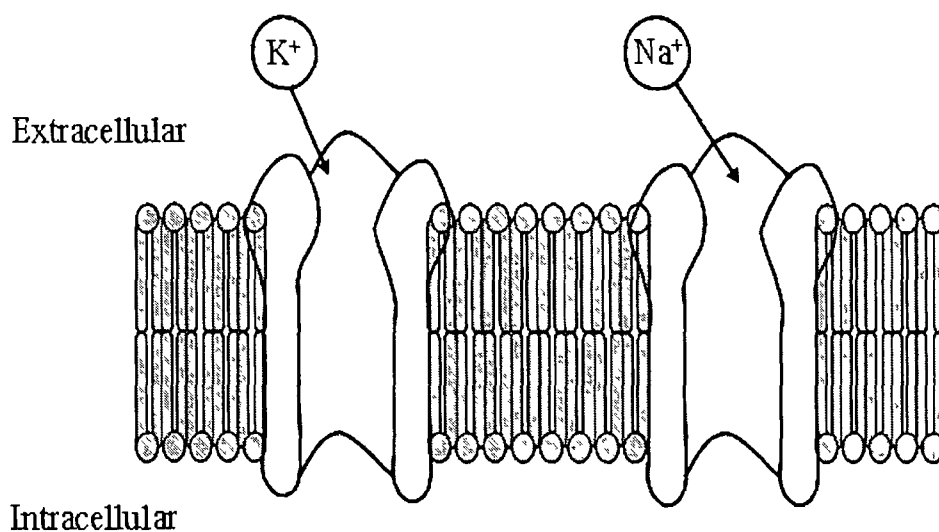


Fig 2.5 Patch of cell neuron membrane

### 2.2.4 Resting potential of Neuron:

Neurons are remarkable because of their electrical properties. There is an electrical potential difference between the inside and outside of a neuron's membrane. This difference is called the "transmembrane potential", "membrane potential," or simply the "voltage" of the cell. Electro physiologists measure the membrane potential by establishing electrical continuity between the inside of a neuron and the inside of a glass

microelectrode. The microelectrode is filled with electrolyte, which contains ions that carry current. A wire from inside the microelectrode leads to an amplifier, and is compared with another wire that serves as an external reference electrode. These two wires allow the amplifier to sense the electrical potential inside and outside the neuron.

Neurons can respond to stimuli and conduct impulses if a potential is established across the cell membrane. There is an unequal distribution of ions of two sides of the membrane. The inside of the neuron is slightly negative relative to the outside. This difference is called resting membrane potential. The resting membrane potential is expressed as  $-70\text{ mV}$ , and  $(-)$  sign indicates that inside of the membrane is negative relative to the outside. The potential is called resting because it occurs when the membrane is not stimulated or conducting impulses. The active transport mechanism of membrane is shown in Fig. 2.6.

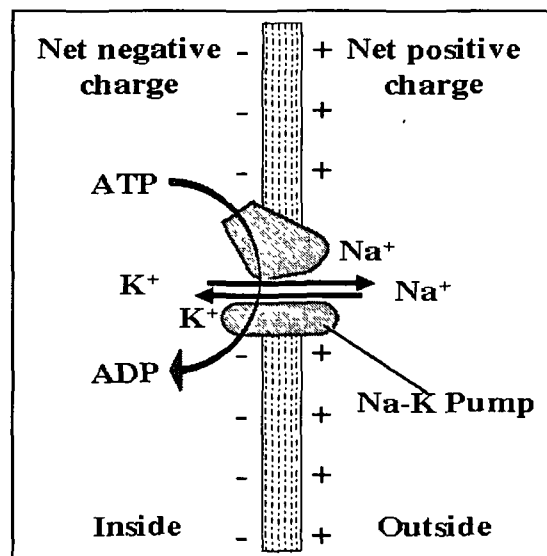


Fig. 2.6: The active transport mechanism

The positive ions responsible for the membrane is Sodium ions and Potassium ions;  $\text{Na}^+$  from the inside to the outside and  $\text{K}^+$  from the outside to the inside. As a result there occur Sodium-potassium pump which is also called active transport mechanism. There is a higher concentration of  $\text{Na}^+$  on the outside than the inside and there is a higher concentration of  $\text{K}^+$  on the inside than the outside.

In a resting nerve cell membrane all the sodium gates are closed and some of potassium gates are open. As a result  $\text{Na}^+$  cannot diffuse through the membrane and largely remain outside of the membrane. Some potassium ions are diffuse outside the membrane. Overall there are lots of positive charge ( $\text{K}^+$ ) inside the membrane and lots of sodium ions ( $\text{Na}^+$ ) plus small number of  $\text{K}^+$  ions outside the membrane. This means that there are more positive ions outside than the inside. In other word resting membrane potential is maintain until the membrane is stimulated.

### **2.2.5 Action potential:**

An action potential is vary rapid change in membrane potential., it occurs when nerve cell is stimulated. Action potential occurs when the membrane is depolarized and  $\text{Na}^+$  channels opens completely . The minimum stimulus needed to achieve an action potentials is called threshold stimulus. If the membrane potential reaches the threshold potential (generally 5-15mv), the voltage gated sodium channels are open and sodium ions diffuse inward and depolarization occurs [4].

The membrane potential of a neuron is measured while injecting current into it. If the stimulating current is above a threshold value, then the neuron generates action potential. During an action potential, the potential of the inside of the neuron becomes more positive than the outside for about few milliseconds. Every action potential of a neuron has roughly the same stereotyped time course. The schematic of arrangement for measurement of action potential in a neuron is shown in Fig. 2.7

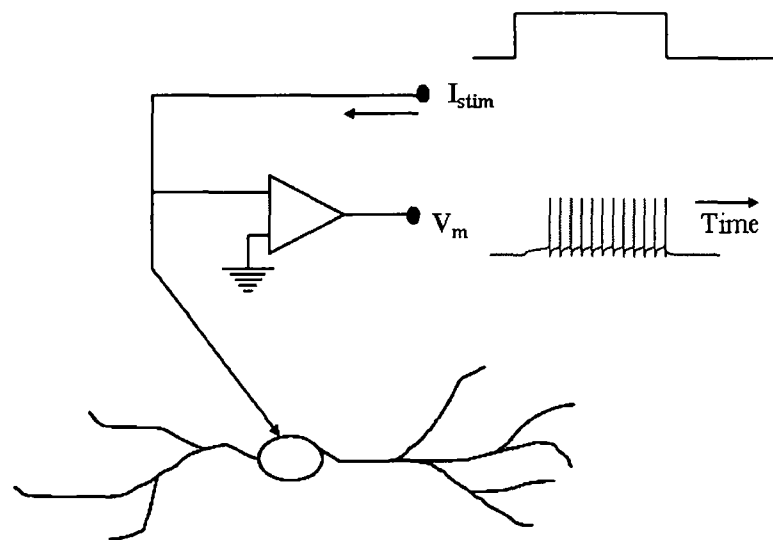


Fig. 2.7: Measurement of action potentials in a neuron.

The dendrite of the neurons receive information from sensory receptors or other neurons. The information is then passed down to the cell body and on to the axon. Once the information is arrived at the axon, it travels down the length of the axon in the form of an electrical signal, known as action potential. The firing of a neuron, referred to as action potential; i.e., the incoming stimuli either produce an action

potentials, if they exceed the neurons threshold value or not. A spike or action potential is a stereotyped impulse of fixed magnitude generated by the neuron. After the firing of an action potential, the neuron enters a refractory period when no further action potentials can be generated. Even with very strong input, it is impossible to excite a second spike during or immediately after a first one. This causes that action potentials in a spike train are usually well separated. The minimal distance between two spikes defines the absolute refractory period of the neuron. The absolute refractory period is followed by a phase of relative refractoriness where it is difficult, but not impossible, to generate an action potential [2].

Neurons in a resting state normally have a membrane potential  $-70\text{mv}$  [1]. This means that the voltage difference between the fluids on the inside of the cell relative to the fluid on the outside of the cell is negative. The cell membrane prevents charged particles such as these from freely diffusing into and out of the cell. There are two basic ways that they can get in or out. The first is with passive transport. Basically the cell has a protein in the cell membrane that it can open and close like a water faucet. It is specific for certain kinds of chemicals like ions. When it opens, then the ions can flow down their gradient from the more concentrated area to the less concentrated area. The other way to get ions in or out of cells is to by active transport. The cell uses some of its own energy to actively pump the chemicals against their gradient. The neuron has a pump that actively pumps three  $\text{Na}^+$  ions out and takes in two  $\text{K}^+$  ions. This means that a net positive charge flows out of the neuron. This is what gives the cell its negative potential. Ions are also what are responsible for the initiation, and transmission of action potentials. When the

neurotransmitters from other firing neurons come in contact with their corresponding receptors on the dendrites of the target neuron it causes those receptors to open or close some of the passive ion transports. This allows the ions to flow into the cell and temporarily change the membrane voltage. If the change is big enough then it will cause an action potential to be fired. Fig. 2.8 shows the basics of how ion flow transmits the action potential down the length of the axon.

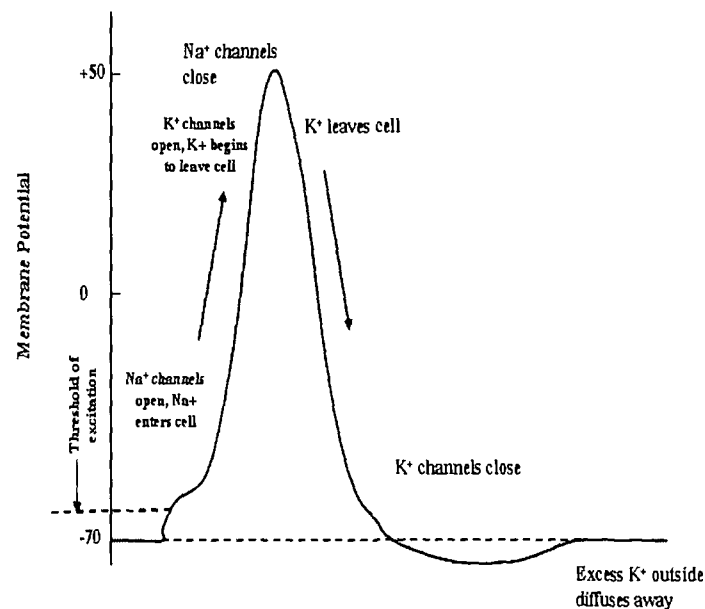


Fig. 2.8: Ion flow in action potential

The first step of the action potential is that the Na<sup>+</sup> channels open allowing a flood of sodium ions into the cell. This causes the membrane potential to become positive.



At some positive membrane potential the  $K^+$  channels open allowing the potassium ions to flow out of the cell.

Next the  $Na^+$  channels close. This stops inflow of positive charge. But since the  $K^+$  channels are still open it allows the outflow of positive charge so that the membrane potential plunges.

When the membrane potential begins reaching its resting state the  $K^+$  channels close.

Now the sodium/potassium pump does its work and starts transporting sodium out of the cell, and potassium into the cell so that it is ready for the next action potential.

Chloride ions also play some role in action potential. At rest the inside of a neuron is more negatively charged relative to the outside of the neuron. Though the intracellular concentration is high for potassium and low for both chloride and sodium, the resting membrane potential opposes potassium and chloride ions from diffusing down their concentration gradients. A change in extracellular chloride potential will eventually lead to a change in intracellular chloride potential; thus, inducing changes in the relative volume of the cell and changes in chloride, potassium, sodium, and internal anion concentrations. However, a change in extracellular chloride potential will not result in a change in the chloride equilibrium potential or membrane potential at steady state. Conversely, a change in extracellular potassium potential will lead to a change in the relative volume of the cell and alter the membrane potential. In addition, a change in extracellular potassium potential will result in changes in chloride, sodium, and internal anion concentrations. Sodium and potassium

ions constantly leak through the membrane. Yet, the sodium-potassium exchange pump maintains the leakage concentration. Activated by adenosine triphosphate (ATP) produced by metabolism, the sodium-potassium exchange-pump pumps three sodium ions into the cell for every two potassium ions pumped out of the cell. Activation of ion channels changes the permeability of the cell membrane to both potassium and sodium. These changes generate electrical signals changing the amount of charge on the cell membrane; thus, changing the membrane potential [6].

### **2.2.6 All or None principle:**

The conduction of nerve impulses is an example of an all-or-none response. In other words, if a neuron responds, then it must respond completely. The greater the intensity of stimulation does not produce a stronger signal but can produce *more* impulses per second. There are different types of receptor response to stimulus, slowly adapting or tonic receptors respond to steady stimulus and produce a steady rate of firing. These tonic receptors most often respond to increased intensity of stimulus by increasing their firing frequency, usually as a power function of stimulus plotted against impulses per second. This can be likened to an intrinsic property of light where to get greater intensity of a specific frequency (color) there have to be more photons, as the photons can't become "stronger" for a specific frequency.

### **2.2.7 Refractory period:**

When membrane has undergone an action potential, a refractory period follows. Thus, although the passive transmission of action potentials across myelinated segments would suggest that action potentials propagate in either

direction, most action potentials travel unidirectionally because the node behind the propagating action potential is *refractory*.

This period arises primarily because of the voltage-dependent inactivation of sodium channels, as described by Hodgkin and Huxley in 1952 [5]. In addition to the voltage-dependent opening of sodium channels, these channels are also inactivated in a voltage-dependent manner. Immediately after an action potential, during the *absolute refractory period*, virtually all sodium channels are inactivated and thus it is impossible to fire another action potential in that segment of membrane. In absolute refractory period, during an action potential a second stimulus will not produce a second action potential.

With time, sodium channels are reactivated in a stochastic manner. As they become available, it becomes possible to fire an action potential, even though with a much higher threshold. This is the *relative refractory period* and together with the absolute refractory period, lasts approximately five milliseconds. In relative refractory period another action potential can be produced if the stimulus is greater than the threshold stimulus. The nerve cell membrane becomes progressively more 'sensitive' (easier to stimulate) as the relative refractory period proceeds. So, it takes a very strong stimulus to cause an action potential at the beginning of the relative refractory period, but only a slightly above threshold stimulus to cause an action potential near the end of the relative refractory period [2]. The schematic of absolute and relative refractive period of action potential is shown in Fig. 2.9.

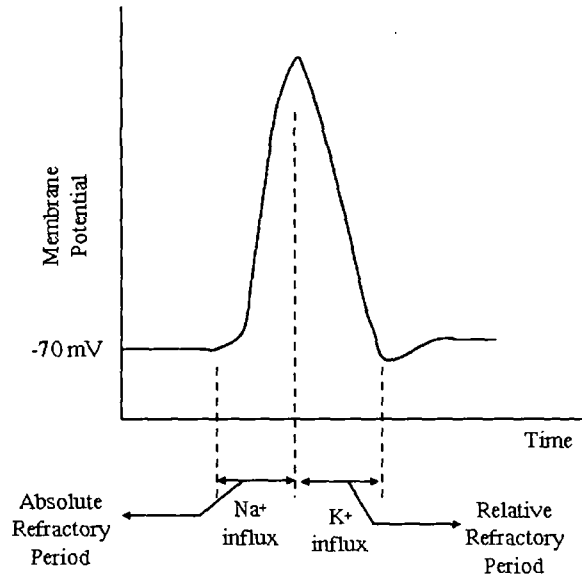


Fig. 2.9: The absolute and relative refractory period.

### 2.2.8 Impulse conduction:

An impulse is simply the movement of action potentials along a nerve cell. Action potentials are localized (only affect a small area of nerve cell membrane). So, when one occurs, only a small area of membrane depolarizes (or 'reverses' potential). As results, for a split second, areas of membrane adjacent to each other have opposite charges (the depolarized membrane is negative on the outside & positive on the inside, while the adjacent areas are still positive on the outside and negative on the inside). An electrical circuit (or 'mini-circuit') develops between these oppositely-charged areas (or, in other words, electrons flow between these areas). This 'mini-circuit' stimulates the adjacent area and, therefore, an action potential occurs. This process repeats itself and action potentials move down the nerve cell membrane. This movements of action potentials is called an impulse.

Impulses typically travel along neurons at a speed of anywhere from 1 to 120 meters per second. The speed of conduction can be influenced by: the diameter of a fiber, temperature, and the presence or absence of myelin.

Neurons with myelinated neuron conduct impulse must faster than the neuron without myelin [3].

### **2.3 Introduction to Synapse:**

A synapse can be defined as a specialized site of functional interaction between neurons. No neurons run directly from the periphery to brain. Normally the initiated signal is relayed by several intermediate neural cells. This interconnection between neurons, called the synapses, behave as a simple switch but also has a simple role in information processing. Neurons are able to respond to stimuli (such as touch, sound, light, and so on), conduct impulses, & communicate with each other. And synapse is point of impulse transmission between two neurons; in general impulse transmitted from axon of presynaptic neuron to dendrite of postsynaptic neuron, which is known as axodendritic synapse. Synapses generally omnidirectional, i.e., transmit signals in only one direction: an axon terminal from the presynaptic cell sends signal that are picked by the postsynaptic cell. The axon terminal of the presynaptic cell contains vesicle filled with neurotransmitter. The most common type of synapse in the vertebrate brain is a chemical synapse.

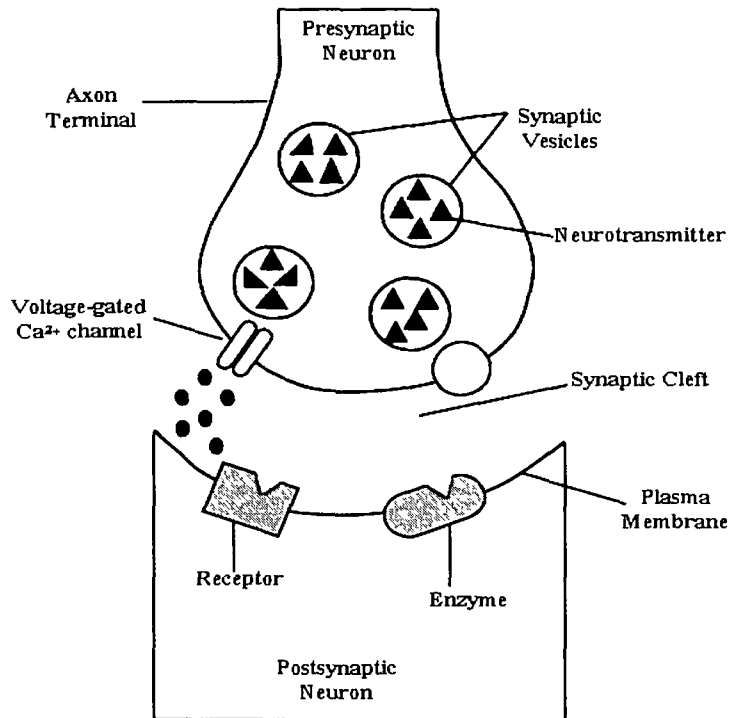


Fig. 2.10: Anatomy of Chemical Synapses

At a synapse, the end of the axon is 'swollen' and referred to as an end bulb or synaptic knob. Within the end bulb are found lots of synaptic vesicles (which contain neurotransmitter chemicals). Between the end bulb and the dendrite (or cell body) of the post-synaptic neuron, there is a gap (15-200nm) commonly referred to as the synaptic cleft as shown in Fig. 2.10.

Since the term synapse was coined at the end of the nineteenth century, this sophisticated structure has attracted tremendous attention, not only because synapses are necessary for neuronal signaling and computation, but also because they undergo long-term modification (synaptic plasticity) that underlie information storage (learning and memory) in the brain. Most synapses in the nervous system are chemical synapses — that is, synaptic transmission is

mediated by a neurotransmitter that is released by the Axon of the presynaptic neuron and that diffuses across a narrow cleft to act on corresponding receptors on the Dendrite of the postsynaptic neuron. So, synapses are cell junctions that are characterized by specialized membrane regions and the accumulation of specific proteins at both the presynaptic and postsynaptic sites of cell contact [7].

### **2.3.1 Types of Synapse:**

Synapses are classified according to the kind of neurotransmission, and/or according to the site.

Three types of synapse can be classified according to the site-

- (i) Axoaxonic synapse.
- (ii) Axosomatic synapse.
- (iii) Axodendritic synapse.

Axoaxonic makes a connection between axon of a one neuron to the axon of another neuron as shown in Fig. 2.11. Its tend to be inhibitory and regulating the postsynaptic neuron.

Axosomatic synapse makes a connection between axon of a presynaptic neuron to the soma or cell body of a postsynaptic neuron.

Axodendritic synapse referring to the synapse between the axon of a one neuron (presynaptic neuron) to dendrite of another neuron (postsynaptic neuron). This types of synapse is most frequent and they tend to be excitatory.

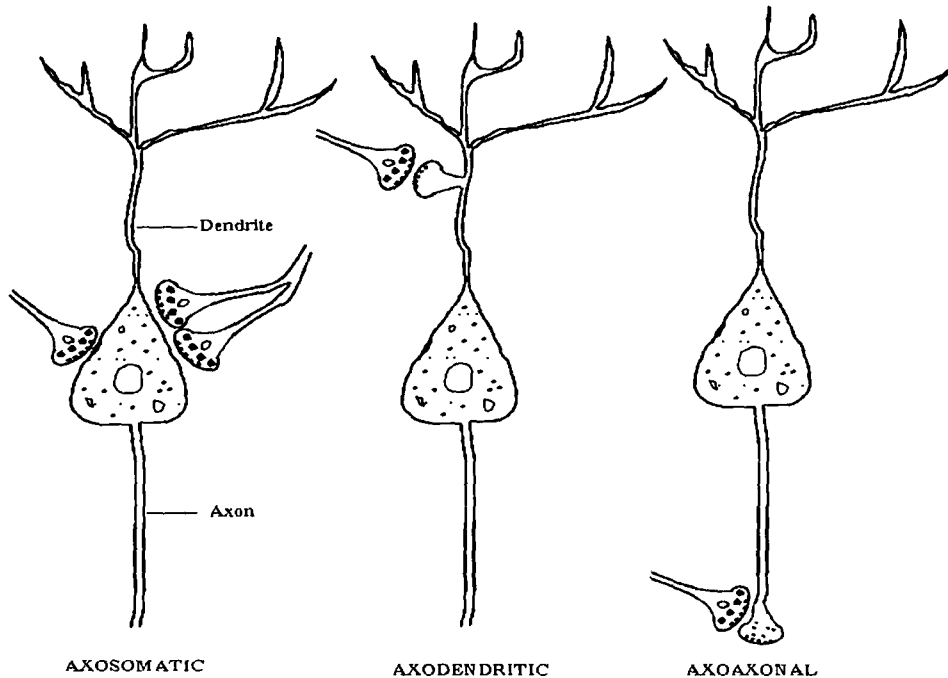


Fig. 2.11: Types of synapses according to site.

The typical and most frequent type of synapse is the one in which the axon of one neuron connects to a second neuron by usually making contact with one of its dendrites or with the cell body.

According to the neurotransmission there are two types of synapse: They are,

- (i) Electrical synapse, and
- (ii) Chemical synapse.

Gap junctions and connexons form electrical synapse (Bennett, 1977). And Chemical synapses are formed by chemical neurotransmitters, where there is a



gap between the presynaptic neuron and postsynaptic neuron, which is known as synaptic cleft.

### **2.3.2 Synaptic Communication:**

The primary mode of communication between two neurons is a biochemical process that occurs at a synapse. The synapse is essentially a junction called synaptic cleft between two neurons namely presynaptic and postsynaptic neurons. Signal from presynaptic neuron to postsynaptic neuron is transmitted through neurotransmitter chemical released by presynaptic neuron terminals into the synaptic cleft. Neurotransmitters diffuse through the cleft and then bind with the specific receptor sites of the membrane of postsynaptic neuron. This binding initiates the opening of transmitter gated ion channels resulting in flow of ions into the cell or out of the post synaptic cell [2].

Primarily synapses are the point of impulse conduction between presynaptic (axon) neuron and postsynaptic (dendrite) neuron. The neurotransmitter released by the presynaptic neuron at synapses excite or inhibit the dendrites and cell body of the postsynaptic neuron. If sufficiently excited an action potential will be generated in the postsynaptic neuron. The neurotransmitter molecules are stored in synaptic vesicles located in the expanded tips of the presynaptic neuron [8]. Some of the neurotransmitters diffuse across the synaptic cleft and bind with receptors in the postsynaptic membrane. In response membrane channel open and ions (sodium, potassium, chloride) enter and exit the postsynaptic neuron. The exchange of ions depolarized or hyperpolarized the postsynaptic neuron.

The synapses can be Excitatory or Inhibitory in nature, according to the effect it causes on the postsynaptic element. Neurotransmitter released at excitatory synapses open ion channels in the postsynaptic membrane, that allow sodium ions ( $\text{Na}^+$ ) and calcium ( $\text{Ca}^+$ ) to enter the cell. The influx of sodium ions causes the membrane to temporally depolarize [9]. This voltage change, which is called Excitatory post synaptic potential (EPSP), are required to reach the threshold point (-55mv approximately) to generate an action potential. Interaction with receptor sites at excitatory synapses opens sodium ( $\text{Na}^+$ ) and potassium ( $\text{K}^+$ ) channels, thereby increasing the permeability of post synaptic membrane to each of this ions. The inward diffusion of sodium ion is greater than outward diffusion of potassium ions, thus the postsynaptic membrane is no longer resting and is called excitatory post synaptic potential (EPSP). The EPSP is shown in Fig. 1.12. The resting membrane potential (RMP) is shown as -70 in Fig. 2.12.

The postsynaptic potential repolarizes to its resting potential (-70mv) within a few milliseconds after the receptor close. This process is accomplished by sodium-potassium pump in the postsynaptic membrane.

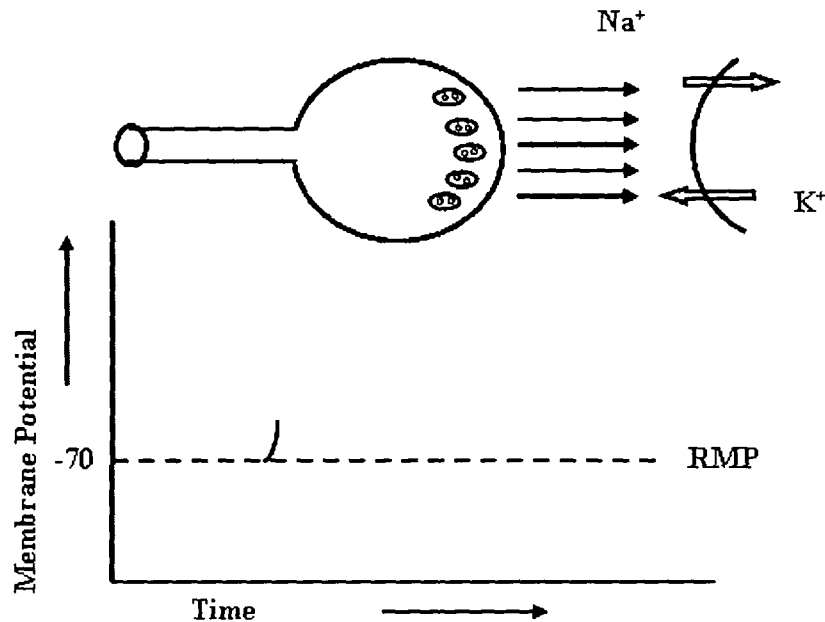


Fig. 2.12: Excitatory Post Synaptic Potential (EPSP).

Inhibitory synapses cause an inhibitory postsynaptic potential (IPSP) because the net effect of neurotransmitter released by the presynaptic membrane hyperpolarized the postsynaptic membrane, which is more difficult to reach the electrical threshold potential to start an action potential. Neurotransmitter released at inhibitory synapses cause ion channels of receptor site to open, which allow the movement of potassium ( $K^+$ ) ion. Then the membrane will temporally hyperpolarize due to potassium ions. This movement of potassium, hyperpolarized the membrane so that the internal potential become more negative than the resting state. Consequently an inhibitory postsynaptic potential (IPSP) established. The potential is called inhibitory because the membrane potential is even

farther from the excitation threshold than in the resting state. The IPSP is shown in Fig. 2.13.

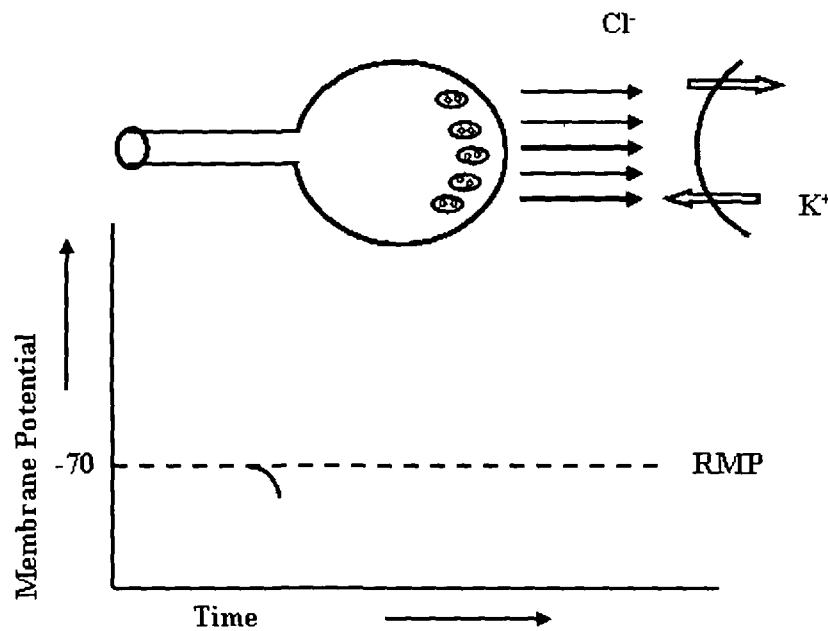


Fig. 2.13: Inhibitory Post Synaptic Potential (IPSP).

An IPSP change the membrane voltage in the postsynaptic neuron which result from synaptic activation of inhibitory neurotransmitter receptors. A postsynaptic potential is called inhibitory when the resulting change in membrane voltage make it more difficult to fire an action potential, lowering the firing rate of action potential.

When an action potential from the presynaptic neuron arrives at its terminals connecting the cleft, neurotransmitters are released into the cleft which diffuse through the cleft and bind with the receptor sites of the postsynaptic

membrane. This binding mechanism opens the ion channels situated at the membrane surface and ions move into or out of the membrane. If the synapse is excitatory, Sodium ions flow into the cell resulting into positive current. As a result the membrane depolarizes. If sufficient number of Sodium channels open, then membrane potential will be greater than the action potential threshold  $V_T$  of the neuron and initiates an action potential. If the synapse is inhibitory, Chloride & Potassium ions move into & out of the cell, resulting into negative current. As a result the membrane hyperpolarizes. If the numbers of Chloride & Potassium channels are sufficiently large then membrane potential will be able to initiate an action potential in negative direction. Excitatory neurotransmitters make membrane potential less negative via increased permeability of the membrane to sodium & therefore tend to excite the postsynaptic membrane. Inhibitory neurotransmitters make membrane potential more negative via increased permeability of the membrane to potassium & therefore tend to inhibit or make less likely the transmission of an impulse [9]-[10].

## 2.4 References:

- [1] Shepherd, G. M. *Neurobiology*, Oxford University Press, 3<sup>rd</sup> Edition, 2005.
- [2] Longstaff, A. *Neuroscience*, Viva Books Private Limited, First Indian Edition 2002.
- [3] Smith, Leslie. S. *Handbook of Nature-Inspired and Innovative Computing: Implementing Neural Models in Silicon*, Springer, 2006, Chapter 13, pp. 433-476.

- 
- [4] Mortimer, J. Thomas. Voltage gated Sodium Ion Channel: From phenomena To Technology, *IEEE Transaction*, 1999, pp. 26-29.
- [5] Hodgkin, A. L. Huxley, A. F. *A Quantitative Description Of Membrane Current And Its Application To Conduction And Excitation In Nerve*. Journal of Physiology, 1952, 117, pp. 500-544.
- [6] Moore, J. W. Stuart, A. E. *Neurons in Action*. Sunderland, MA: Sinauer Associates, Inc., 2001.
- [7] Cowan, W. M. Sudhof, T. C. Stevens, C. F. *Synapses*, The Johns Hopkins University Press, 2003.
- [8] Plonsey, M. J. R. *Bioelectromagnetism – Principles and Applications of Bioelectric and Biomagnetic Fields*. Oxford University Press, 1995, Chapter 10.
- [9] Farquhar, E. Hasler, P. A Bio-physically inspired silicon neuron, *IEEE Transactions on Circuits and systems*, March 2005, Vol. 52, No. 3, pp. 477-488.
- [10] G. Roy. A simple electronic analog of the squid axon membrane: The NEUROFET, *IEEE Transactionson on Biomedical Engineering*, 1972, vol. BME-18, pp. 60–63.

# **Chapter 3**

## **General Overview of Neuron Modeling**

## General Overview of Neuron Modeling

### 3.1 Introduction:

Neuron models are used in neuromorphic engineering aiming at understanding of real neuronal systems and are gaining better, possibly brain like performance for systems being built. In recent times the term neuromorphic has been used to describe analog, digital or mixed-mode analog/digital VLSI systems that implement models of neuronal systems (for perception, motor control, or sensory processing) as well as software algorithms. A key aspect of neuromorphic design is to understanding how the morphology of individual neurons, circuits, and overall architectures create desirable computations, affect how information is represented, influences robustness to damage, incorporates learning and development, and facilitates evolutionary change. Neuromorphic engineering takes inspiration from biology, physics, mathematics, computer science and engineering to design artificial neural systems, such as vision systems, head-eye systems, auditory processors, and autonomous robots, whose physical architecture and design principles are based on those of biological nervous systems. Neuromorphic systems are basically artificial systems and can be realized in analog VLSI, and they range from vision chips to synaptic conductances. By building and operating neuromorphic systems, we can have depth knowledge of computational principles of neural networks and systems. Here we reviewed of some publications concerning the development of model of neuron based on Hodgkin – Huxley equations and subsequent electronic models based on the similarities between biological and semiconductor physics.



Neuroengineering, or more precisely Bio-neuroengineering which is inseparable part of Bioelectronics, is an interdisciplinary area, with the common goal of analyzing the function of the nervous system, developing methods to restore damaged neurological function & creating artificial neuronal systems by integrating physical, chemical, mathematical & engineering tools.

The development of artificial circuit models that simulate the behavior of biological neuron is one of today's most promising directions of investigation in the field of neurobio and neuromorphic engineering. Two main classes of models of spiking neurons have been implemented in silicon, namely conductance based model, such as Hodgkin and Huxley (H-H) model and Integrate and fire (I-F) model such as McGregor model. I-F model is employed to reproduce some phenomenological properties of biological neurons that are specially focused on the designers. The latter is employed to design the electrophysiological properties of biological neuron accurately. Conductance based model details allow for a dynamics of a neuron membrane potential and spike generation.

### **3.2 Conductance based model:**

These types of silicon neurons contain analog circuits that emulate the physics of a real ionic conductance and are typically based on prototypical ion conductance models that obey Hodgkin-Huxley principles. The Conceptual basis of the H-H model equation is given by the stochastic motion of ions through channel proteins with the cell membrane, driven by potential difference across the cell membrane and regulated by potential dependent conductances. In 1952 H-H explained how action potentials

are generated through the electrical excitability of neuronal membrane. Action potential are arises from the synergistic action of sodium and potassium channels, each of which open and close in a voltage dependent fashion.

Conductance based models allow for detailed dynamics of a neuron's membrane potential and spike generation. They imitate the biological neurons' response by modeling several ion channels, like sodium, potassium, calcium, etc. Advantages of conductance models are the possibility of modeling post-inhibitory rebounds, bursting, and the multiple-compartmental structure of a single neuron. Thus Hodgkin- Huxley conductance based models provides an excellent description of the electrical behavior of the neuron. The Hodgkin and Huxley (H-H) equation is generally used by biomedical engineers and neuroscientist to model analog circuit for axonal membrane. If a neuron is considered as a signal processing unit, the synapses and dozens of different types of neurotransmitters discovered thus far that can act on transmitter-gated ion channels in synapses must be examined. Thus far, many neuron models were proposed for explaining the active principle of neuron such as the famous Hodgkin-Huxley (H-H) model.

### **3.2.1 Hodgkin-Huxley Membrane Model:**

Hodgkin- and Huxley showed that the current can be carried through the membrane either by charging the membrane capacity or by movement of ions through the resistances in parallel with the capacity. Hodgkin- and Huxley described that the electrical behaviour of membrane may be represented by the equivalent circuit shown in Fig 3.1.

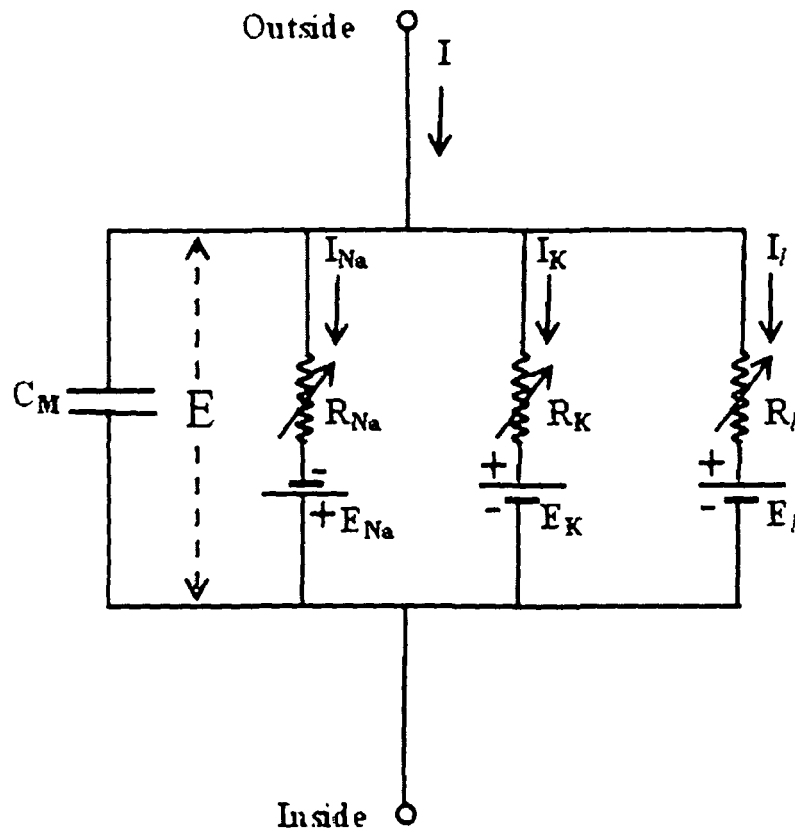


Fig. 3.1: Electrical circuit representing membrane.  $R_{Na} = 1/g_{Na}$ ;  $R_K = 1/g_K$ ;  $R_l = 1/g_l$ .  $R_{Na}$  and  $R_K$  vary with time and membrane potential; the other components are constant.

As described by Hodgkin and Huxley, the current passing through the biological membrane can either be the capacitive current, which is by charging the membrane capacitance or ionic current which is due to movement of ions through the resistances in parallel with the capacitance. So, for analysis of Hodgkin and Huxley model, the total current is divided into capacitive current

and ionic current. The expression of capacitive current described by Hodgkin and Huxley is given by-

$$I_C = C_m (dV / dt) \quad (3.1)$$

And the ionic part of the total current is composed of sodium ions ( $I_{Na}$ ) current, potassium ions ( $I_K$ ) current and other ions ( $I_l$ ) current and given by-

$$I_i = I_{Na} + I_K + I_l \quad (3.2)$$

Thus the total membrane current is

$$I = I_C + I_i \quad (3.3)$$

In the capacitive current,  $V$  is the displacement of the membrane potential from its resting value,  $C_M$  is the membrane capacitance per unit area which is assumed to be constant,  $t$  is time. Hodgkin and Huxley in their series of papers showed that the ionic permeability of the membrane can be expressed in terms of ionic conductances ( $g_{Na}$ ,  $g_K$  and  $g_l$ ). The respective ionic currents given by Hodgkin and Huxley are –

$$I_{Na} = g_{Na} (E - E_{Na}) \quad (3.4)$$

$$I_K = g_K (E - E_K) \quad (3.5)$$

$$I_l = \bar{g}_l (E - E_l) \quad (3.6)$$

Where  $E_{Na}$  and  $E_K$  are the equilibrium potentials for the sodium and potassium ions.  $E_l$  is the potential at which the leakage current due to chloride and other ions is zero. For practical application the above three equations can be written in the form –

$$I_{Na} = g_{Na} (V - V_{Na}) \quad (3.7)$$

$$I_K = g_K (V - V_K) \quad (3.8)$$

$$I_l = \bar{g}_l (V - V_l) \quad (3.9)$$

Where,

$$V = E - E_r \quad (3.10)$$

$$V_{Na} = E_{Na} - E_r \quad (3.11)$$

$$V_k = E_k - E_r \quad (3.12)$$

$$V_l = E_l - E_r \quad (3.13)$$

And  $E_r$  is the absolute value of the resting membrane potential.  $V$ ,  $V_{Na}$ ,  $V_K$  and  $V_l$  can be measured as displacement from the resting membrane potential.

At steady state condition the capacitive component of total current is zero since at steady state  $(dV/dt) = 0$ . The individual ionic currents are related with their respective ionic conductances ( $g_{Na}$ ,  $g_K$  etc), equilibrium potential of respective ions ( $E_{Na}$ ,  $E_K$  and  $E_l$ ) and membrane potential ( $E$ ) [1]. The total membrane current is a function of time and voltage and is given by –

$$I = C_m (dV/dt) + g_K n^4 (V - V_K) + g_{Na} m^3 h (V - V_{Na}) + g_l (V - V_l) \quad (3.14)$$

In order to introduce the concept of resting and action potential related to biological neurons, the general equation for the total current passing through the patch of membrane given by Hodgkin and Huxley can be expressed as -

$$I_{tot} = C_m (dv/dt) + g_K (V - E_K) + g_{Na} (V - E_{Na}) + I_p \quad (3.15)$$

Where,  $I_p$  is current due to Na -K pump, which can be split into two separate currents, Sodium pump current  $I_p(Na)$ , and Potassium pump current  $I_p(K)$ . Because of its small contribution, Na-K pump current can be neglected.

From the current expression, the resting potential expression can be written as-

$$V_m = \frac{(E_k + NK E_{Na})}{(1 + NK)} \quad (3.16)$$

Where,  $NK = (g_{Na}) / (g_K)$  is the sodium/potassium conductance ratio.

Now, if an ionic current is injected-

$$I_{ext} = C_m \left( \frac{dv}{dt} \right) + g_K (V - E_K) + g_{Na} (V - E_{Na}) \quad (3.17)$$

inside the cell through the membrane neglecting the Na-K active pump current  $I_p$ , it will shift the resting potential of the membrane to a new steady value. Therefore, constant current  $I_{ext}$  applied for a short time  $\Delta t$  will shift the membrane potential to a new steady value given by-

$$V_m^* = \left[ \frac{(E_k + NK E_{Na})}{(1 + NK)} \right] + \left[ \frac{I_{ext}}{(g_K + g_{Na})} \right] \quad (3.18)$$

Now if the  $I_{ext}$  current is turn off, the membrane current will decay back to its original resting value  $V_m$ . The simulated output profile of H-H model is shown in Fig 3.2.

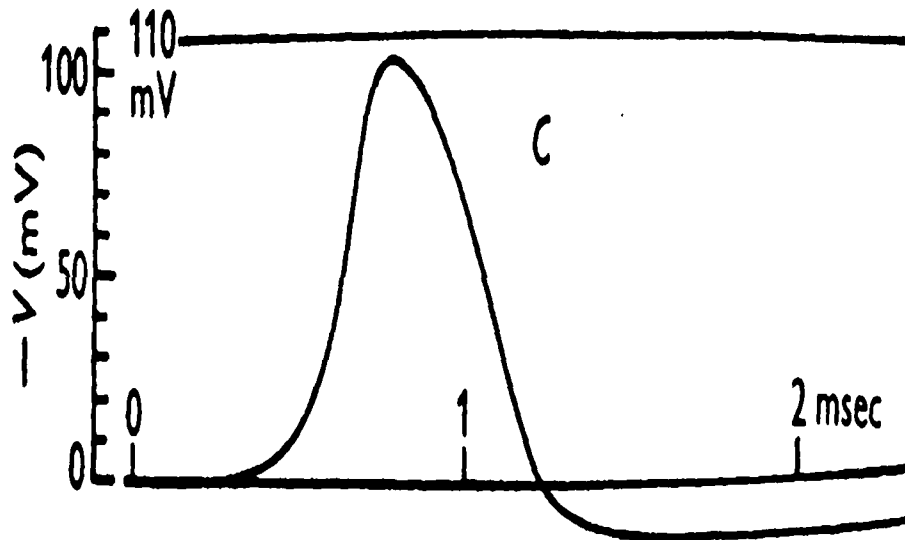


Fig. 3.2: The simulated output of H-H model

After these historical developments, many researchers in the field of bio-neuroengineering proposed different models of biological neurons. The dynamics of those models is quantitatively and qualitatively similar to Hodgkin-Huxley mechanisms which implement their specific equations.

### 3.2.2 Lewis Membrane Model:

Edwin R. Lewis published several electronic membrane models that are based on the Hodgkin-Huxley equations. Lewis membrane model proposed by Edwin R. Lewis, uses discrete transistors and associated components for the sodium and potassium conductances, synaptic connections, and other functions of electronic membrane model [2]. All these are parallel circuits connected between nodes representing the inside and outside of the membrane. Lewis implemented the electronic membrane model as shown in

Fig. 3.3, with active filters for sodium and potassium conductances and multipliers.

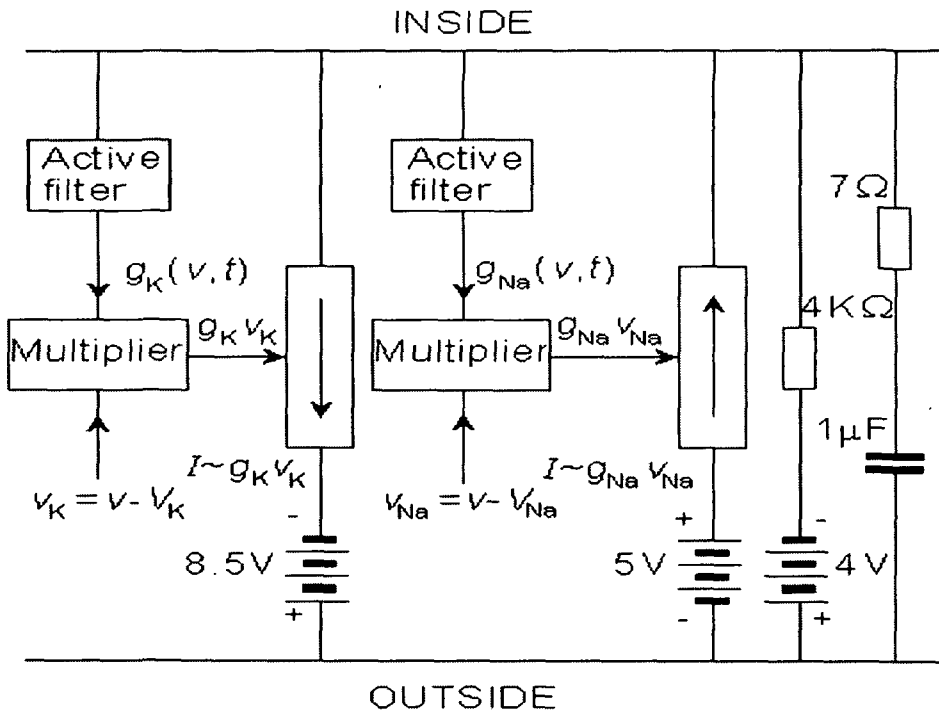


Fig. 3.3: The block diagram of Lewis Membrane Model

Since the output of the model is the transmembrane voltage  $V_m$ , the potassium current can be evaluated by multiplying the voltage corresponding to  $G_K$  by  $(V_m - V_K)$ . The Lewis model is an accurate physical analogy to the Hodgkin-Huxley expressions and the behavior of the output voltage  $V_m$  corresponds to that predicted by the Hodgkin-Huxley equations. The electronic circuits in the Lewis neuron model has provision for inserting (and varying) not only such constants as  $G_{K \max}$ ,  $G_{Na \max}$ ,  $V_K$ ,  $V_{Na}$ ,  $V_{Cl}$ , which enter the Hodgkin-Huxley formulation, but also  $\tau_h$ ,  $\tau_m$ ,  $\tau_n$ , which allow modifications from the Hodgkin-Huxley equations. In the following, the components of the model are discussed separately.



### 3.2.2.1 Potassium Conductance of Lewis Membrane model:

The circuit simulating the potassium conductance of Lewis membrane model is shown in Fig 3.4. The potassium conductance function  $G_K(V_m, t)$  is generated from the simulated membrane voltage through a nonlinear active filter according to the Hodgkin-Huxley model (in the figure separated with a dashed line). The three variable resistors in the filter provide a control over the delay time, rise time, and fall time. The value of the potassium conductance is adjusted with a potentiometer, which is the amplitude regulator of a multiplier. The multiplier circuit generates the function  $G_K(V_m, t) \cdot v_K$ , where  $v_K$  is the difference between the potassium potential ( $V_K$ ) and membrane potential ( $V_m$ ). The multiplier is based on the quadratic function of two diodes.

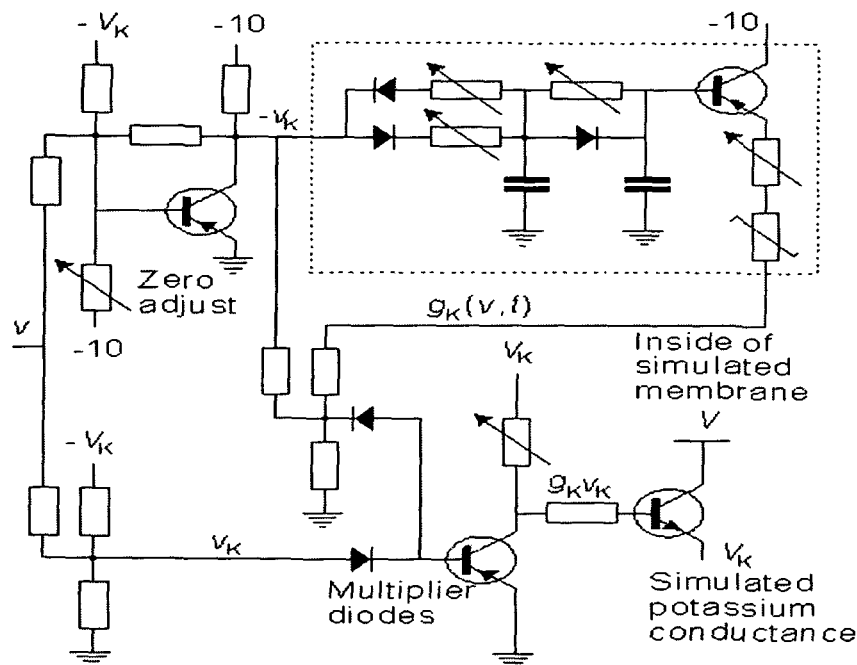


Fig. 3.4: The circuit simulating the potassium conductance of the Lewis membrane model.

### 3.2.2.2 Sodium Conductance of Lewis Membrane model:

In the Lewis circuit simulating the sodium conductance, Lewis omitted the multiplier on the basis that the equilibrium voltage of sodium ions is about 120 mV more positive than the resting voltage. Because of the interest in small membrane voltage changes, the gradient of sodium ions may be considered constant. The circuit simulating the sodium conductance is shown in Fig 3.5. The time constant of the inactivation is defined according to a varistor. The inactivation decreases monotonically with the depolarization, approximately following the Hodgkin-Huxley model.

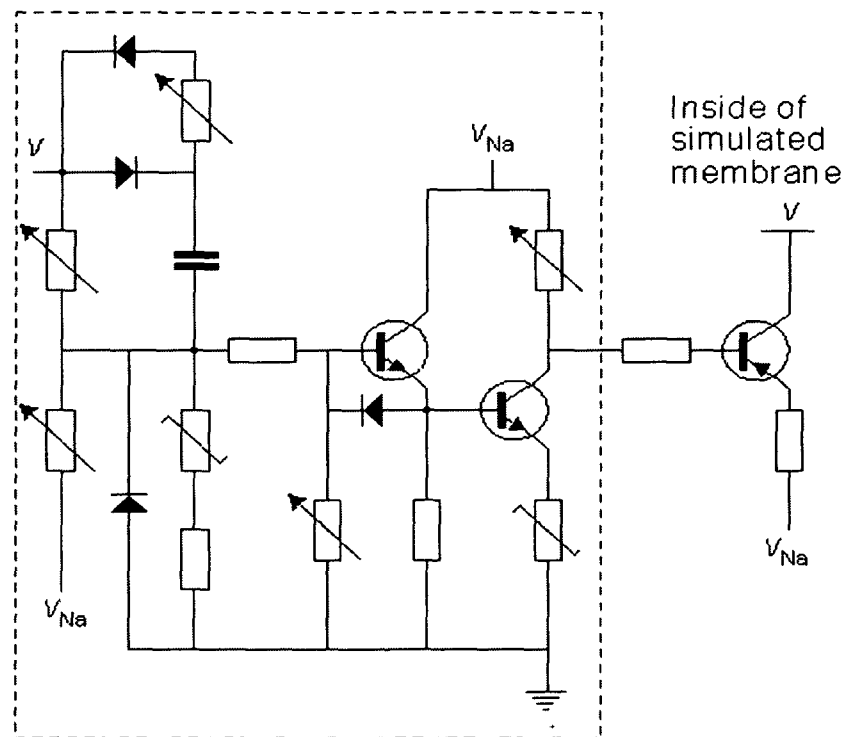


Fig. 3.5: The circuit simulating the sodium conductance of the Lewis membrane model.

### 3.2.2.3 Simulated Action Pulse of Lewis Membrane model:

By connecting the components of the membrane model as in Fig 3.6 and stimulating the model analogously to the real axon, the model generates a membrane action pulse. This simulated action pulse follows the natural action pulse very accurately. Fig 3.7 illustrates a single action pulse generated by the Lewis membrane model. The goal of Lewis model is to simulate the behavior of a neuronal network, including coupled neuron.

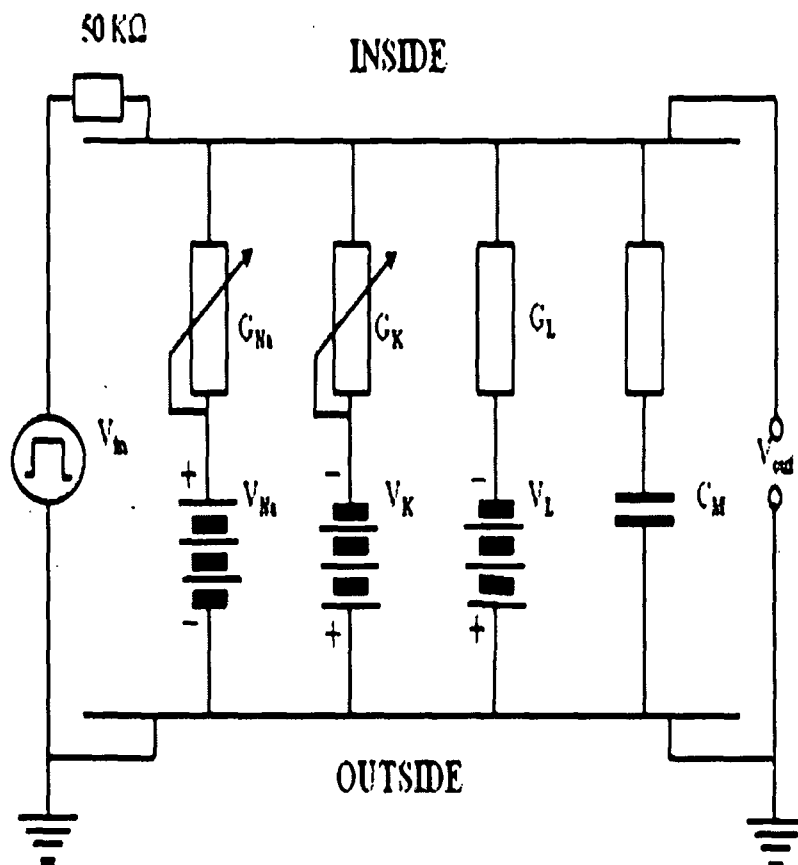


Fig. 3.6: The complete Lewis membrane model

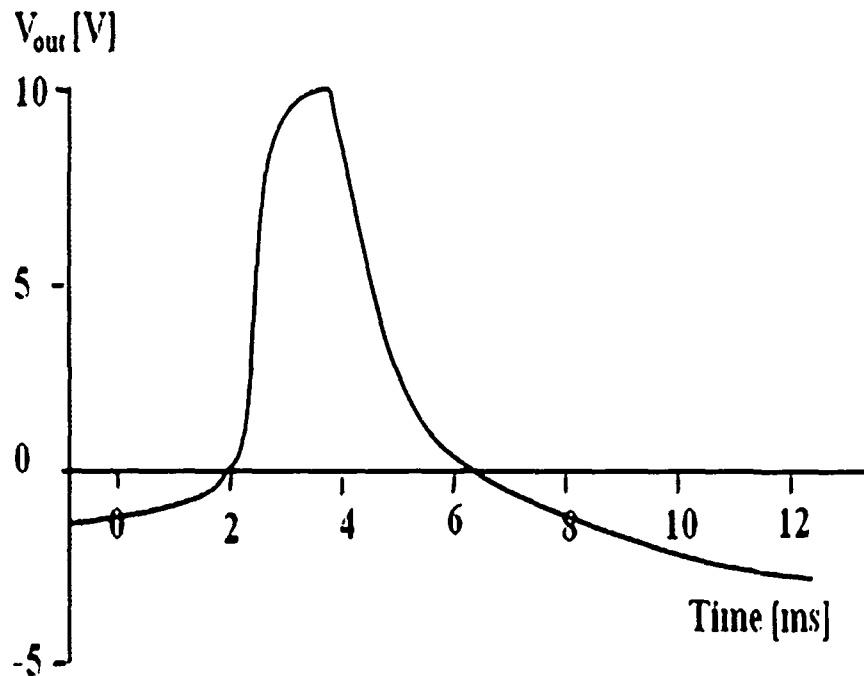


Fig. 3.7: Single action potential pulse generated by Lewis Membrane Model

### 3.2.3 Roy Membrane Model:

Guy Roy published an electronic membrane model in 1972 and gave it the name "Neurofet". His model, analogous to Lewis's, is also based on the Hodgkin-Huxley model. Guy Roy used Field Effect Transistors (FETs) to simulate the sodium and potassium conductances. FETs are well known as adjustable conductors. So the multiplying circuit of Lewis may be incorporated into a single FET component (Fig 3.8). In the Roy model the conductance is controlled by a circuit including an operational amplifier, capacitors, and resistors. This circuit is designed to make the conductance

behave according to the Hodgkin-Huxley model. Roy's main goal was to achieve a very simple model rather than to simulate accurately the Hodgkin-Huxley model. Nevertheless, the measurements resulting from his model, shown in Fig 3.9 and 3.10, are reasonably close to the results obtained by Hodgkin and Huxley. Fig 3.9 illustrates the steady-state values for the potassium and sodium conductances as a function of applied voltage. Note that for potassium conductance the value given is the steady-state value, which it reaches in steady state. For sodium the illustrated value is  $G'_{Na} = G_{Na\max} m^3 \infty h_0$ ; it is the value that the sodium conductance would attain if  $h$  remained at its resting level ( $h_0$ ). The full membrane model was obtained by connecting the potassium and sodium conductances in series with their respective batteries and simulating the membrane capacitance with a capacitor of 4.7 nF and simulating the leakage conductance with a resistance of 200 kΩ. The results from the simulation of the action pulse are illustrated in Fig 3.10 [3]

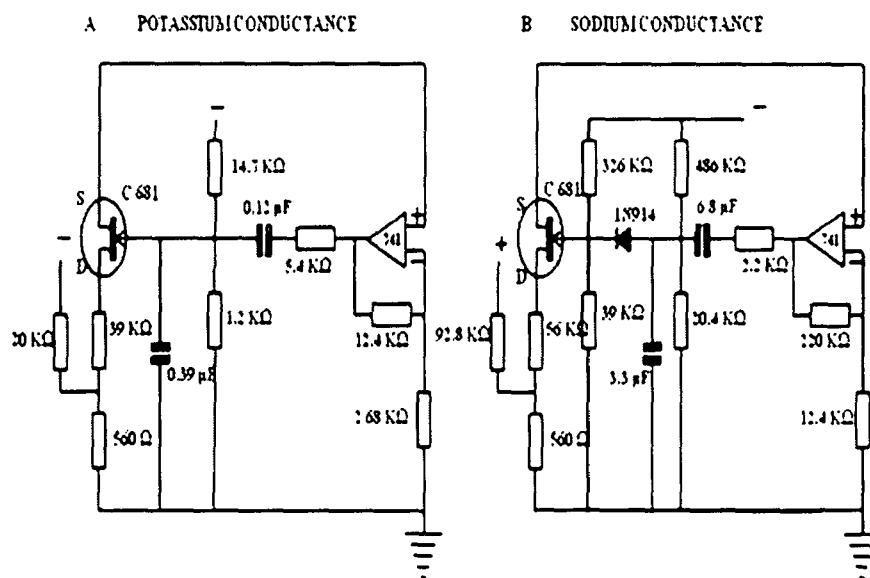


Fig. 3.8: The circuits simulating (A) sodium and (B) potassium conductances in the Roy Membrane Model

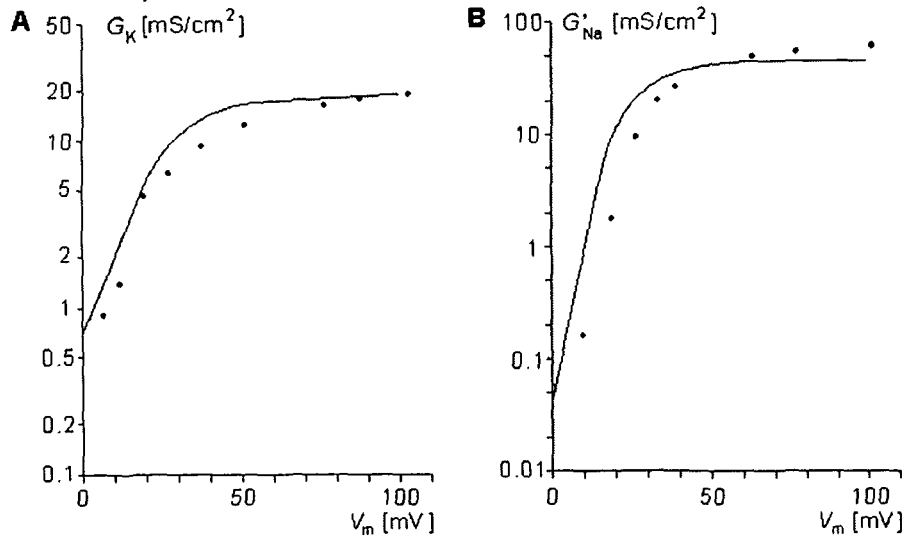


Fig. 3.9: Steady-state values of the (A)  $G_K$  and (B)  $G'_{Na}$  as a function of membrane voltage clamp in the Roy model (solid lines), compared to the measurements of Hodgkin and Huxley (dots).  $V_m$ , the transmembrane voltage, is related to the resting value of the applied voltage clamp.

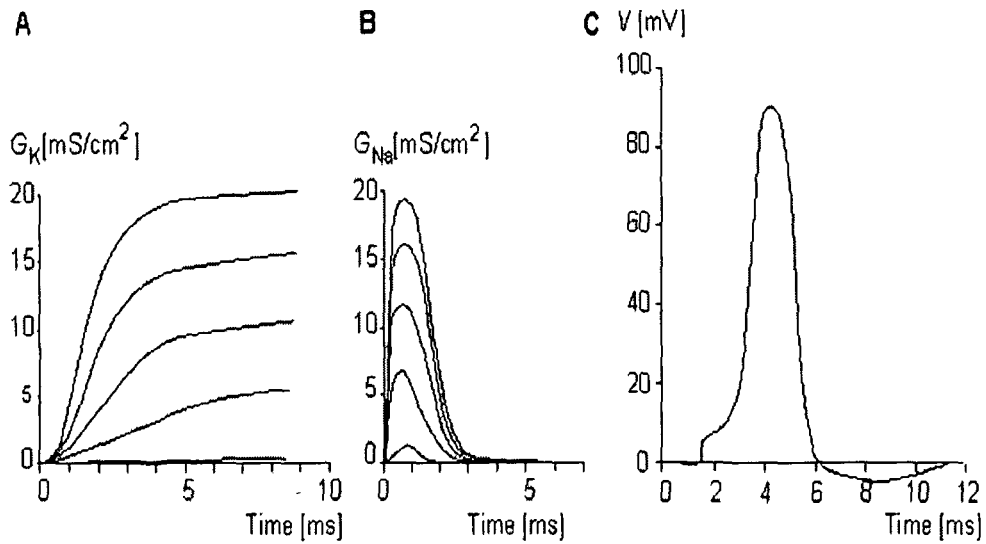


Fig. 3.10: Voltage-clamp measurements made for (A) potassium and (B) sodium conductances in the Roy model. The voltage steps are 20, 40, 60, 80, and 100 mV. (C) The action pulse simulated with the Roy model.

### 3.2.4 Farquhar and Hasler Membrane Model:

There is clear analogy between biological neuron and semiconductor physics. Hodgkin-Huxley realized non-linear conductance using resistors. But biological channels have exponential current relationship to the voltage on the membrane which can not be simply realized using resistor. E. Farquhar and P. Hasler [4] proposed a model of sodium and potassium channel type neuron circuit which can generate action potential. The proposed model of E. Farquhar and P. Hasler is shown below in Fig. 3.11.

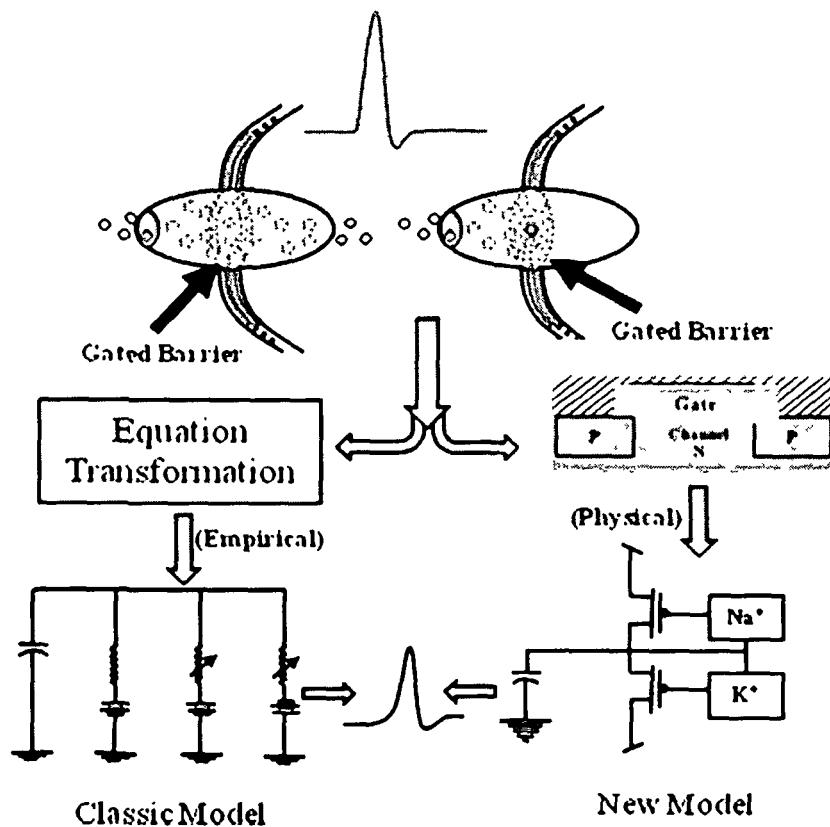


Fig. 3.11 The figure shows the model proposed by E. Farquhar and P. Hasler

The Fig.3.11 shows the transition from bio-physics to semiconductor physics. The proposed model of E. Farquhar and P. Hasler can be realized for linear conductances using Bipolar Junction Transistor (BJT) or a sub-threshold mode Metal Oxide Semiconductor Field Effect Transistor (MOSFET). MOSFET has higher preference over BJT because of its extremely low power dissipation in sub-threshold mode. As mentioned earlier, the proposed model of neuron circuit of E. Farquhar and P. Hasler consists of sodium and potassium channel circuits. The sodium channel circuit of E. Farquhar and P. Hasler is shown in Fig. 3.12 below, and it contains a band pass filter and a band pass control circuit which controls the sodium channel transistor and it is observed that the response of band pass filter is that of sodium channel response. Similarly, the potassium channel circuit of E. Farquhar and P. Hasler is shown below in Fig. 3.13. By combining the two channel circuits of E. Farquhar and P. Hasler a complete neuron circuit model is proposed, which is shown in Fig. 3.14. The results obtained by E. Farquhar and P. Hasler closely matches with the biological data.



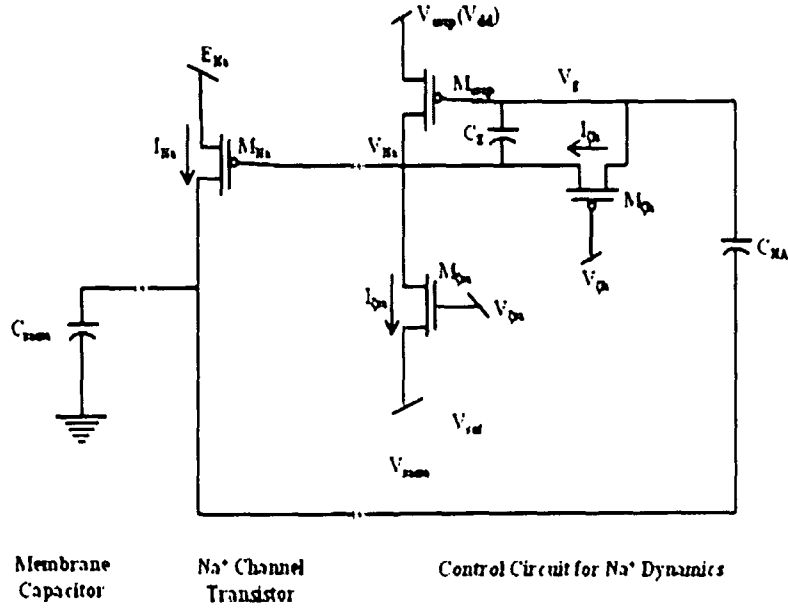


Fig. 3.12: The sodium channel circuit model of E. Farquhar and P. Hasler

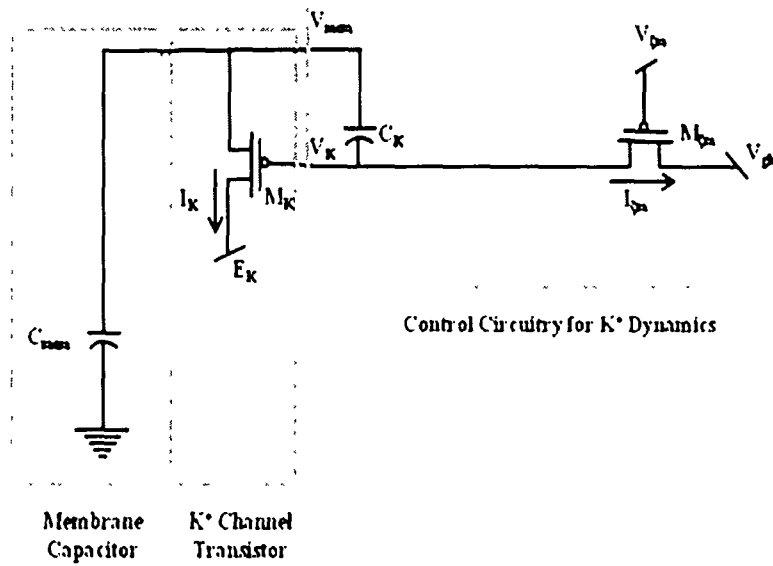


Fig. 3.13: The potassium channel circuit model of E. Farquhar and P. Hasler

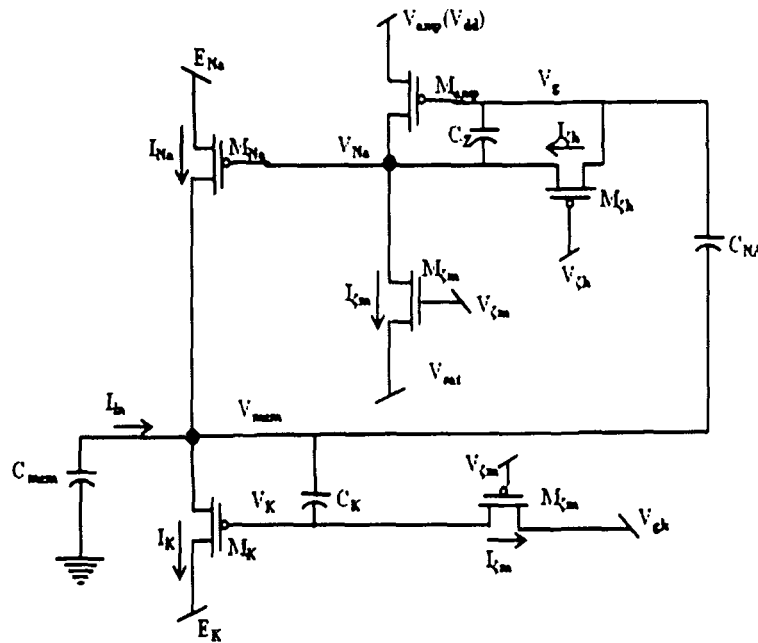


Fig. 3.14: The neuron circuit model using both sodium and potassium channel circuit of E. Farquhar and P. Hasler

The experimentally measured action potential generated by the circuit model developed by E. Farquhar and P. Hasler is shown in Fig. 3.15. The action potential generated is quite similar to the biological one.

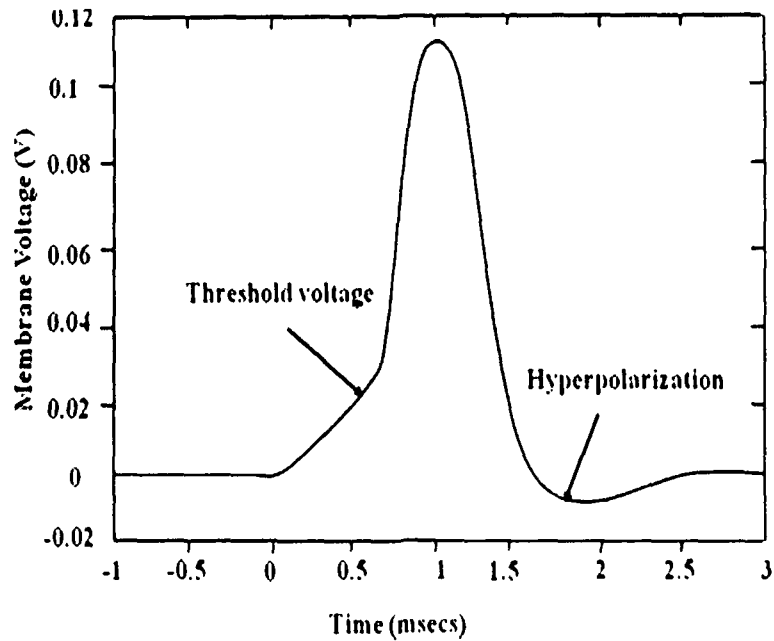


Fig. 3.15: The action potential generated by the neuron circuit model of E. Farquhar and P. Hasler

The physical principles governing ion flow in biological neurons share some interesting similarities to electron flow through channels of a MOS transistor. A simple electrical circuit can be designed which seeks to exploit these similarities to produce an artificial silicon neuron circuit which behaves in a manner similar to a biological neuron. Artificial neurons are designed to process information in a way that directly mimics the processing that is found in biological neurons.

### 3.3 Integrate and Fire (I&F) model:

Integrate and fire (I&F) models are less realistic than conductance-based ones, but require fewer transistors and less silicon real-estate. They allow for the implementation of large, massively parallel networks of neurons in a single VLSI device. I&F neurons integrate pre-synaptic input currents and generate a

voltage pulse analogous to an action potential when the integrated voltage reaches a spiking threshold. Networks of I&F neurons have been shown to exhibit a wide range of useful computational properties, including feature binding, segmentation, pattern recognition, onset detection, and input prediction. Many variants of these circuits were built during the 1950s and 1960s using discrete electronic components.

### 3.3.1 I & F model of Mead:

The first simple VLSI version was probably the Axon-hillock circuit, proposed by Carver Mead and colleagues in the late 1980s (Mead, 1989) [5]. It reduces the complexity of a single component with a single conductance. The Integrate & Fire model of Carver Mead is shown in Fig 3.16.

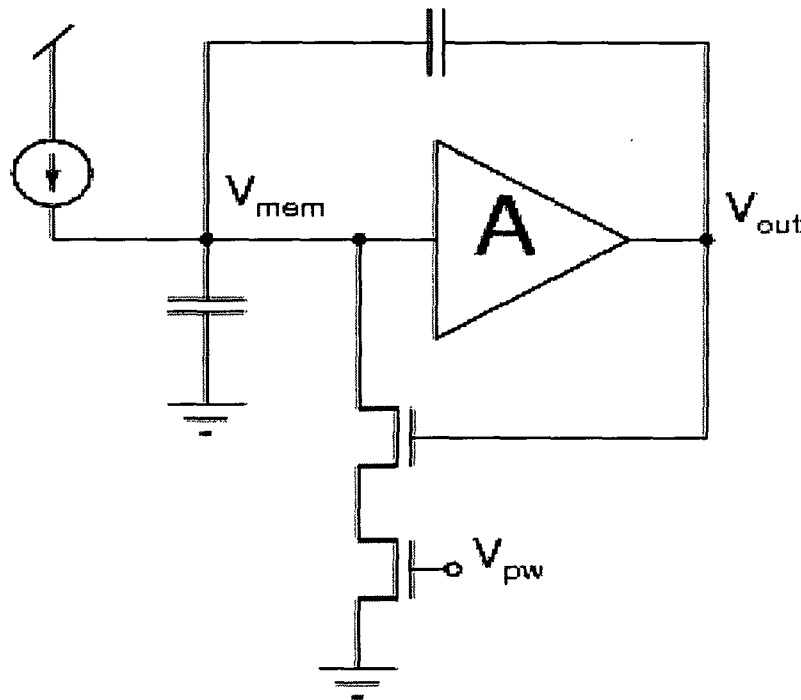


Fig. 3.16: The Axon Hillock Integrate and Fire circuit of C. Mead.

In this model, a capacitor that represents the neuron's membrane capacitance integrates current input to the neuron. When the capacitor potential crosses the spiking threshold a pulse  $V_{out}$  is generated and the membrane potential  $V_{mem}$  is reset. This circuit captures the basic principle of operation of biological neurons, but cannot faithfully reproduce all of the dynamic behaviors observed in real neurons. In addition it has the drawback of dissipating non-negligible amounts of power while the membrane potential  $V_{mem}$  crosses the amplifier's switching threshold [6].

The basic circuit of this model consists of a capacitor  $C$ , parallel with a resistor  $R$ , driven by current  $I$ . The basic Integrate and Fire model of neuron is shown in Fig 3.17.

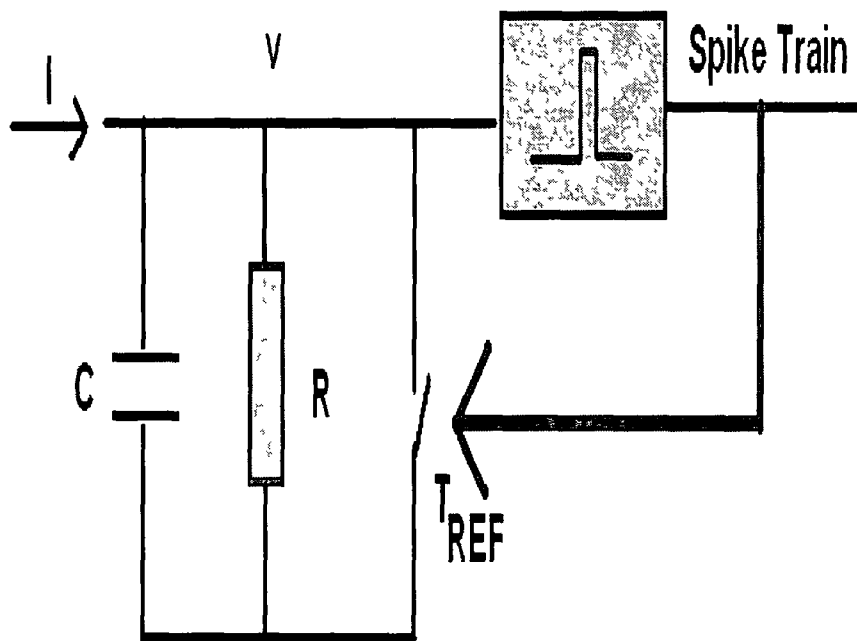


Fig 3 17 Basic Integrate and Fire circuit

The driving current is split in to two components:

$$I = I_R + I_C \quad (3.19)$$

Where  $I_R$  is the resistive current passes through the  $R$ , and  $I_C$  is the capacitive component.

$$\text{Thus, } I = V / R + C (dv / dt) \quad (3.20)$$

Where  $V$  is the membrane potential. A spike will occur when  $V$  reaches a threshold  $V_{TH}$ . After the occurrence of spike next spike cannot occur due to refractory period [7].

### 3.3.2 Leaky integrate and fire model:

The family of leaky integrate-and-fire (LIF) neuron models has a simplified spike generation mechanism while providing an accurate approximation of the membrane potential and other neuron properties like refractory properties and adaptation to stimuli. Simplification of spike generation allows for improved computation speed as compared with conductance based models. This model is a very simple mechanism of spike generation and dendritic integration. Abbott & Kepler (1990) have shown that the more complex H-H model can be reduced to an LIF model in the limit that the membrane loading time is the dominant time scale of the neuronal dynamics [8]-[9]. The model provides a good description of subthreshold integration of synaptic input and injection current that the neuron received. The Leaky Integrate and Fire model of neuron is shown in Fig 3.18.

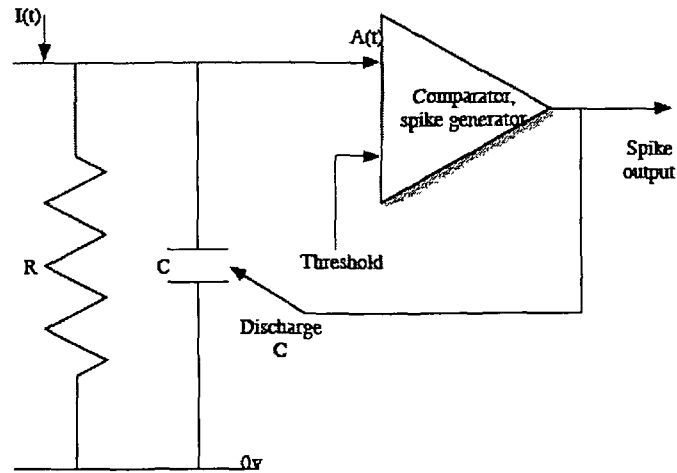


Fig. 3.18: The leaky integrate and fire model

The resistor  $R$  models the overall leakage of the membrane, and the  $C$  models the overall capacitance of the membrane. The time constant  $\tau = RC$ . When a spike occurs the capacitor will be discharged. In this neuron model, the dendrites are modeled as a single point at which the synaptic inputs are summed, while current leaks away linearly. The voltage like state variable at point  $A$  is described by:

$$\frac{dA}{dt} = -\frac{A}{\tau} + I(t) \quad (3.21)$$

Where  $\tau$  is the time constant of the point neuron (i.e. a reciprocal) measure of its leakiness), and  $I(t)$  is the total external input to the neuron. In the presence of positive input, the activity  $A$  can rise to the threshold  $\theta$ . When this is crossed from below, the neuron emits a spike, and  $A$  is reset to some initial value. The mechanism of spike generation is generally ignored in the model, and the output is characterized entirely by the sequence of spike times. This type of neuron is sometimes known as a point neuron, because all the

geometry of the dendrite has been shrunk to a single point. If  $R$  is infinite, then the neuron is not leaky, and it simply integrates its input until this reaches threshold. If  $\tau$  is small, then more recent inputs have a larger effect on  $A$ . If  $I(t)$  is made up of a number of excitatory synaptic inputs, each of which is not large enough to cause  $A$  to exceed  $\theta$ , then the neuron will act as a coincidence detector, firing when a number of its excitatory inputs occur at about the same time, allowing  $A$  to reach  $\theta$  in spite of the leakage.

As integrate and fire model is described by the dynamics of membrane potential  $V(t)$ .

$$C_m \frac{dv}{dt} = - \frac{C_m}{\tau_m} [v(t) - V_0] + I_S(t) + I_{inj}(t) \quad (3.22)$$

Where  $C_m$  is the membrane potential,  $v_0$  is the resting potential,  $\tau_m$  is the passive membrane time constant,  $I_S(t)$  a current describing the effect of synaptic input.  $I_{inj}(t)$  is the current injected in to the neuron. The first term in the right is the current due to the passive leak of the membrane, and the passive membrane time constant is related to the neuron's capacitance and leak resistance  $R_m$  of the membrane potential by  $\tau_m = R_m C_m$ . For subthreshold potentials the respond of the model to periodic deterministic input is

$$v(t) = V_0 + e^{-t/\tau_m} \int_0^t \frac{I_{inj}(t')}{C_m} e^{t'/\tau_m} dt' \quad (3.23)$$

Where it is assumed that the membrane potential at the initial time  $t_0$  is at the resting potential  $v(t_0) = V_0$ . When the membrane potential reaches the threshold  $V_{th}$  a spike is generated and the membrane potential is reset to its initial value  $V_{reset}$ . The main interest in the integrate-and fire neuron model is



stochastic synaptic input. In the case of current synapses, the synaptic current is described by

$$I_S(t) = C_m \sum_{k=1}^{N_E} a_{E,k} S_{E,k}(t) + C_m \sum_{k=1}^{N_I} a_{I,k} S_{I,k}(t) \quad (3.24)$$

As in the case of homogeneous synaptic input, the excitatory and inhibitory synaptic inputs,  $S_{E,k}(t)$  and  $S_{I,k}(t)$ , are described as a series of  $\delta$ -function inputs to each synapse.

$$\left. \begin{aligned} S_{E,k}(t) &= \sum_{t_{E,k}} \delta(t - t_{E,k}), \text{ and} \\ S_{I,k}(t) &= \sum_{t_{I,k}} \delta(t - t_{I,k}) \end{aligned} \right\} \quad (3.25)$$

where  $t_{E,k}$  and  $t_{I,k}$  are the times of the synaptic input spikes for the excitatory and inhibitory synapses, respectively. Thus leaky integrate fire model gives the membrane potential for injected current and details of the synaptic input for current synapses and conductance synapses [10].

Nonlinear integrate-and-fire models have been considered in different regimes. These can roughly be categorized by three criteria; whether they are deterministic or stochastic, whether the applied signal is static or time dependent, and whether this is a sub- or suprathreshold signal, i.e. whether the signal may drive the membrane voltage above the threshold in absence of random noise.

### 3.4 References:

- [1] Hodgkin, A. L. Huxley, A. F. A Quantitative Description Of Membrane Current And Its Application To Conduction And Excitation In Nerve, *Journal of Physiology*, 1952, 117, pp. 500-544.

- 
- [2] Malmivuo, J. Plonsey, R. *Bioelectromagnetism – Principles and Applications of Bioelectric and Biomagnetic Fields*, Oxford University Press, 1995, Chapter 10.
- [3] Roy, G. A simple electronic analog of the squid axon membrane: The NEUROFET, *IEEE Trans. Biomed. Eng.*, 1972, vol. BME-18, pp. 60–63.
- [4] Farquhar, E. Hasler, P. A Bio-physically inspired silicon neuron, *IEEE Transactions on Circuits and systems*, Vol. 52, No. 3, March 2005, pp. 477-488.
- [5] Mead, C. A. *Analog VLSI and Neural Systems*, Addison-Wesley, Reading, MA, 1989.
- [6] Indiveri, Dr. Giacomo. Douglas, Dr. Rodney. Smith, Dr. Leslie S. Silicon Neurons, *from Scholarpedia*. [www.scholarpedia.org/article/Silicon\\_neurons](http://www.scholarpedia.org/article/Silicon_neurons). 1987.
- [7] Gerstner, Kistler, *Spiking Neuron Models. Single Neurons, Populations, Plasticity*. Cambridge University Press, 2002.
- [8] Kepler, Thomas B. Abbott, L. F. *Model Neurons: From Hodgkin-Huxley to Hopfield, Statistical Mechanics of Neural Networks*, Springer-Verlag, Berlin, 1990, pp. 5-18.
- [9] Kepler, Thomas B. Abbott, L. F. Marder, Eve. Reduction of conductance-based neuron models, *Biol. Cybern.*, 66, 381-387 (1992).
- [10] Burkitt, A. N. A Review of the Integrate and Fire Neuron Model: II. Inhomogeneous Synaptic Input & Network Properties, *Biol. Cybern.*, 95: 97-112 (2006).

# **Chapter 4**

## **General Overview of Synapse Modeling**

## General Overview of Synapse Modeling

### 4.1 Introduction:

Modeling and simulation of the electrical activity of neuron including the synapse provides important tools for characterization and prediction of neuronal function. Such model has important applications in the field of neurobioengineering for simulation of receptor function and electrical activity of the postsynaptic cell. In the field of neuromorphology, such model may be used for simulation of agonist-receptor function of postsynaptic cell.

The electrical mechanism of synapse is shown in Fig. 4.1(a). The synaptic equivalent circuit is shown in Fig. 4.1(b), where  $I$  is the total current from ionic channels of all synapses and  $E_1, E_2, \dots, E_M$  represent the chemical potentials of each corresponding ions. For example,  $E_M$  may be  $E_{Na}$  or may be  $E_{Cl}$ . The total current  $I$  help to stimulate the postsynaptic neuron to initiate an action potential [1].

Fig. 4.1(c) shows the equivalent circuit of a synapse which consists of a presynaptic neuron, synaptic cleft and postsynaptic neuron. Here,  $C_M$  represents the capacitance of the lipid bilayer of postsynaptic membrane. The conductance  $g_{Na}$ ,  $g_K$ ,  $g_{Cl}$ , and  $g_o$  represent the membrane permeability of Sodium, Potassium, Chloride and other ions.  $E_{Na}$ ,  $E_{Cl}$ , and  $E_K$  are the chemical potentials of Sodium, Chloride and Potassium.  $E_o$  is the resting potential.

From the Fig. 4.1(b), the total current can be written as

$$I = I_m + I_o - I_{Na} + I_{Cl} + I_K \quad (4.1)$$

If  $V_m$  be the postsynaptic membrane potential established by the ionic and capacitive membrane current then

$$I = C(dV_m / dt) + g_O(V_m - E_O) - g_{Na}(V_m - E_{Na}) + g_{Cl}(V_m - E_{Cl}) + g_K(V_m - E_K) \quad (4.2)$$

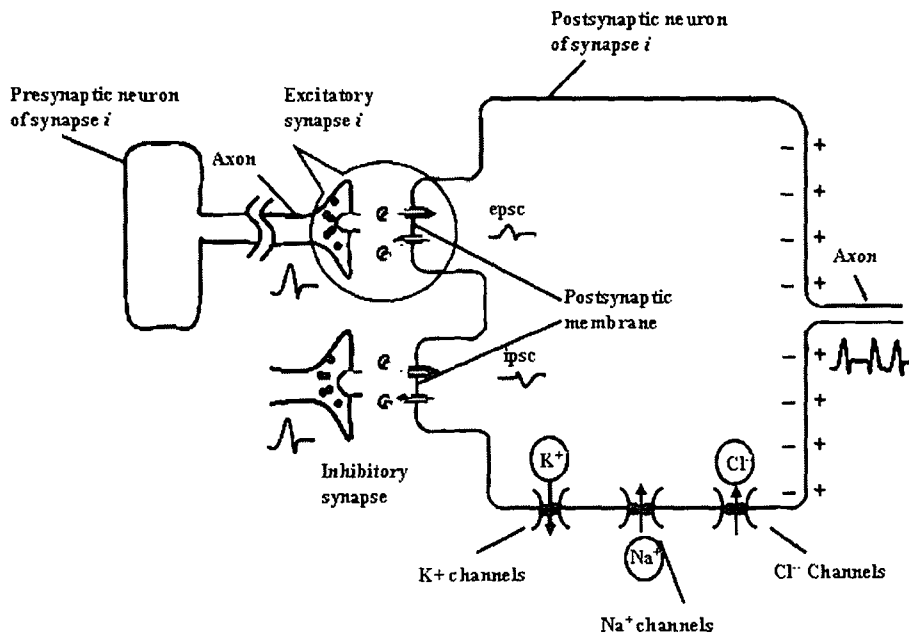


Fig. 4.1(a): Electrical mechanism of synapse

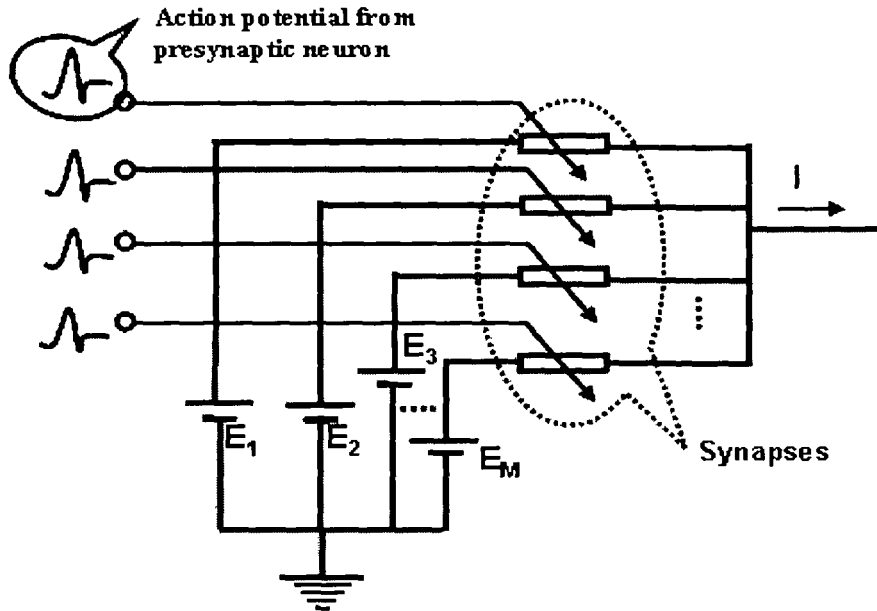


Fig. 4.1(b): Equivalent circuit of a presynaptic neuron

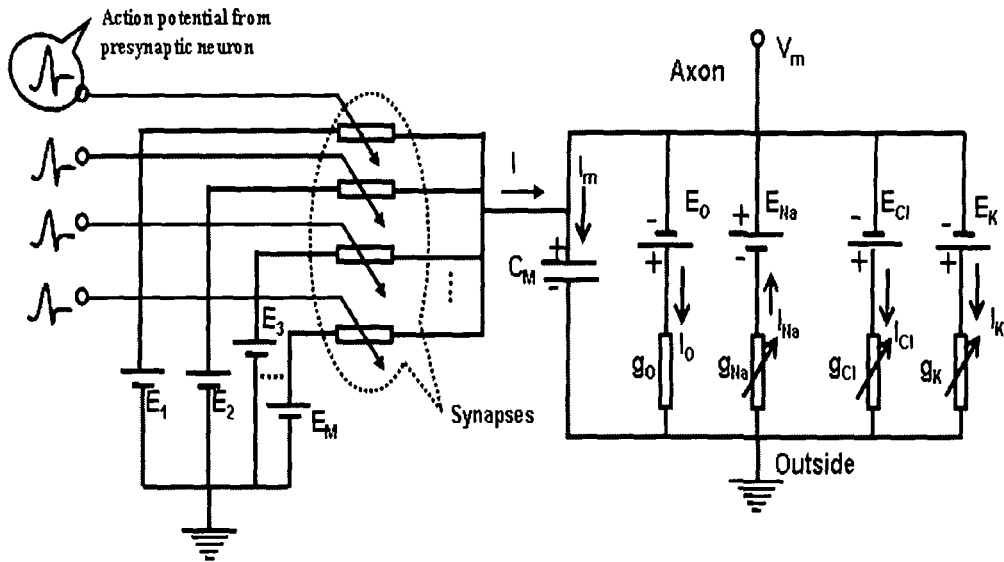


Fig. 4.1(c): Electrical equivalent circuit of synapse

## 4.2 Synaptic Neuron Models:

Modeling and simulation of neuron provides important tools for prediction of function of neurons at excitatory and inhibitory states. Such model has important applications in the field of neurobioengineering for simulation of receptor binding function and electrical activity of the postsynaptic cell. It is stated in literature [2] that FET is the ideal electronic element to simulate the axon membrane conductances. Theory of Metal-oxide Semiconductor Field-Effect Transistor (MOSFET) is therefore essential to understand the synaptic neuron model.

### 4.2.1 Theory of Metal-oxide Semiconductor Field-Effect Transistor (MOSFET):

The basic structure of Metal Oxide Semiconductor Field Effect Transistor (MOSFET) is shown in Fig. 4.2. MOSFET is a Metal Oxide Semiconductor (MOS) capacitor that has been made between two  $n^+$  (i.e., heavily doped  $n$ -type) contact regions in a  $p$ -type semiconductor. The *gate* ( $G$ ) (or MOS capacitor electrode) has a length  $L$  and a width  $Z$ , as shown in Fig. 4.2.

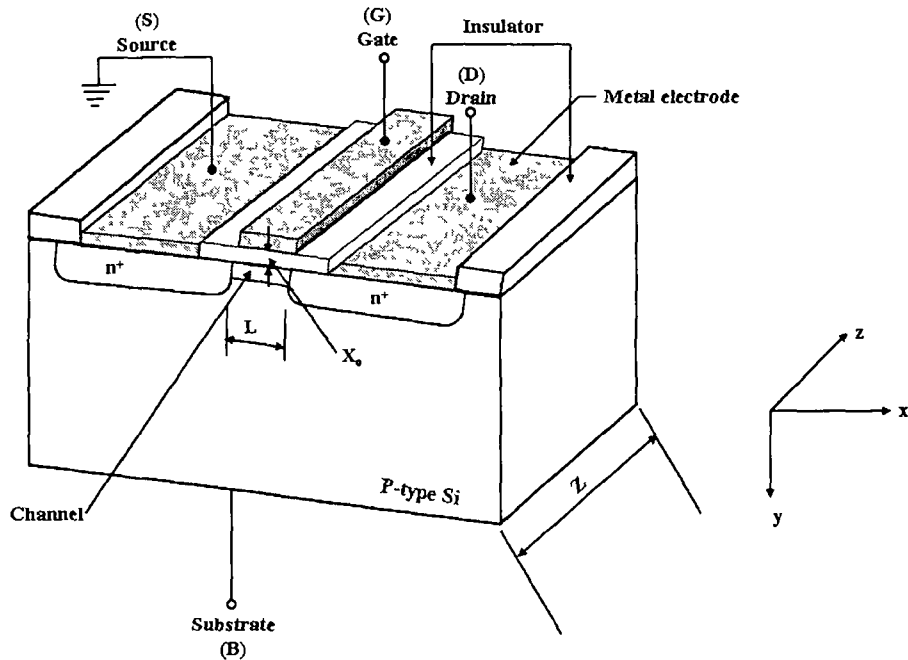


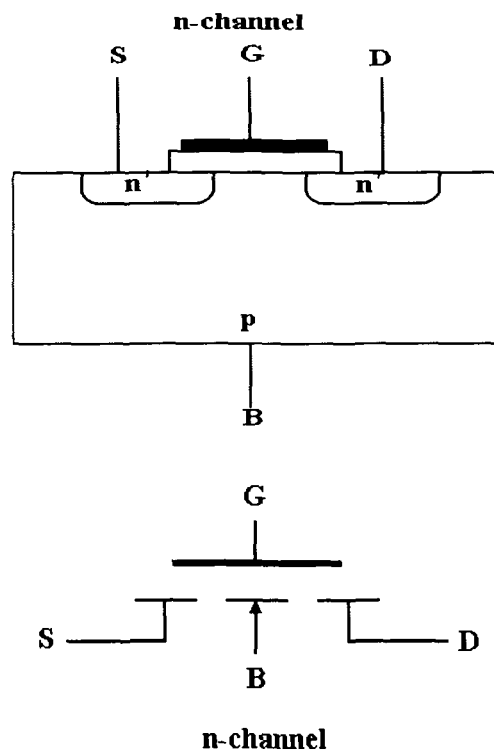
Fig 4.2. Structure of an  $n$ -channel enhancement-mode MOSFET

The  $n^+$  regions are called the *source* ( $S$ ) and *drain* ( $D$ ) regions. Their main function is to establish a low-resistance contact to the two ends of the  $n^+$ -type inversion layer, and a very high resistance contact to the  $p$ -type semiconductor substrate. Indeed the  $n^+$  regions can supply electrons to the inversion layer, as is required there for conduction, but they can not supply holes to the  $p$ -type substrate, so they are a very poor ohmic contact to the substrate. They form  $pn$  junctions with the substrate, with the polarity of bias between the source and drain regions and the substrate being such as to inhibit current flow (actually a leakage current will flow across the  $n^+p$  junction at the drain, but it is very small, so the source and drain are effectively isolated when there is no inversion layer connecting them). In practice, only a negligible current can flow between the two  $n^+$  regions unless a surface inversion layer is formed. This implies that current flows between source and drain only when we apply



a voltage between gate and substrate that is greater than the threshold voltage for the MOS capacitor.

The device shown in Fig. 4.2 is called an *n-channel enhancement-mode* MOSFET: a *p-channel enhancement-mode* MOSFET can be made by using  $p^+$  contact regions in an *n*-type semiconductor substrate. The array of possible MOSFETs is indicated in Fig. 4.3, with the arrow indicating the direction from *p*-type to *n*-type.



\* Fig. 4.3(a)(i) : Enhancement mode MOSFET structure and Circuit symbol (n-channel)

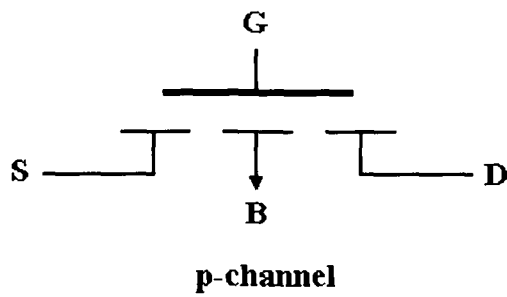
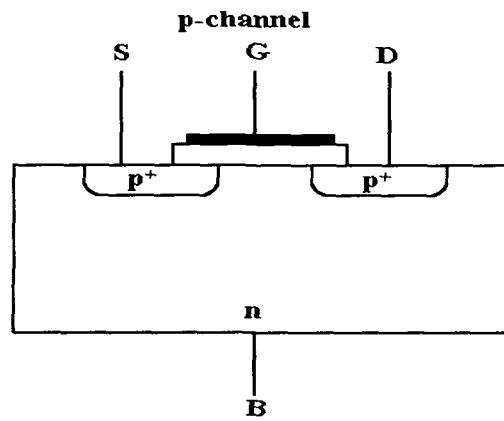


Fig. 4.3(a)(ii) : Enhancement mode MOSFET structure and Circuit symbol (p-channel)

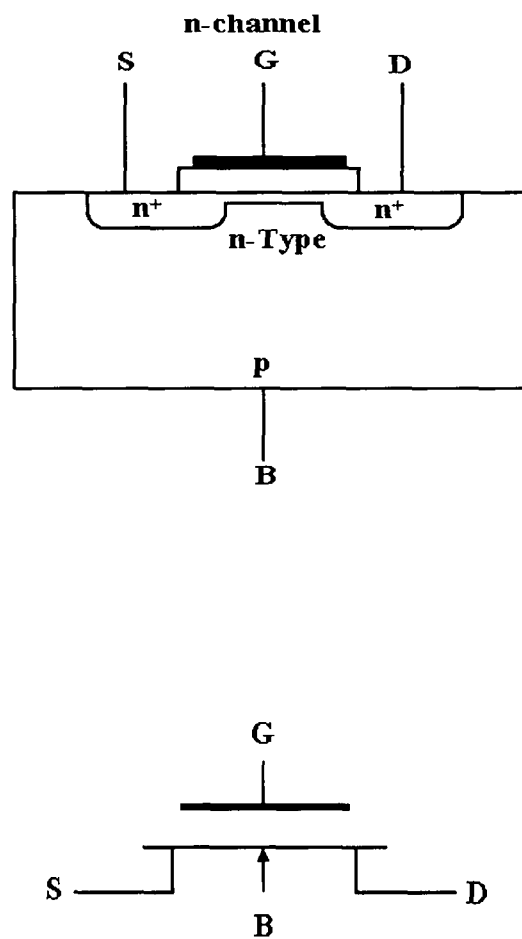


Fig. 4.3(b)(i) : Depletion mode MOSFET structure and Circuit symbol (n-channel)

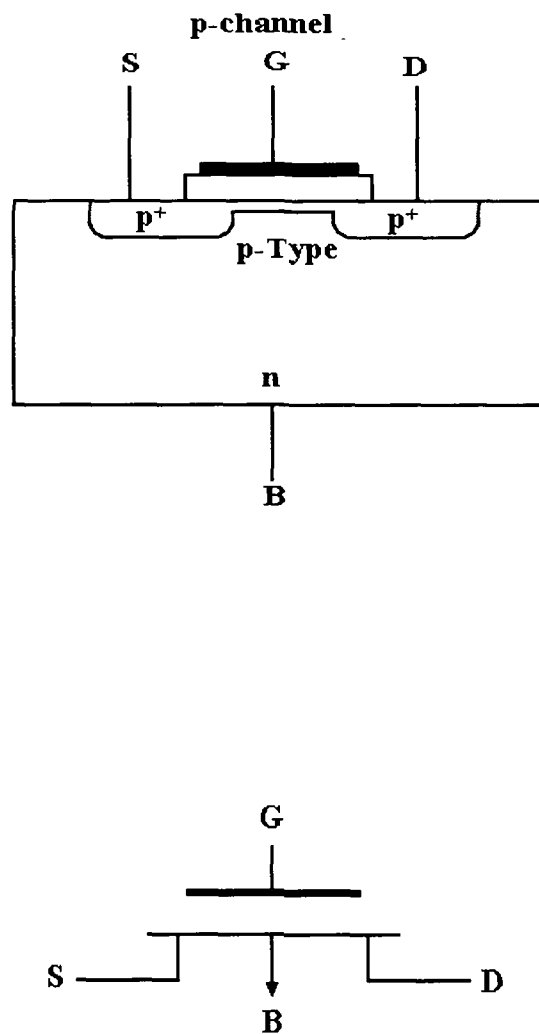


Fig. 4.3(b)(ii) : Depletion mode MOSFET structure and Circuit symbol (p-channel)

The line connecting the source and drain is continuous for depletion mode devices (channel exists for zero gate-source bias) and discontinuous for enhancement-mode devices (channel does not exist for zero gate-source bias). When MOSFETs are used as discrete devices, the substrate contact (labeled  $B$  for *body* in the figure) is usually connected to the source. In integrated circuits that use only one channel type, all of the transistors have a common substrate. Under these circumstances, it is common practice for a significant number of these devices to have their source terminals connected to other circuit components, not to the substrate. This connection results in complicated relationship between the gate-source voltage and drain current. Here it is assumed that, the source and substrate are connected together.

#### **4.2.1.1 Drain Characteristics for the Enhancement-Mode MOSFET:**

The basic electrical characteristics of a MOSFET can be described by a set of curves in which the drain current  $I_{DS}$  is plotted as a function of the drain-source voltage  $V_{DS}$  for given values of the gate-source voltage  $V_{GS}$ . These curves are called the *drain* (or output) *characteristics* of the MOSFET. Other curves, called *input characteristics*, relate the drain current  $I_{DS}$  to the gate-source voltage  $V_{GS}$  for given values of the drain-source voltage  $V_{DS}$ .

Typical output characteristics for an  $n$ -channel enhancement-mode MOSFET are shown in Fig. 4.4(a). Fig. 4.4(b) shows a typical input characteristic of a MOSFET, pointing out the regions of operation.

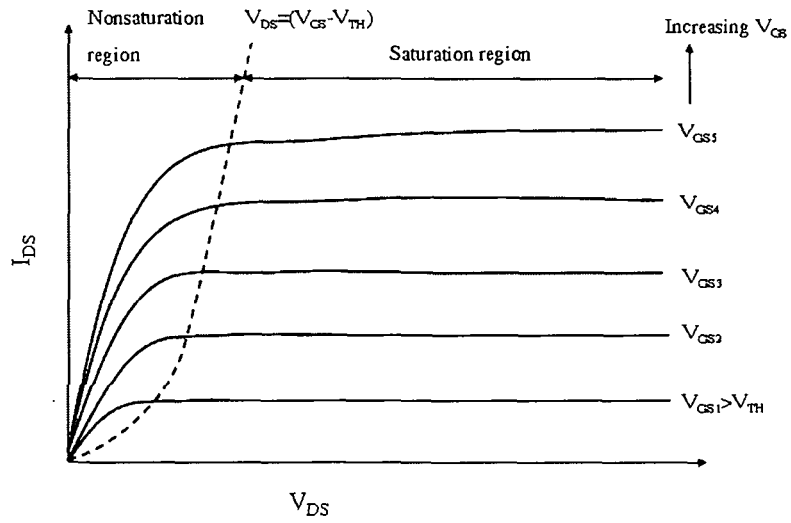


Fig. 4.4(a): Output Characteristics of an  $n$ -channel enhancement mode MOSFET

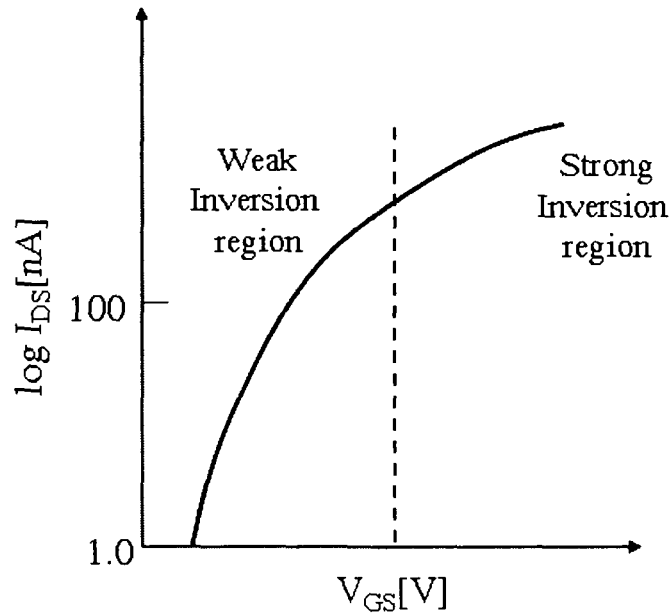


Fig. 4.4(b): Input Characteristics of an  $n$ -channel enhancement mode MOSFET

The drain nonsaturation characteristics are defined by the equation

$$I_{DS} = \beta[(V_{GS} - V_{TH})V_{DS} - \frac{V_{DS}^2}{2}] \quad (4.3)$$

The quantities  $\beta$  and  $V_{TH}$  are device parameters that must be either measured or calculated. The drain characteristics shown in Fig. 4.4(a) indicates that there are two basic regions of operation of the MOSFET, corresponding to very low  $V_{DS} \ll (V_{GS} - V_{TH})$  (*nonsaturation region*) and very high  $V_{DS} \gg (V_{GS} - V_{TH})$  (*saturation region*) values of the drain voltage. The basic characteristics for these two regions can be derived now. The locus of points dividing the saturation region from the nonsaturation region is defined by

$$V_{DS} = (V_{GS} - V_{TH}) \quad (4.4)$$

For digital applications, the MOSFET operates on both sides of the curves specified by equation (4.4). For analog applications, the MOSFET is usually operated in saturation.

Considering Fig. 4.5, a drain voltage  $V_{DS}$  is applied to MOSFET under the condition  $V_{GS} > V_{TH}$ , necessary to ensure that a conducting channel has been formed between the source and drain regions, where  $x$  is the distance coordinate measured along the length of the channel from source to drain.

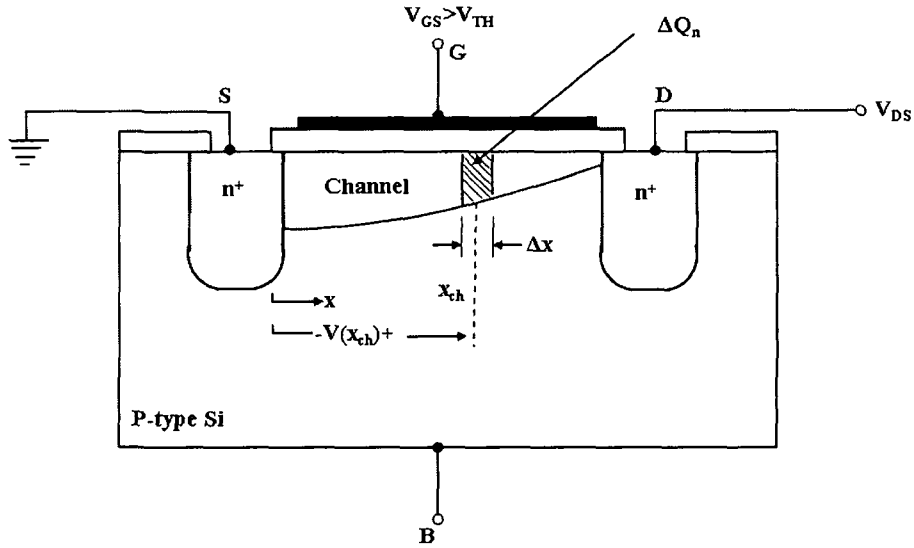


Fig. 4.5: Shape of the channel width of an  $n$ -channel enhancement mode MOSFET, caused by the applications of a large drain-source voltage  $V_{DS}$ .

The application of  $V_{DS}$  will cause a voltage drop along the channel which is indicated by the function  $V(x)$ , and whose value varies from 0 to  $V_{DS}$  as it proceeds from the source to the drain. As indicated, the potential at a point  $x_{ch}$ , as shown in Fig. 4.5, by  $V(x_{ch})$ . The existence of such a potential implies that the voltage between the gate and a small section of channel placed at  $x_{ch}$  is

$$V'_{GS} = V_{GS} - V(x_{ch}) \quad (4.5)$$

The width and charge density at each point in the channel are then determined by  $V'_{GS}$  and will vary along the  $x$  direction as indicated in Fig. 4.5. In particular, the channel will show maximum width at the source end and minimum width at the drain end. The charge in the differential section  $\Delta x$  of channel at  $x_{ch}$  is then given by

$$\Delta Q_n = \Delta C_{ox}(V'_{GS} - V_{TH}) \quad (4.6)$$



$$\text{where } \Delta C_{ox} = \epsilon_{ox} W \frac{\Delta x}{x_o} \quad (4.7)$$

In equation (4.7),  $C_{ox}$  is the capacitance of oxide layer,  $\epsilon_{ox}$  is the dielectric constant of the oxide,  $x_o$  is the oxide thickness, and  $W$  is the width of the device.

The charge  $\Delta Q_n$  can also be written in terms of  $V_{GS}$  and  $V(x_{ch})$  by using equation (4.5) as

$$\Delta Q_n = \Delta C_{ox} [V_{GS} - V(x_{ch}) - V_{TH}] \quad (4.8)$$

To calculate the drain current that flows under these conditions, it is first noticed that the time needed for carriers (electrons) to flow across the section  $\Delta x$  at  $x_{ch}$  is

$$\Delta t = \frac{\Delta x}{v_n} = - \frac{\Delta x}{\mu_n E(x_{ch})} \quad (4.9)$$

Where  $E(x_{ch})$  is the field in the channel at  $x_{ch}$  induced by the application of  $V_{DS}$ . The minus sign in equation (4.9) derives from the definition of the positive direction of  $E(x)$ . Thus, the current flowing through the section  $\Delta x$  can be written as

$$I_{DS} = \frac{\Delta Q_n}{\Delta t} \quad (4.10)$$

By using equation (4.8), we can rewrite equation (4.10) in the form

$$I_{DS} = \frac{\Delta C_{ox} [V_{GS} - V(x_{ch}) - V_{TH}]}{\Delta t} \quad (4.11)$$

Using equation (4.7), we write equation (4.11) as

$$I_{DS} = -\frac{\mu_n \epsilon_{ox} W}{x_0} [V_{GS} - V(x_{ch}) - V_{TH}] E(x_{ch}) \quad (4.12)$$

$$\text{Since } E(x_{ch}) = -\left. \frac{dV(x)}{dx} \right|_{x=x_{ch}} \quad (4.13)$$

we obtain

$$I_{DS} dx = \frac{\mu_n \epsilon_{ox} W}{x_0} [V_{GS} - V(x_{ch}) - V_{TH}] dV(x) \quad (4.14)$$

Equation (4.14) represents the current  $I_{DS}$  flowing through a section of width  $\Delta x$  centered at  $x$ . The channel, in its turn, is formed of a large number of such sections, all of which are connected in series, going from the source to the drain. Moreover, the same current  $I_{DS}$  must flow through each section for a given  $V_{DS}$ . Therefore, the equation (4.14) can be integrated as follows:

$$I_{DS} \int_0^L dx = \frac{\mu_n \epsilon_{ox} W}{x_0} \int_0^{V_{DS}} [(V_{GS} - V_{TH}) - V] dV \quad (4.15)$$

Carrying out the integration and dividing by the channel length  $L$ , the  $I_{DS}$  current can be obtained as-

$$\begin{aligned} I_{DS} &= \frac{\mu_n \epsilon_{ox} W}{x_0 L} [(V_{GS} - V_{TH}) V_{DS} - \frac{V_{DS}^2}{2}] \\ &= \beta [(V_{GS} - V_{TH}) V_{DS} - \frac{V_{DS}^2}{2}] \end{aligned} \quad (4.16)$$

This is exactly equation (4.3), when  $\beta$  value is set as-

$$\beta = \mu_n C_{ox} \frac{W}{L} \quad (4.17)$$

Where  $C_{ox}$  is the capacitance of the gate oxide per unit area.

In equation (4.17),  $\mu_n$  is constant up to sufficiently large values of  $V_{GS}$  and  $\beta$  begins to decrease when  $V_{GS}$  becomes large enough. Equation (4.17) states that, for a given type of channel (given  $\mu$ ), the parameter  $\beta$  can be determined directly once the gate width  $W$ , the gate length  $L$ , and oxide properties ( $X_o$  and  $\epsilon_{ox}$ ) are known.

At low drain voltages, i.e., for  $V_{DS} \ll (V_{GS} - V_{TH})$ , the quadratic term in  $V_{DS}$  in equation (4.16) can be neglected. Thus, under this assumption, we can write

$$I_{DS} = \beta(V_{GS} - V_{TH})V_{DS} \quad (4.18)$$

Equation (4.18) states that the low drain voltage characteristics are a series of straight lines passing through the origin, with slopes that increase as  $V_{GS}$  increases. In general, each of these characteristics can be described by the equation

$$I_{DS} = G_{DS}V_{DS} \quad (4.19)$$

where  $G_{DS}$  is called the *drain-source conductance* of the MOSFET. From equation (4.18) and (4.19), we have

$$G_{DS} = \beta(V_{GS} - V_{TH}) \quad (4.20)$$

The variation in channel width with  $V_{DS}$  has given the physical key to obtaining the basic MOSFET equation (equation (4.16)). However, this derivation is valid only as long as  $V_{DS} \ll (V_{GS} - V_{TH})$ , i.e., when the MOSFET is operated in the so-called nonsaturation region, because when  $V_{DS} = (V_{GS} - V_{TH})$  the channel will (in principle) be reduced to zero width at the drain end. The physical situation is shown in Fig. 4.6(a): the channel is said to be *pinched off*

at the drain. The drain current that flows under this condition can be calculated from equation (4.16) by substituting  $V_{DS}=(V_{GS}-V_{TH})$ . The result is

$$I_{DS} = \frac{\beta}{2}(V_{GS} - V_{TH})^2 \quad (4.21)$$

By differentiating equation (4.16), it is found that the drain current has a horizontal tangent at  $V_{DS}=(V_{GS}-V_{TH})$ , as indicated in the drain characteristics of Fig. 4.4(a).

For the current given by equation (4.21) to flow, it is necessary that some very high velocity electrons exist in a thin region near the drain. Then, the channel is in practice not pinched down to exactly zero width, but rather to a point where there are just enough electrons to carry the drain current when each electron is traveling at its maximum velocity.

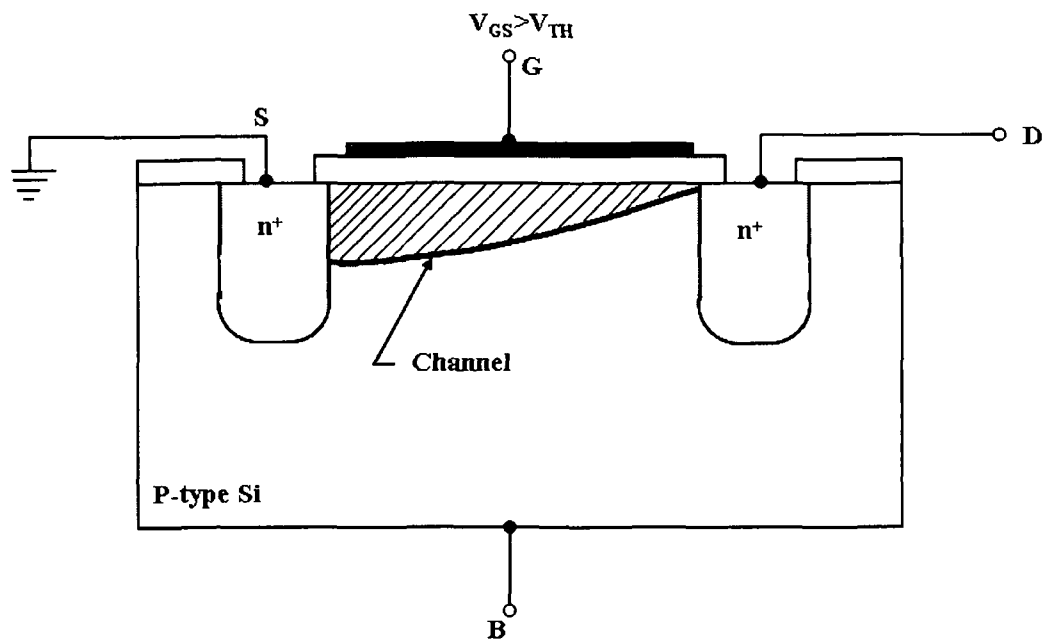


Fig. 4.6(a): Shape of the channel width of an *n*-channel enhancement mode MOSFET for  $V_{DS}=(V_{GS}-V_{TH})$

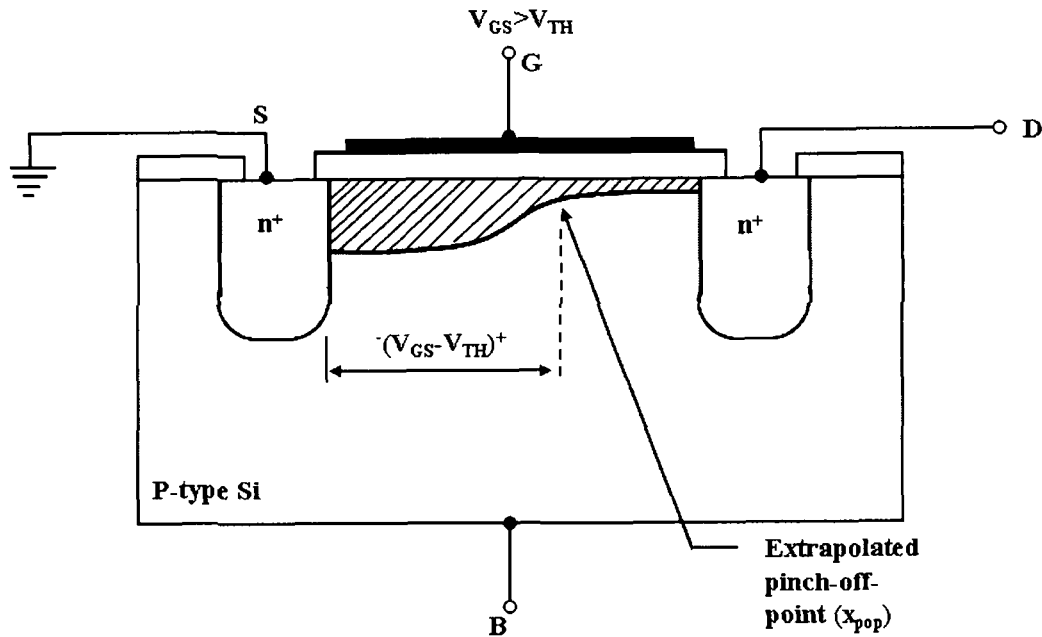


Fig. 4.6(b): Shape of the channel width of an  $n$ -channel enhancement mode MOSFET for  $V_{DS} > (V_{GS} - V_{TH})$

The presence of thin pinched-off region is more evident when  $V_{DS}$  is increased beyond  $(V_{GS} - V_{TH})$ . When this happens, the actual channel pinch-off point, indicated by  $x_{pop}$  in Fig. 4.6(b), will shift very slightly from drain toward the source. The voltage drop from source to the pinch-off point,  $V(x_{pop})$ , will be exactly  $(V_{GS} - V_{TH})$ , since this is the value needed to reduce the channel charge and width to zero. The remainder of the applied drain voltage,  $[V_{DS} - (V_{GS} - V_{TH})]$ , is dropped across the region from the extrapolated pinch-off point ( $x_{pop}$ ) to the drain, and the charge in this region can be neglected.

Thus, it follows that the non-pinched-off portion of the channel behaves like a MOSFET that has a gate length  $L = x_{pop}$  and is always operated at  $V'_{DS} = (V_{GS} - V_{TH})$ . The total charge in the non-pinched-off portion of the channel and the voltage drop across it are practically fixed at the values they have when  $V_{DS} = (V_{GS} - V_{TH})$ , so to a first approximation the current  $I_{DS}$  flowing in the channel will be independent of  $V_{DS}$  for all values of  $V_{DS} > (V_{GS} - V_{TH})$ . In other words, the drain current  $I_{DS}$  saturates at its pinch-off value. As a consequence we can extend the drain current characteristics horizontally from the pinch-off point to larger values of  $V_{DS}$  (see Fig. 4.4(a)). Thus, at large drain voltages, i.e., for  $V_{DS} \gg (V_{GS} - V_{TH})$ , the drain current  $I_{DS}$  in this region is given by equation (4.21).

The MOSFET is said to be operated in the *saturation mode*. From a circuit point of view, the fact that  $I_{DS}$  can be independent of  $V_{DS}$  implies that the output current  $I_{DS}$  is controlled entirely by the input voltage  $V_{GS}$ . Moreover, the output terminals of the MOSFET are therefore represented as a  $V_{GS}$ -controlled current source instead of a conductance as in the nonsaturated operation mode.

The physical phenomena just described and the corresponding electrical behavior of the MOSFET are summarized in Table 4.1.

In the preceding analysis, the channel length  $L$  can be considered as constant. In reality,  $L$  is determined by the distance between the depletion regions surrounding the source and drain. The widths of these regions are functions of the source-substrate and drain-substrate biases. The width of the drain depletion region increases with drain voltage, thereby decreasing the channel length, which increases the gradient of carrier concentration, and therefore

increases the channel current. This increase in channel current due to *channel length modulation* is called the *Early effect*. Because the dependence of  $I_{DS}$  on  $L$  is explicit (through the parameter  $\beta$ ) in equations (4.16) and (4.21), we can solve directly for the drain conductance  $G_{DS}$  of the MOSFET.

Table 4.1 Basic properties of an  $n$ -Channel Enhancement-Mode MOSFET

Gate & drain bias conditions	Channel conditions	Drain Characteristics
$V_{GS} \leq V_{TH}$ and $V_{DS} \geq 0$	No inversion layer $Q_n = 0$	$I_{DS} = 0$
$V_{GS} > V_{TH}$ and $0 < V_{DS} \ll (V_{GS} - V_{TH})$	Inversion layer exists $Q_n = C_{ox}(V_{GS} - V_{TH})$	$I_{DS} = \beta (V_{GS} - V_{TH}) V_{DS}$ Voltage controlled conductance
$V_{GS} > V_{TH}$ and $0 < V_{DS} \leq (V_{GS} - V_{TH})$	Inversion layer exists Decreasing channel thickness near drain	$I_{DS} = \beta \left[ (V_{GS} - V_{TH}) V_{DS} - \frac{V_{DS}^2}{2} \right]$
$V_{GS} > V_{TH}$ and $V_{DS} \geq (V_{GS} - V_{TH})$	Inversion layer exists pinch-off near drain	$I_{DS} = \frac{\beta}{2} (V_{GS} - V_{TH})^2$ Voltage controlled current source

Because the drain current is inversely proportional to  $L$ , the drain conductance (which manifest itself as a nonzero slope on the drain characteristics for large values of  $V_{DS}$ ) is proportional to  $I_{DS}$  and inversely proportional to  $L$ . Usually, this conductance is approximated by a constant depending on the given

process and device geometry. Because the conductance is proportional to  $I_{DS}$ , in this approximation the extrapolated drain curves all intersect the voltage axis at a single point, which is  $V_{DS} = -V_0$ . Thus, to take into account the channel-length modulation, the term  $G_{DS} V_{DS}$  can be simply added to the expressions of the drain current just obtained [3].

### **4.2.2 Neuron Model for Excitation and Inhibition of Postsynaptic Membrane of Levine, Marvin et al:**

The postsynaptic membrane of a single neuron can have excitatory and inhibitory transmitter-gated ion channels. Generally, excitatory channels are specific to sodium ions and inhibitory channels are specific to chloride ions. The excitatory and inhibitory ionic current control the change in membrane potential. The influx of sodium ions causes an excitatory postsynaptic membrane potential (EPSP), whereas the influx of chloride ions causes an inhibitory postsynaptic membrane potential (IPSP). When excitation predominates, the membrane potential increases. If a sufficient number of transmitter gated sodium channels are open, then the membrane potential exceeds the threshold for initiating an action potential. When inhibition predominates, the membrane potential decreases (or hyperpolarizes), and triggering of an action potential is impeded.

In the excitatory and inhibitory postsynaptic circuit model of Levine, Marvin et al, the variable conductance of the transmitter-gated ion channels is represented by MOSFET. The MOSFET is chosen because as described in MOSFET theory that it functions as a voltage controlled conductance in the linear region (equation (4.20)). For analysis, rewriting the equation (4.20):



$$G_{DS} = \beta(V_{GS} - V_{TH}) \quad (4.22)$$

Where,  $\beta = \mu_n C_{ox} \frac{W}{L}$  (from equation (4.17)). And  $G_{DS}$  is the conductance of the MOSFET,  $V_{GS}$  is the gate voltage,  $V_{TH}$  is the threshold voltage,  $C_{ox}$  is the capacitance of the gate oxide,  $\mu$  is the electron mobility constant,  $W$  is channel width, and  $L$  is the channel length.

The excitatory and inhibitory postsynaptic circuit model of Levine, Marvin et al is shown in Fig 4.7.

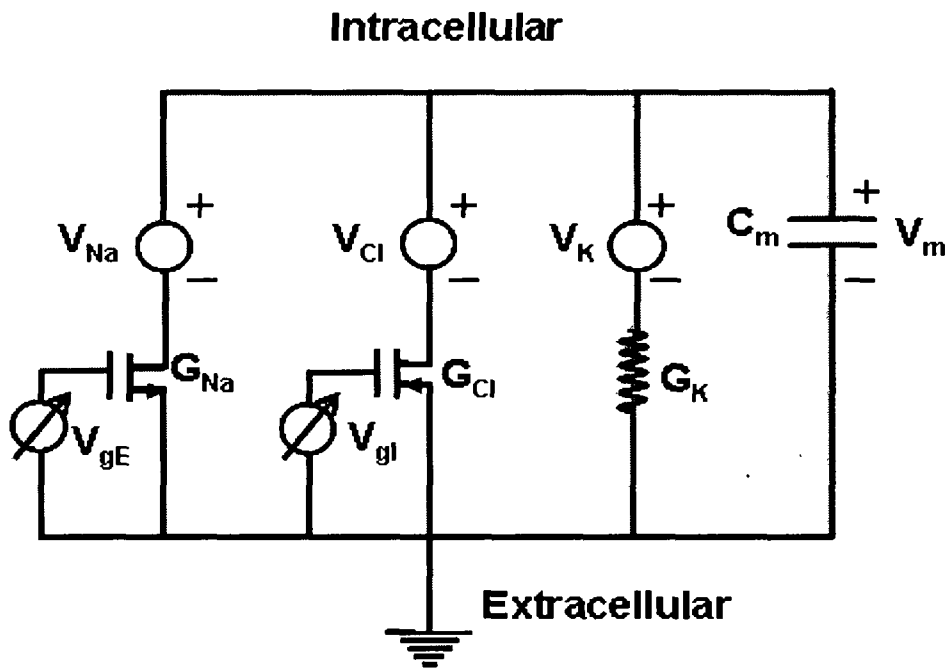


Fig. 4.7: Excitatory and inhibitory postsynaptic circuit model of Levine, Marvin et al

In this model, an NMOSFET represents the conductance of the transmitter-gated sodium channels and a PMOSFET represents the conductance of the

transmitter-gated chloride channels.  $C_m$  represents the capacitance of the lipid bilayer;  $V_{Na}$ ,  $V_{Cl}$  and  $V_K$  are the Nernstian membrane potentials for sodium, chloride and potassium;  $G_K$  is the conductance of non-gated potassium channels;  $G_{Na}$  is the conductance of transmitter-gated sodium channels; and  $G_{Cl}$  is the conductance of the transmitter-gated chloride channels.  $V_{gE}$  and  $V_{gI}$  are the gate input voltages applied to elicit MOSFET conductances  $G_{Na}$  and  $G_K$  respectively.

The postsynaptic membrane potential  $V_m$  is controlled by the conductance of the transmitter-gated ion channels. From Fig. 4.7, the  $V_m$  is established by the ionic and capacitive membrane current, given by the following equation:

$$C \left( \frac{dV_m}{dt} \right) + (V_m - V_{Na}) G_{Na} + (V_m - V_{Cl}) G_{Cl} + (V_m - V_K) G_K = 0 \quad (4.23)$$

In SPICE simulation, the membrane potential  $V_m$  is obtained as a function of the relative weighting of the ionic conductances.

The conductance of the transmitter-gated channels is controlled by transmitter-receptor binding activity. The MOSFET conductance  $G_{DS}$  is controlled by the gate voltage. In the excitatory and inhibitory postsynaptic circuit model of Levine, Marvin et al, the MOSFET gate voltage functionally represents the transmitter-receptor binding activity. The simulation input voltage applied to the MOSFET gate is expressed as:

$$V_g(t) = V_o[(1 - \exp(-k_1 t)) + \exp(-k_2 t) u(t - t_m)] \quad (4.24)$$

Where  $u(t - t_m)$  is the Heaviside function, and  $V_o$  is a voltage proportional to the maximum attainable conductance, when all the transmitter-gated channels for

a specific ion are open. The component values assigned in this model, for SPICE simulation, are based on the physical parameters of biologic neurons.

Fig 4.8 shows the simulated result of the excitatory and inhibitory postsynaptic circuit model of Levine, Marvin et al.

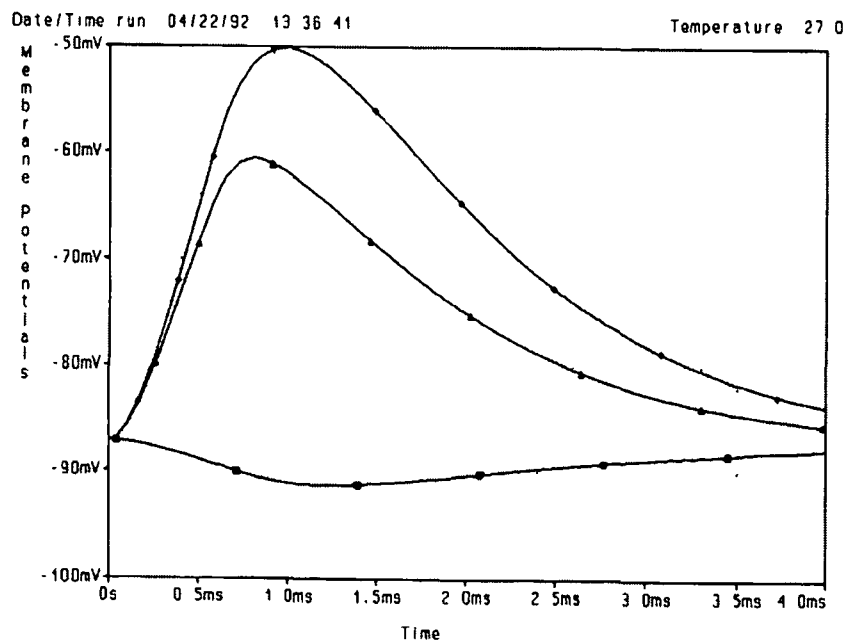


Fig 4.8 Simulated result of the excitatory and inhibitory postsynaptic circuit model of Levine, Marvin et al

The top waveform represents the EPSP, the bottom waveform the IPSP and middle waveform the potential arising from combined excitation and inhibition. The postsynaptic membrane potential  $V_m$  is established by spatial summation and temporal integration of the membrane current. The simulation output for the excitatory case illustrates an EPSP with sufficient amplitude for triggering an action potential. The output in the inhibitory case shows an EPSP that would suppress the triggering of an action potential. The output from

combined excitation and inhibition demonstrates the formation of a membrane potential based on the relative weighting of the sodium and chloride conductances.

The excitatory and inhibitory postsynaptic circuit model of Levine, Marvin et al, is a physiologically motivated model which provides a practical method for simulating the structure and function of the postsynaptic membrane. The simulation result shows the effects of excitation and inhibition on a single neuron. This model demonstrates the basic mechanism of integrative decision-making that occurs at the postsynaptic region of the neuron [4].

### **4.2.3 Synaptic Neuron Model of Levine, Marvin et al:**

Michael D. Levine, Marvin F. Eisenberg, and Thomas L. Fare proposed a model of postsynaptic membrane at neuromuscular junction. This neuromuscular junction occurs biochemically between presynaptic membrane and postsynaptic membrane. In this circuit model of postsynaptic membrane, excitatory transmitter gated ion channels are simulated with a metal-oxide semiconductor field effect transistor (MOSFET). MOSFET is considered here because it functions as a voltage controlled resistor. Due to binding of neurotransmitter with the receptor of postsynaptic membrane, there will be influx of Sodium to the cell. If sufficient number of Sodium channels opens then membrane potential exceeds the threshold and generates an action potential.

The postsynaptic membrane basically consists of transmembrane protein ion channels and lipid bilayer. Fig. 4.9 shows the circuit model for membrane. Simulation of the model yields an output representing the overall membrane potential of the postsynaptic region [5].

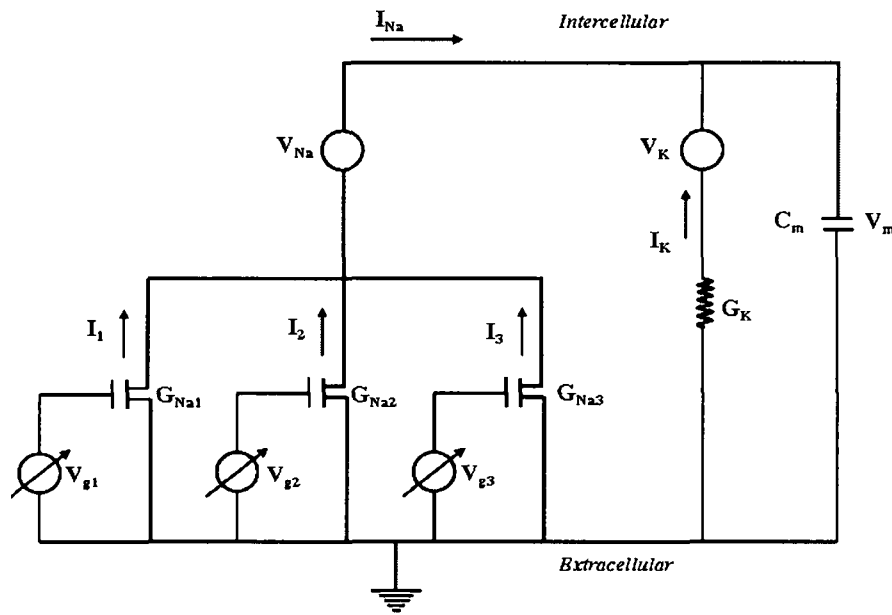


Fig. 4.9: Circuit model of Levine, Eisenberg, and Fare for the membrane of the postsynaptic region.

In this model  $C_m$  represents the capacitance of lipid bilayer.  $V_{Na}$  and  $V_k$  represent the Nernstian membrane potential for sodium and potassium.  $G_k$  represents the conductance of non-gated potassium channel.  $G_{Na1}$ ,  $G_{Na2}$ ,  $G_{Na3}$  represent conductance of acetylcholine-gated sodium channels.  $V_{g1}$ ,  $V_{g2}$  and  $V_{g3}$  are the MOSFET gate voltages used for obtaining transmitter gated sodium conductances

The membrane is divided into three patches to demonstrate the sodium current.

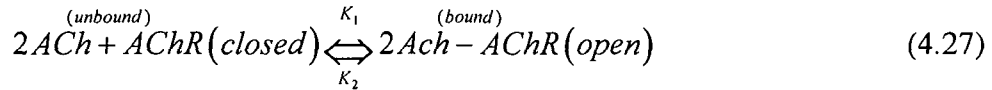
$$I_{Na} = I_1 + I_2 + I_3 \quad (4.25)$$

Due to spatial summation of sodium current through the open acetylcholine gated channels, the membrane potential  $V_m$  will be increased.

$$C_m (dV_m / dt) + (V_m - V_{Na}) G_{Na} + (V_m - V_k) G_k = 0 \quad (4.26)$$

Where  $G_{Na}$  is the total sodium conductance and  $G_k$  is the total potassium conductance of the postsynaptic membrane. Levine et al. [5] got the membrane potential  $V_m$  by spatial and temporal varying acetylcholine-gated sodium conductance  $G_{Na}$  and simulation is done using Personal Computer Simulation Program with Integrated Circuit Emphasis (SPICE) software.

The conductance of the acetylcholine-gated sodium channels in a patch of membrane is controlled by activity of transmitter-receptor binding [6]. Analogous to this is the MOSFET conductance  $G_{DS}$  which is controlled by the gate voltage of the MOSFET. In the Levine et al. model of the postsynaptic membrane, the MOSFET gate voltage functionally represents the transmitter-receptor binding activity. For the simplest case, binding is governed by the chemical reaction:



Where  $K_1$  and  $K_2$  are the rate constant for the forward reaction and the reverse reaction respectively. These rate constants are analogous to the time constants utilized by the exponential voltage function in SPICE. The simulation input voltage applied to the MOSFET gate is expressed as

$$V_g(t) = V_o [1 - \exp(-k_1 t)] + \exp(-k_2 t) u(t - t_m) \quad (4.28)$$

Where  $u(t - t_m)$  is the Heaviside function, and  $V_o$  is a voltage proportional to the maximum attainable conductance of the membrane patch when all the acetylcholine-gated sodium channels are open.

The Heaviside function is generally used in the mathematics of control theory and signal processing to represent a signal that switches on at a specified time and stays switched on indefinitely. It is also used in structural mechanics together with the Dirac delta function to describe different types of structural loads. It was named after the English polymath Oliver Heaviside [7].

Fig 4.10 shows the simulated postsynaptic membrane potential of Levine et al. model of the postsynaptic membrane.

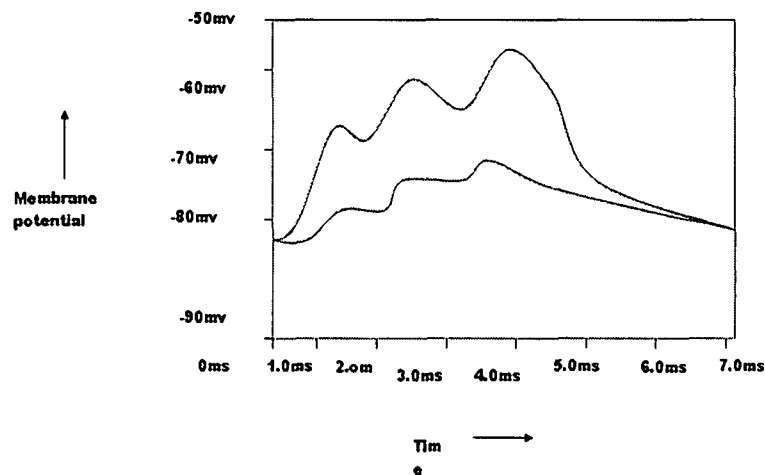


Fig 4 10 Simulated Postsynaptic Membrane Potential of Model of Levine, Eisenberg, and Fare

The top waveform represents the normal postsynaptic membrane potential and the bottom waveform represents the pathologic state postsynaptic membrane potential. The  $V_m$  is established by spatial summation and temporal integration of the acetylcholine-gated sodium current. When  $V_m$  exceeds a threshold value, in the -60 to -40 millivolt range, as shown in the simulation of the normal case, the voltage-gated sodium channels open causing initiation of an action potential. The simulation output in the case of

myasthenia gravis illustrates the degraded membrane potential secondary to the pathologic function of the acetylcholine-gated channels. This model is generally applicable in the field of neuropharmacology for simulation of receptor function and electrical activity of the postsynaptic cell.

### 4.3 References:

- [1] Zhang, X. A Mathematical Model of a Neuron with Synapses based on Physiology, *Nature Proceedings, npre*, 1703.1, (2008)
- [2] Guy, R. A simple Electronic Analog of the Squid Axon Membrane: The NEUROFET, *IEEE Transaction on Biomedical Engineering*, Vol. BME-19, Issue: 1, 60-63, 1972.
- [3] Grattarola, M. Massobrio, G. *Bioelectronics Handbook: MOSFETs, Biosensors, and Neurons*, McGraw Hill, 1998.
- [4] Levin, M. D. Eisenberg, M. F. et al. A Physiologic-Based Circuit Model of Excitation and Inhibition in the Postsynaptic Neuron, *IEEE Conference on Circuits and Systems*, pp. 268 - 269 vol.1. ISBN: 0-7803-0510-8, (1992)
- [5] Levin, M. D. Eisenberg, M. F. et al. A Physiologic-based Circuit Model of the Postsynaptic Region at Neuromuscular Junction, *IEEE Conference on Circuits and Systems*, pp. 1602 - 1603 vol.4. ISBN: 0-7803-0785-2, (1992)
- [6] Kandel, Schwartz, E. J. Jessell, T. *Principles of Neural Science*, McGraw-Hill, 3rd Ed., pp. 235-243. 1991.
- [7] [http://en.wikipedia.org/wiki/Heaviside\\_step\\_function](http://en.wikipedia.org/wiki/Heaviside_step_function)



# **Chapter 5**

## **Study on the Development of Neuron Models: Integrate-and-Fire Based Models**

## **Study on the Development of Neuron Models: Integrate-and-Fire Based Models**

In this chapter a study on the development of two neuron models based on Integrate-and-Fire based concept has been carried out. The description of two models and their simulation results have been presented and compared with the results obtained by the previous researchers.

### **5.1 Introduction:**

Each silicon neuron in the artificial network system has one or more inputs and produces an output; each input having a weighting factor, which modifies the value entering the neuron. The neuron mathematically compares the integrated inputs with a threshold limit, and if the integrated input value is greater than the threshold limit then output the result or more precisely an action potential is generated.

The basic circuit that can be used to simulate the action of a neuron both for resting and excitation is shown in Fig. 5.1. The resistor associated with each input (with conductances  $W_1, W_2, W_3$ ) simulates the synaptic weights and ' $V_{th}$ ' is equivalent to the neuron threshold potential. Threshold potential will decide whether neuron will fire or not. The synaptic weights are less flexible, they have positive values only [1].

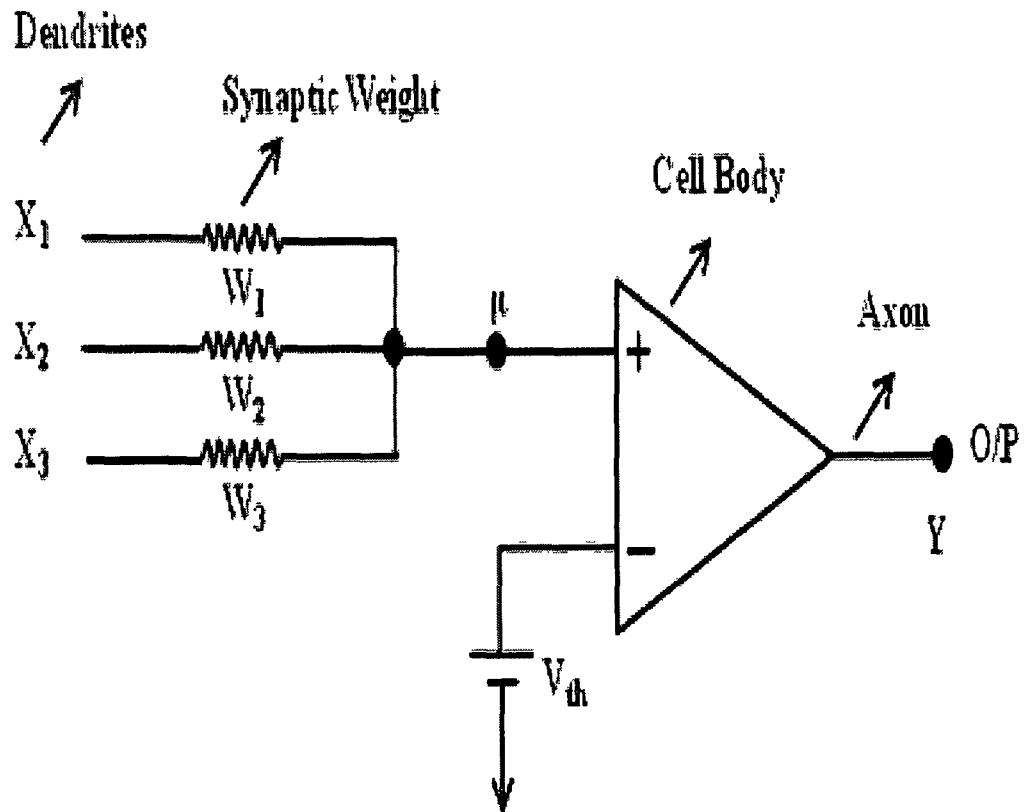


Fig 5.1 Basic Silicon Neuron model

The net input to the amplifier can be determined by using the following equation.

$$W_1(X_1 - \mu) + (X_2 - \mu)W_2 + (X_3 - \mu)W_3 = \left(\frac{1}{R_{eqv}}\right) \cdot \mu \quad (5.1)$$

Where,  $X_1, X_2, X_3$  are input voltages, and ' $\mu$ ' is the input to the amplifier.  $W_1, W_2, W_3$  are the conductance values representing the weight of each input, and ' $R_{eqv}$ ' is the input resistance of the amplifier. Assuming ' $R_{eqv}$ ' to be very large, the expression of input to the amplifier can be written as–

$$\mu = \frac{\sum_{i=1}^n (X_i W_i)}{\sum_{i=1}^n (W_i)} \quad (5.2)$$

The output voltage ' $Y$ ' is then given by –

$$Y = A [\mu - V_{th}] \quad (5.3)$$

Where,  $A$  = amplifier gain and ' $V_{th}$ ' is the amplifier threshold voltage.

Based on this basic principle, two analog circuits have been developed and studied to simulate the behaviour of biological neurons.

## 5.2 Integrate-and-Fire Based Model 1:

The circuit diagram of the model when the neuron is stimulated/excited is shown in Fig. 5.2. In this circuit there are three input signals. The neuron integrates the inputs and compares it with a threshold value, which will define whether the neuron will fire or not. And if integrated input is above the threshold limit, then it fires i.e. generation of action potential. In case of biological neuron the threshold limit is generally 5 – 15mV less negative than the resting potential. Here, the threshold limit is considered as 60mV. The threshold limit is given by the threshold stimulus. The Table 5.1 summarizes the different components used in silicon neuron of Fig. 5.2.

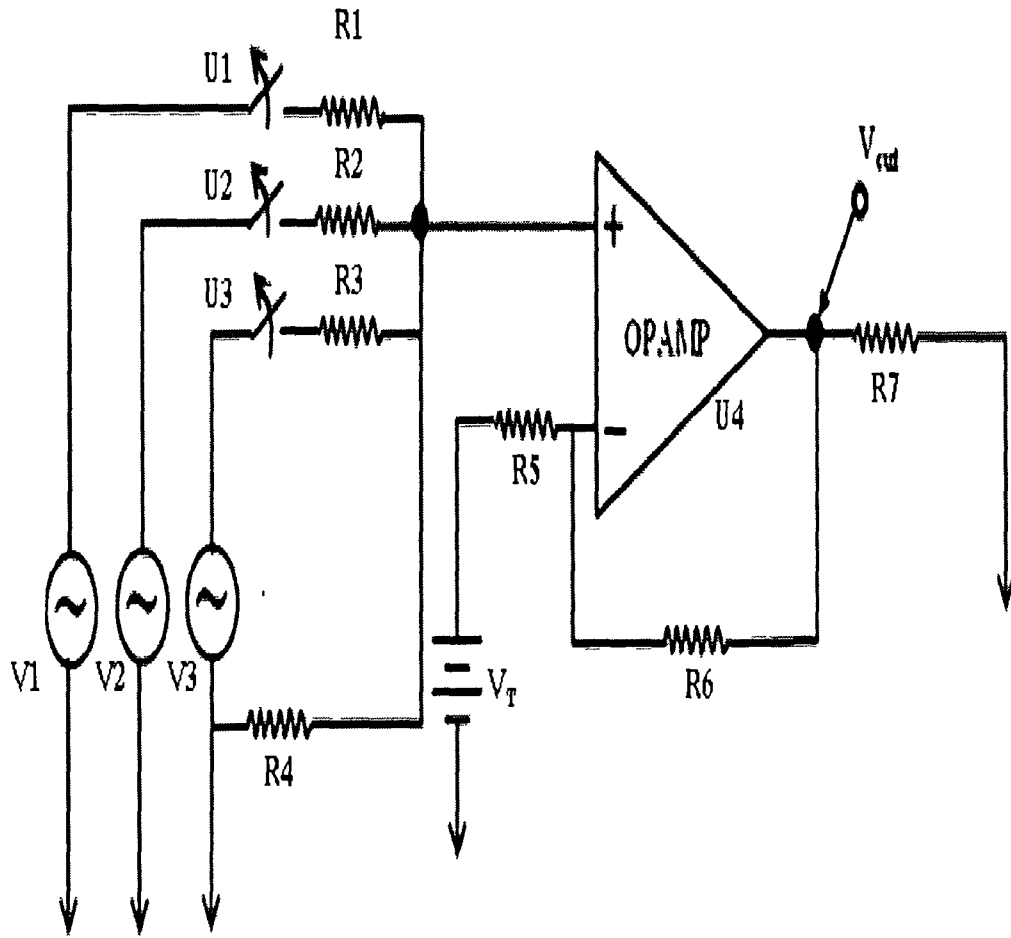


Fig 5 2 Proposed electrical model of neuron (Excitation)

**TABLE 5.1**  
DIFFERENT COMPONENTS USED IN THE PROPOSED MODEL OF NEURON OF FIG. 5.2

Sl. No	Component Name	Component Details	Unit	Value
01	V1	A.C. Voltage Source	Volt	0V
02	V2	A.C. Voltage Source	Volt	75mV
03	V3	A.C. Voltage Source	Volt	95mv
04	R1	Resistor	Ohms	1.5K
05	R2	Resistor	Ohms	1K
06	R3	Resistor	Ohms	1K
07	R4	Resistor	Ohms	1K
08	R5	Resistor	Ohms	1K
09	R6	Resistor	Ohms	1.17K
10	R7	Resistor	Ohms	1K
11	U1	Switch	Transmission time	3 ms
12	U2	Switch	Transmission time	3 ms
13	U3	Switch	Transmission time	3 ms
14	U4	Op-Amp ( $\mu$ 741)		
15	V <sub>T</sub>	Threshold Voltage	Volt	60mV

The circuit diagram of the model when the neuron is not disturbed or stimulated or more precisely membrane is resting i.e., when there is no input to the neuron is shown in Fig. 5.3.

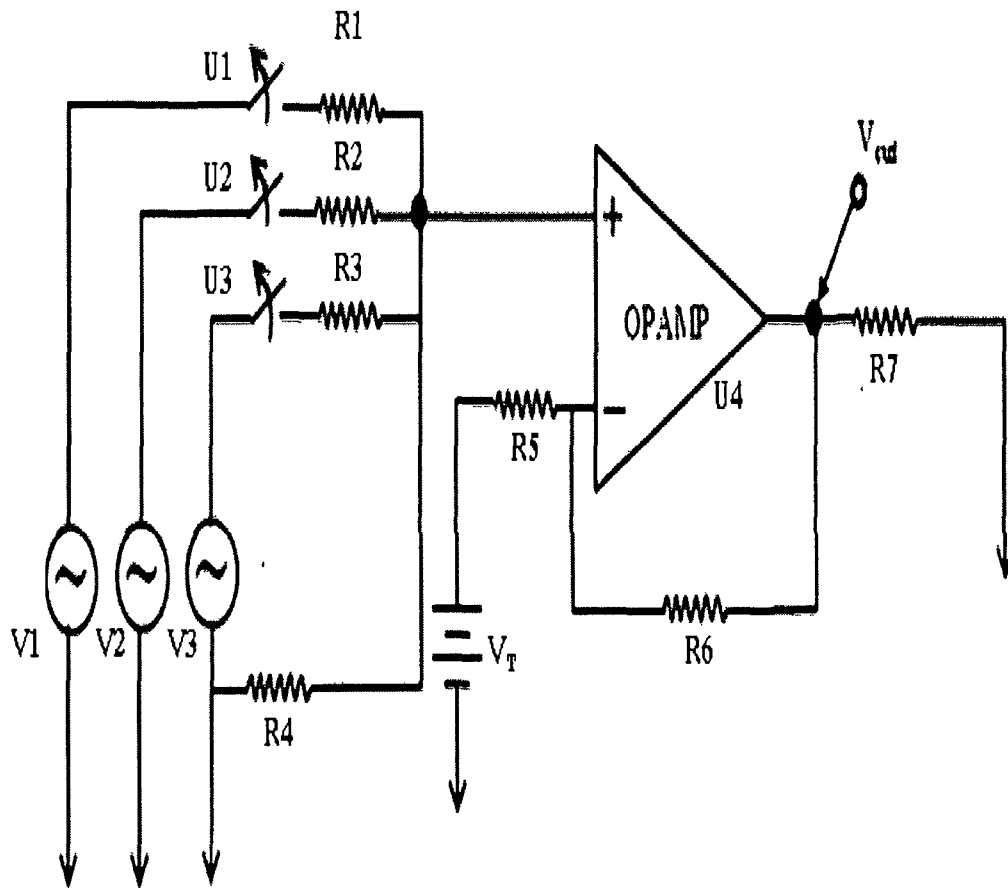


Fig. 5 3: Proposed electrical neuron model at rest.

The different components and their values for the proposed electrical circuit of neuron of Fig. 5.3 are summarized in Table 5.2.

TABLE 5.2  
DIFFERENT COMPONENTS USED IN THE PROPOSED MODEL OF NEURON OF FIG. 5.3

Sl. No	Component Name	Component Details	Unit	Value
01	V1	A.C. Voltage Source	Volt	0V
02	V2	A.C. Voltage Source	Volt	0V
03	V3	A.C. Voltage Source	Volt	0V
04	R1	Resistor	Ohms	1.5K
05	R2	Resistor	Ohms	1K
06	R3	Resistor	Ohms	1K
07	R4	Resistor	Ohms	1K
08	R5	Resistor	Ohms	1K
09	R6	Resistor	Ohms	1.17K
10	R7	Resistor	Ohms	1K
11	U1	Switch	Transmission time	3 ms
12	U2	Switch	Transmission time	3 ms
13	U3	Switch	Transmission time	3 ms
14	U4	Op-Amp ( $\mu$ 741)		
15	$V_T$	Threshold Voltage	Volt	60mV

### 5.2.1 Results:

Here, in the proposed excitable neuron model, shown in Fig. 5.2, the integrated input to the neuron is higher than the threshold potential, so the neuron should fire i.e., an action potential should initiate. The ORCAD simulation result when the net input to the neuron is higher than the threshold stimulus of the proposed model of excitable neuron of Fig. 5.2 is shown in Fig. 5.4, where the neuron is fired. The simulated action potential is very



similar to the experimentally recorded ones i.e., with real excitable actions of the neuron.

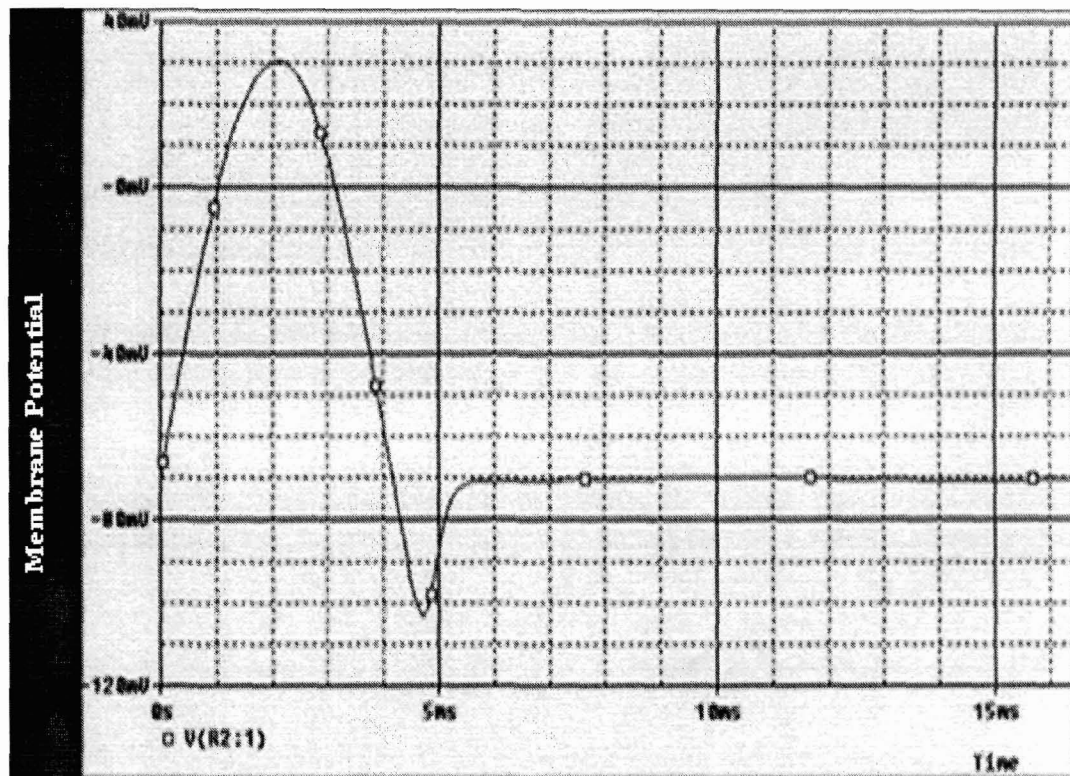


Fig. 5.4: The simulation result of excitable neuron model of Fig. 5.2

In the second case of the proposed model of Fig. 5.3, the integrated input to the neuron is zero i.e., lower than the threshold potential, so the neuron should not fire i.e., it should remain in its resting potential i.e.,  $\sim 70$  mV. And the ORCAD simulation result when the membrane is at rest of Fig. 5.3 is shown in

Fig. 5.5. The simulated resting potential is very similar to the experimentally recorded ones i.e., with real neuron.

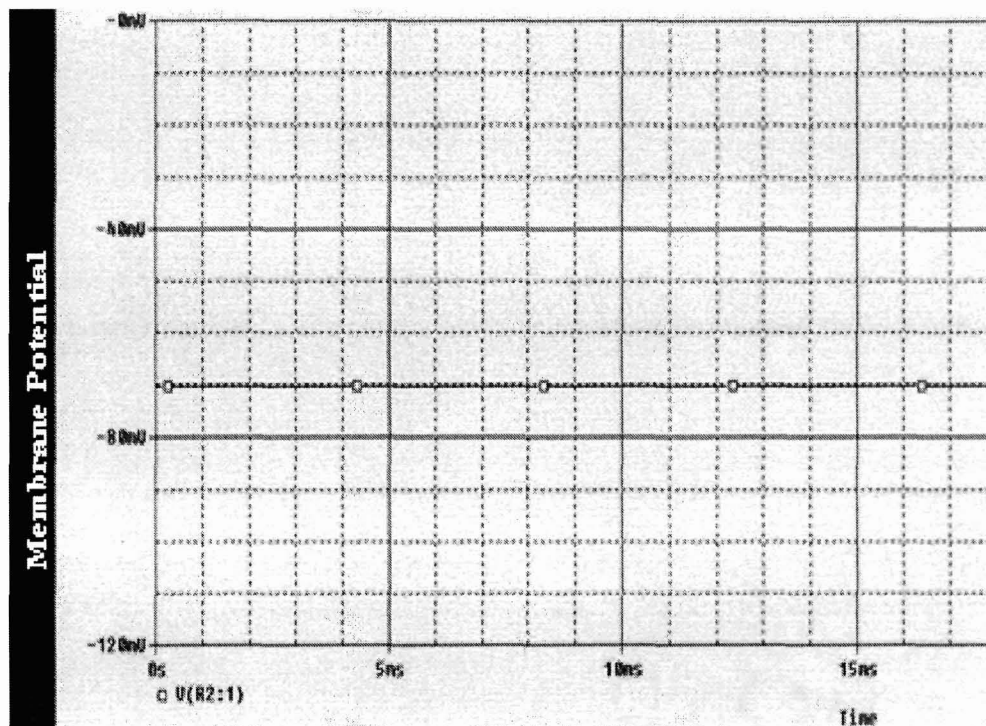


Fig. 5.5: The simulation result of proposed model electrical neuron at rest.

The results obtained from simulation of proposed model of silicon neuron for excitation are compared with those reported by previous researchers and are given in Table 5.4.

### **5.3 Integrate-and-Fire Based Model 2:**

In this model the neuron is supposed to be composed of dendritic regions and the soma. The dendritic regions have three dendritic terminals and receive input from presynaptic neurons. The circuit diagram of proposed model is shown in Fig. 5.6. Each dendritic region receives input or action potential from three different presynaptic neurons. Each dendritic region generates action potential if the integrated input of that specific region crosses the threshold value, which is required for the impulse to be transmitted from presynaptic neuron to the postsynaptic region. So, the post synaptic neuron has three input signals from the three dendritic regions for spatial summation.

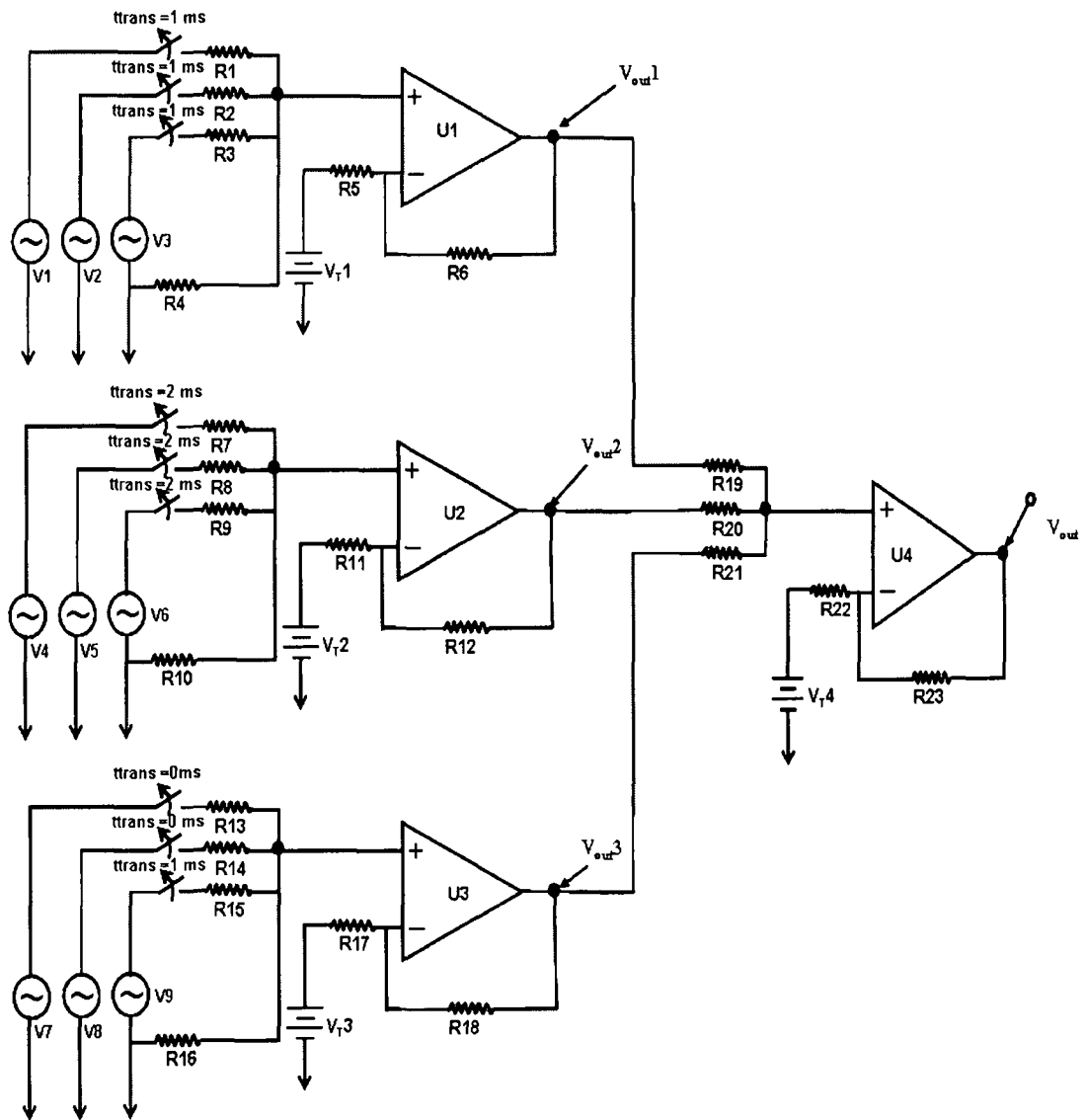


Fig. 5.6: Proposed electrical model of neuron

### 5.3.1 Results:

Each input to a specific dendritic region of the proposed model (shown in Fig. 5.6) is connected with the synaptic weight values which modifies the input. In this model, overall effect of all presynaptic terminals of synapse is spatially integrated and brought to a single point value. This single value is compared with the threshold (60mv) value. If the integrated value is greater than the threshold value then impulse will be transmitted to postsynaptic neuron. The output of each dendritic region is shown in Fig. 5.7.

The post synaptic membrane integrates the input from the three dendrites and compares with the threshold value. The threshold value will define whether the post synaptic membrane will fire or not. If integrated input is above the threshold limit, then the membrane will fire. i.e., an action potential will be generated, and if it is bellow threshold limit, then the membrane will not be fired. In the case of biological neuron the threshold limit is generally considered as 5 – 15mV less negative than the resting potential.

In this case, threshold limit considered is 60mV for dendritic region as well as for soma for ORCAD simulation. The integrated input of the proposed model is higher than the threshold potential, so an action potential should be generated. The simulated action potential is shown in Fig. 5.8. The component values assigned in the model for ORCAD simulation is given in Table 5.3.

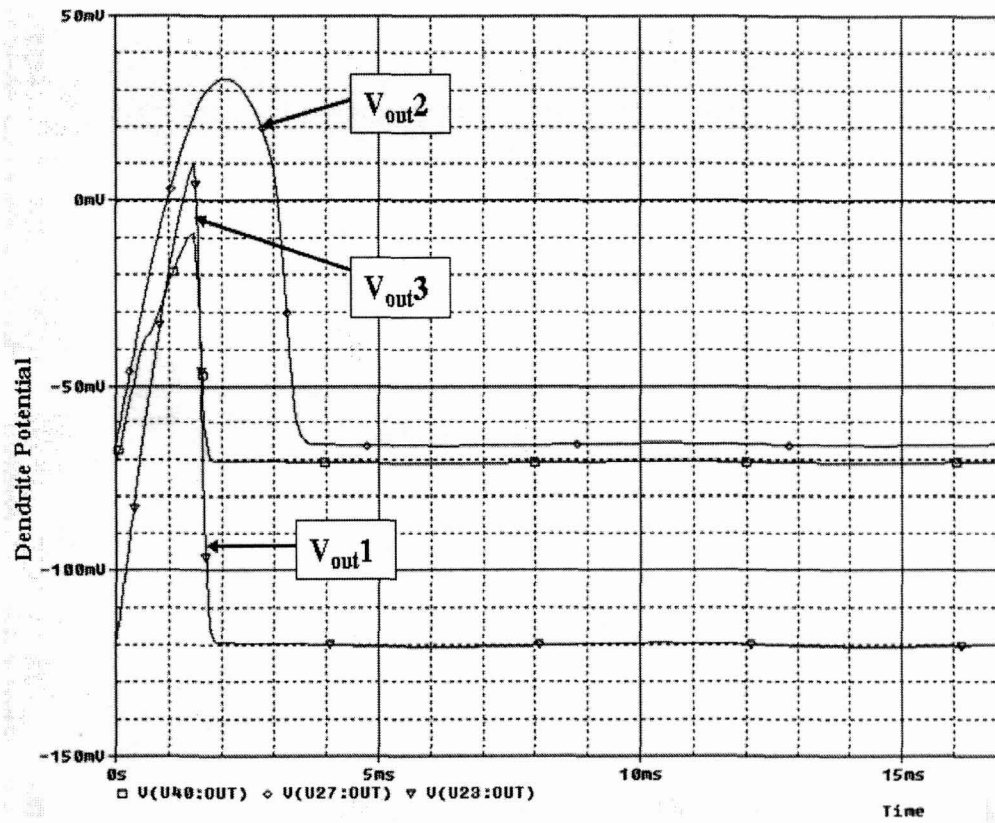


Fig. 5.7: The simulation output of dendritic regions

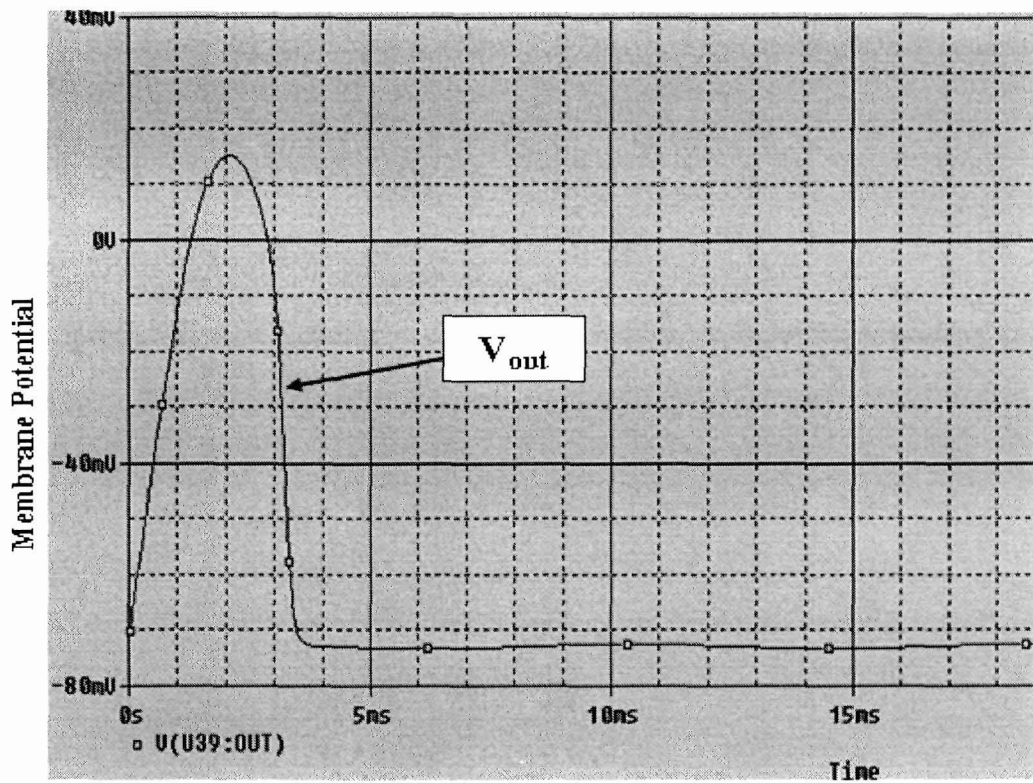


Fig. 5.8: The simulation result of neuron model of Fig. 5.6

TABLE 5.3  
DIFFERENT COMPONENTS USED IN THE PROPOSED MODEL OF NEURON OF FIG. 5.6

Sl. No	Component Name	Component Details	Unit	Value
01	V1	A.C. Voltage Source	Volt	0mV
02	V2	A.C. Voltage Source	Volt	100mV
03	V3	A.C. Voltage Source	Volt	80mV
04	V4	A.C. Voltage Source	Volt	0mV
05	V5	A.C. Voltage Source	Volt	95mV
06	V6	A.C. Voltage Source	Volt	70mV
07	V7	A.C. Voltage Source	Volt	0mV
08	V8	A.C. Voltage Source	Volt	55mV
09	V9	A.C. Voltage Source	Volt	65mV
10	R1	Resistor	Ohms	1.5K
11	R2	Resistor	Ohms	1K
12	R3	Resistor	Ohms	1K
13	R4	Resistor	Ohms	1K
14	R5	Resistor	Ohms	1K
15	R6	Resistor	Ohms	1K
16	R7	Resistor	Ohms	2K
17	R8	Resistor	Ohms	1K
18	R9	Resistor	Ohms	1K
19	R10	Resistor	Ohms	1K
20	R11	Resistor	Ohms	1K
21	R12	Resistor	Ohms	1.1K
22	R13	Resistor	Ohms	1.7K
23	R14	Resistor	Ohms	1K
24	R15	Resistor	Ohms	1K
25	R16	Resistor	Ohms	1K
26	R17	Resistor	Ohms	1K
27	R18	Resistor	Ohms	1.18K
28	R19	Resistor	Ohms	4K
29	R20	Resistor	Ohms	4K
30	R21	Resistor	Ohms	0.01K
31	R22	Resistor	Ohms	10K
32	R23	Resistor	Ohms	0.15K
33	V <sub>T1</sub>	Threshold Voltage	Volt	60mV
34	V <sub>T2</sub>	Threshold Voltage	Volt	60mV
35	V <sub>T3</sub>	Threshold Voltage	Volt	60mV
36	V <sub>T4</sub>	Threshold Voltage	Volt	60mV
37	U1,U2,U3,U4	Op-Amp ( $\mu$ 741)		



The results obtained from simulation of proposed model of neuron are compared with the previous proposed model and are also given in Table 4.3 and a close similarity is found.

TABLE 5.4  
COMPARISON OF SIMULATION RESULTS

Sl. No.	Threshold limit to initiate action potential	Peak value of Action Potential	Time to attain peak value	Total Duration
Lewis model [2]	6 mV	10 V (clamped)	3.8 ms	6 ms
Roy model [2]	8 mV	95 mV	2.3 ms	5 ms
Farquhar, Hasler model [3]	25 mV	110 mV	1 ms	1.5 ms
See Fig. 5.4	- 60 mV	30 mV	2 ms	5 ms
See Fig. 5.8	- 60 mV	15 mV	2 ms	3.5 ms

## 5.4 References:

- [1] Indiveri, G. Douglas, R. Smith, L. S. Silicon Neurons; *Scholarpedia*; [http://www.scholarpedia.org/article/Silicon\\_neurons#Conductance-based\\_models](http://www.scholarpedia.org/article/Silicon_neurons#Conductance-based_models); (2008).
- [2] Malmivuo, J. Plonsey, R. *Bioelectromagnetism – Principles and Applications of Bioelectric and Biomagnetic Fields*, Oxford University Press, 1995, Chapter 10.
- [3] Farquhar, E. Hasler, P. A Bio-physically inspired silicon neuron, *IEEE Transactions on Circuits and systems*, Vol. 52, No. 3, March 2005, pp. 477-488.

## **Chapter 6**

### **Study on the Development of Synapse Model: Integrate-and-Fire Based Model**

## **Study on the Development of Synapse Model: Integrate-and-Fire Based Model**

Over past few years, excellent models were proposed to simulate post synaptic neuron both for excitatory and inhibitory states. In this chapter a study on the development of synapse model based on Integrate-and-Fire based concept has been carried out. Simulation of the model yields an output representing the overall membrane potential of the postsynaptic region. The description of the model and its simulation results have been presented and compared with the results obtained by the previous researchers.

### **6.1 Introduction:**

As explained in chapter 4, referring to the electrical mechanism of synapse (Fig. 4(a), (b), (c)), when an impulse from the presynaptic neuron arrives at postsynaptic neuron, neurotransmitters are released from the presynaptic neuron. Because of which Sodium ions flow into the cell of the postsynaptic membrane resulting into positive current in case of excitatory synapse and the membrane depolarizes. If the postsynaptic membrane depolarizes sufficiently, then the postsynaptic membrane initiates an action potential. In the case of inhibitory synapse, Chloride ions move into the cell, making the postsynaptic membrane hyperpolarize, resulting into negative current. If the hyperpolarization of the postsynaptic membrane is sufficiently large then the postsynaptic membrane will be able to initiate an action potential, but in negative direction. Fig. 4.1(c) of chapter 4 shows the electrical equivalent circuit of a synapse which consists of a presynaptic neuron, synaptic cleft and postsynaptic neuron. Rewriting the equation 4.2:

$$I = C(dV_m / dt) + g_o(V_m - E_o) - g_{Na}(V_m - E_{Na}) + g_{Cl}(V_m - E_{Cl}) + g_k(V_m - E_k) \quad (6.1)$$

The expression of total current is composed of capacitive current and ionic current. The basic circuit which can be used to simulate the action of synapse is shown in as Fig. 5.1 in chapter 5 [1]-[3].

In the model developed, each presynaptic neuron has one or more inputs and produces an output; each input having a weighting factor, which modifies the value entering the synapse. The synapse mathematically compares the integrated inputs with a threshold limit, and if the integrated input value is greater than the threshold limit then synapse outputs the result or more precisely an action potential is generated. In the case of excitatory synapse, the synapse mathematically compares the integrated inputs with a threshold limit, and though in this case the integrated input value is less than the threshold limit then also an action potential is generated in positive direction. In the case of inhibitory synapse, the synapse mathematically compares the integrated inputs with a threshold limit, and if the integrated input value is greater than the threshold limit, an action potential is generated but in negative direction.

## **6.2 A Simple Integrate-and-Fire Based Circuit Model for Excitatory and Inhibitory Synapse:**

The membrane of post synaptic neuron has two types of ion channels – excitatory and inhibitory, whereas these channels are ion specific. Sodium ions specific channels are excitatory in nature and Chloride ions specific channels are inhibitory in nature. And the diffusion of Sodium ions into the cell causes a membrane potential in positive direction which is known as excitatory postsynaptic membrane potential (EPSP) whereas the flow of Chloride ions

causes a membrane potential in negative direction which is known as inhibitory postsynaptic membrane potential (IPSP).

When an action potential from the presynaptic neuron arrives at its terminals connecting the cleft, neurotransmitters are released into the cleft which diffuse through the cleft and bind with the receptor sites of the postsynaptic membrane. This binding mechanism opens the ion channels situated at the membrane surface and ions move into or out of the membrane. If the synapse is excitatory, Sodium ions flow into the cell resulting into positive current. As a result the membrane depolarizes. If sufficient number of Sodium channels open, then membrane potential will be greater than the action potential threshold  $V_T$  of the neuron and initiates an action potential. If the synapse is inhibitory, Chloride ions move into the cell, resulting into negative current. As a result the membrane hyperpolarizes. If the number of Chloride channels are sufficiently large then membrane potential will be able to initiate an action potential in negative direction.

Here, excitatory and inhibitory synapses based on integrate-and-fire models are developed. The circuit model for the excitatory synapse is shown in Fig. 6.1. The different component values used in the model is given in Table 6.1.

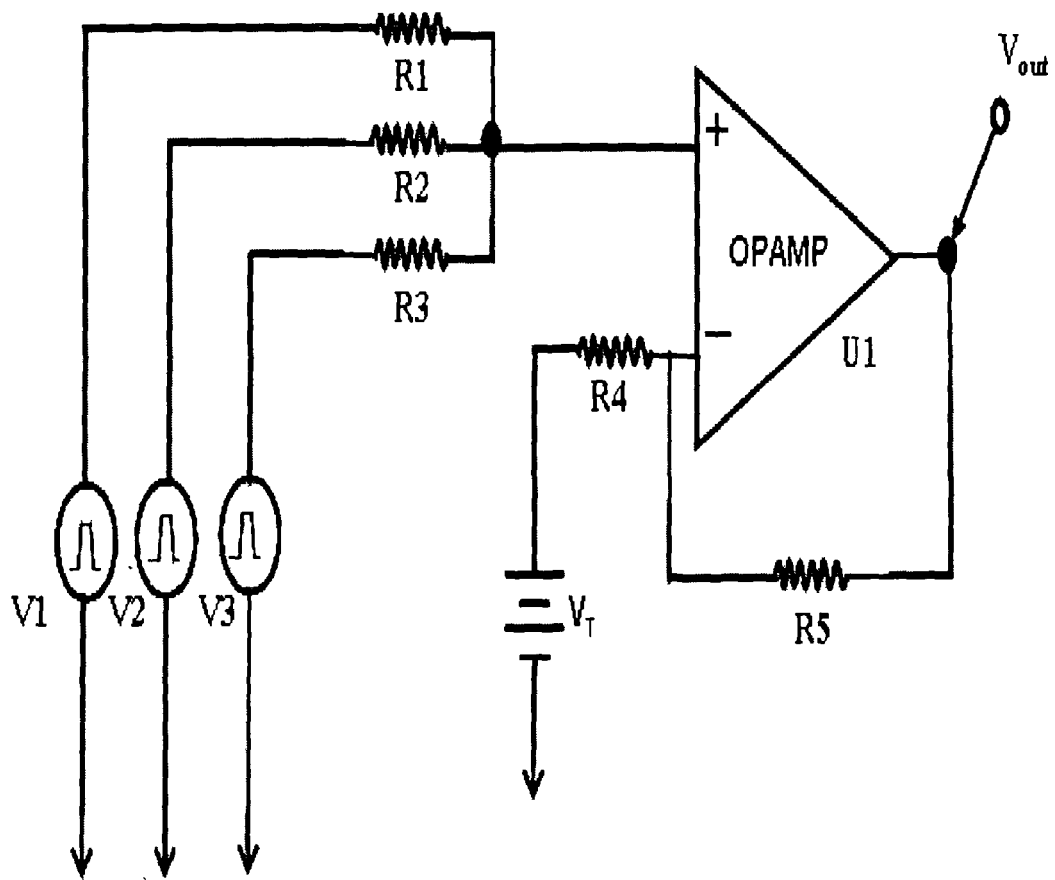


Fig. 6.1. Electrical circuit model of excitatory synapse

TABLE 6.1  
DIFFERENT COMPONENTS USED IN THE PROPOSED MODEL OF NEURON OF FIG. 6.1

Sl. No	Component Name	Component Details	Unit	Value
01	V1	A.C. Voltage Source(Pulse)	Volt	5mV
02	V2	A.C. Voltage Source(Pulse)	Volt	5mV
03	V3	A.C. Voltage Source(Pulse)	Volt	40mV
04	R1	Resistor	Ohms	33.33K
05	R2	Resistor	Ohms	20K
06	R3	Resistor	Ohms	0.1K
07	R4	Resistor	Ohms	2K
08	R5	Resistor	Ohms	2.34K
09	U1	Op-Amp ( $\mu$ 741)		
10	$V_T$	Threshold Voltage	Volt	60mV

The circuit model for the inhibitory synapse is shown in Fig. 6.2. The different component values used in the model is given in Table 6.2.

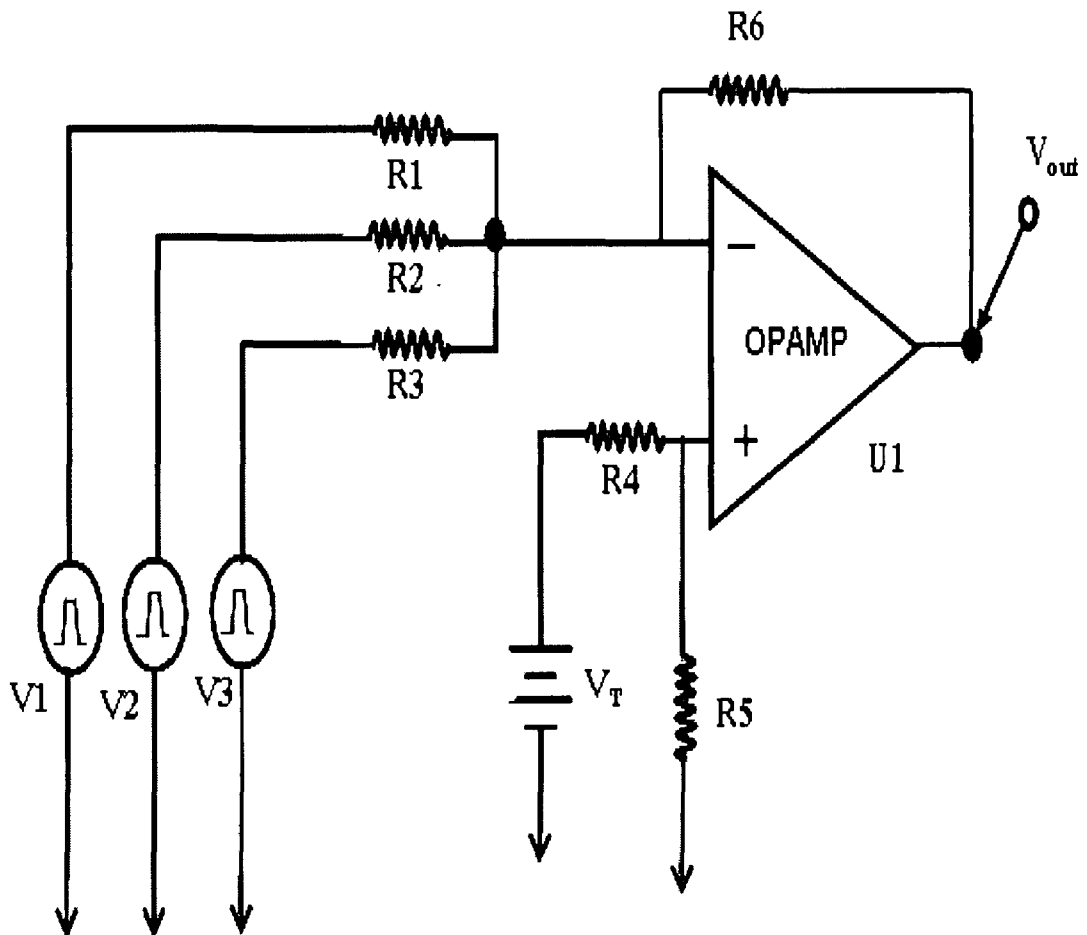


Fig. 6.2: Electrical circuit model of inhibitory synapse



**TABLE 6.2**  
DIFFERENT COMPONENTS USED IN THE PROPOSED MODEL OF NEURON OF FIG. 6.2

Sl. No	Component Name	Component Details	Unit	Value
01	V1	A.C. Voltage Source(Pulse)	Volt	40mV
02	V2	A.C. Voltage Source(Pulse)	Volt	30mV
03	V3	A.C. Voltage Source(Pulse)	Volt	40mV
04	R1	Resistor	Ohms	0.5K
05	R2	Resistor	Ohms	0.1K
06	R3	Resistor	Ohms	0.1K
07	R4	Resistor	Ohms	0.5K
08	R5	Resistor	Ohms	0.0001K
09	R6	Resistor	Ohms	0.13K
09	U1	Op-Amp ( $\mu$ 741)		
10	V <sub>T</sub>	Threshold Voltage	Volt	60mV

### 5.2.1 Results:

The simulation output for excitatory synapse is shown in Fig. 6.3, which illustrates an EPSP with sufficient amplitude for triggering an action potential.

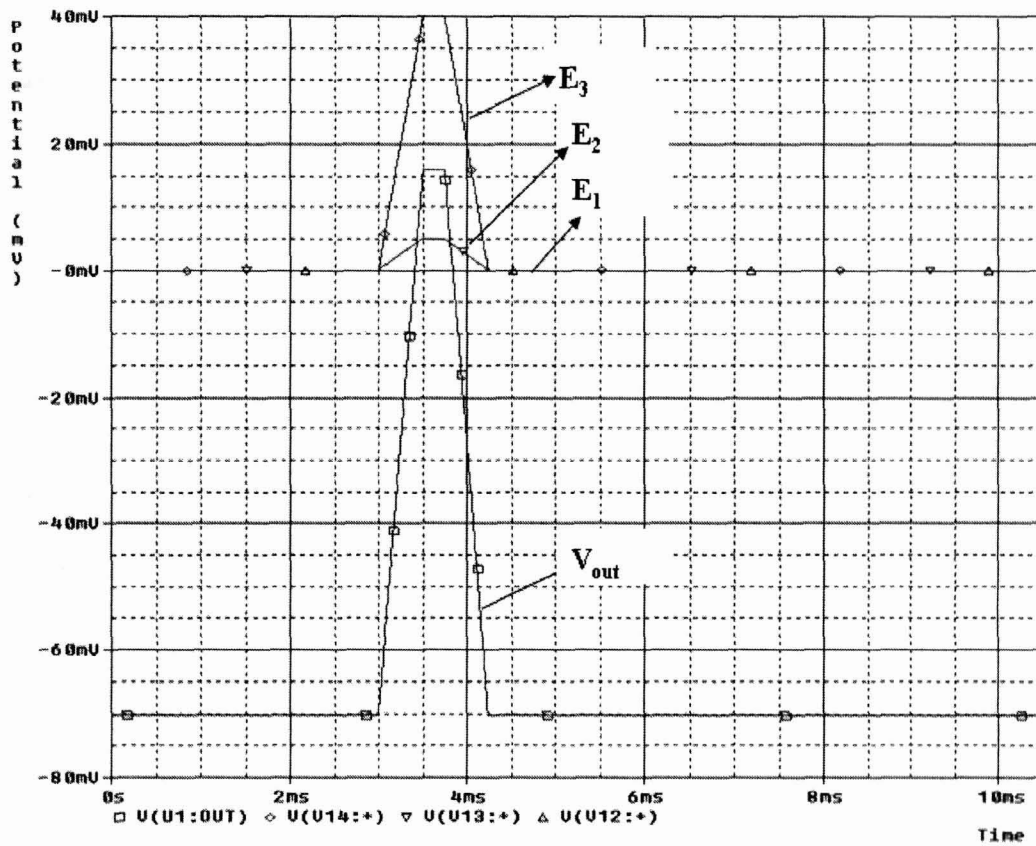


Fig. 6.3: The output profile of excitatory synapse

The simulation output for inhibitory synapse is shown in Fig. 6.4, which illustrates an IPSP with sufficient amplitude for triggering an action potential in negative direction.

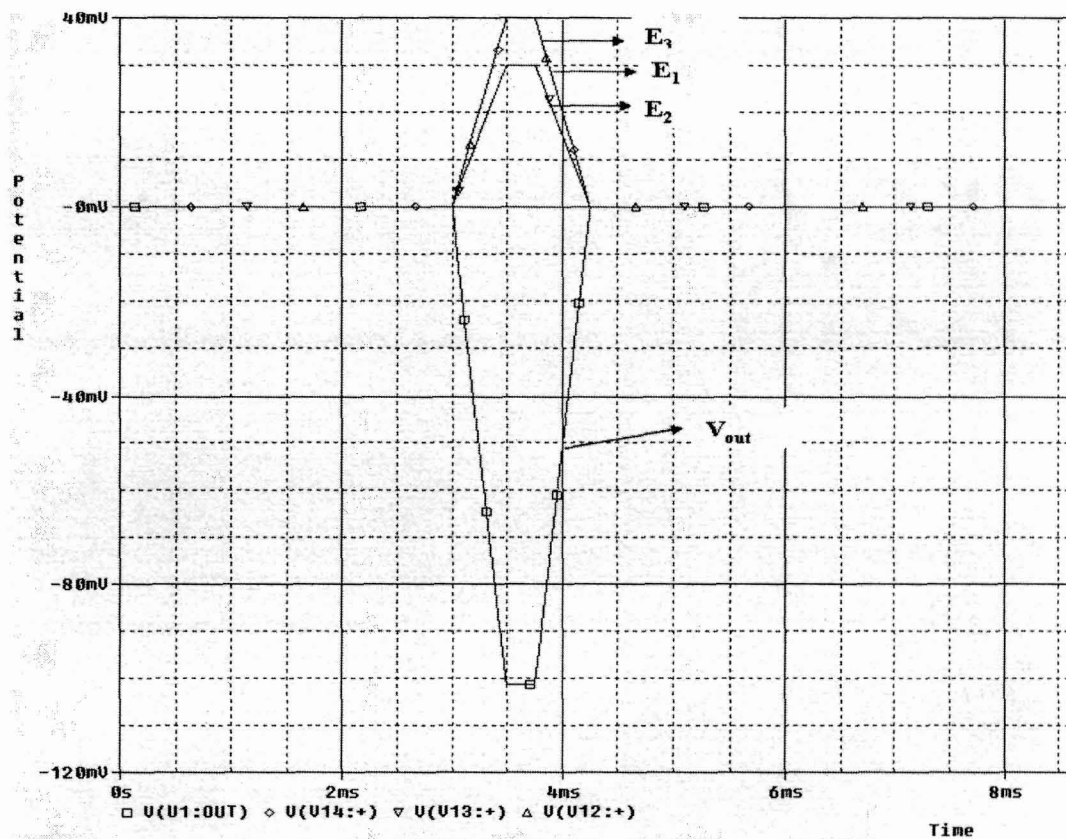


Fig. 6.4: The output profile of Inhibitory synapse.

The results obtained from simulation are compared with those reported by previous researchers and are given in Table 6.3.

**TABLE 6.3**  
**COMPARISON OF SIMULATION RESULTS**

Sl. No.	Threshold limit to initiate action potential	Peak value of Impulse	Time to attain peak value	Total Duration of EPSP/IPSP
[4]	- 40 mV	40 mV	1 ms	10 ms
[5]	- 60 mV to - 40 mV	-52 mV (inhibitory)	3.5 ms	6 ms
See Fig. 6.3	- 60 mV	15 mV	0.5 ms	1.25 ms
See Fig. 6.4	- 60 mV	-110 mV (inhibitory)	0.5 ms	1.25 ms

In the conclusion of this work, it can be summarized that, simple electrical models both for excitatory and inhibitory synapses have been developed by considering a synapse to be made of presynaptic terminals, cleft and postsynaptic membrane. The overall effect of all presynaptic terminals is integrated and then reduced to a single point. The single point value is compared with threshold to produce an output. Models demonstrate the basic mechanism of neuron namely the effects of excitation and inhibition.

### 6.3 References:

- [1] Hodgkin, A. L. Huxley, A. F. A Quantitative Description of Membrane Current and Its Application to Conduction and Excitation In Nerve, *Journal of Physiology*, 117, pp. 500-544 (1952).

- 
- [2] Hodgkin, A. L. Huxley, A. F. Katz, B. Measurement of Current Voltage Relations In The Membrane Of The Giant Axon Of Loligo, *Journal Of Physiology*, 1952, 116,424-448.
- [3] Indiveri, G. Douglas, R. Smith, L. S. Silicon Neurons; *Scholarpedia*; [http://www.scholarpedia.org/article/Silicon\\_neurons#Conductance-based\\_models](http://www.scholarpedia.org/article/Silicon_neurons#Conductance-based_models); (2008).
- [4] Mahowald, M. Douglas, R. A silicon neuron, *Nature*, Vol 354, 19/26 December 1991.
- [5] Levine, M. D. Eisenberg, M. F. Fare, T. L. A Physiologic-Based Circuit Model of the Postsynaptic region at the Neuromuscular Junction, *IEEE Proceedings*, pp. 1602 - 1603, ISBN : 0-7803-0785-2.

# **Chapter 7**

## **Some Aspects of Development of Biologically Motivated Circuit Models of Synapses**

## **Some Aspects of Development of Biologically Motivated Circuit Models of Synapses**

In this chapter a study on the development of three biologically motivated/inspired synapse models has been carried out. The modeling theories and description of the models and their simulation results have been presented and compared with the previously obtained results.

### **7.1 Introduction:**

In the first synapse model, the variable conductance of ion channels of post synaptic neuron, dependence on the transmitters diffused through the synaptic cleft and bind with the receptor sites of the post synaptic membrane of neuron, is represented by MOSFET. MOSFET is chosen because it functions as a voltage controlled conductance in the linear region, analogous to the variable conductance of the transmitter gated ion channels of post synaptic region of neuron. This analog is incorporated into the famous Hodgkin-Huxley (H-H) model of neuron at the synaptic cleft. Simulation is performed in MATLAB environment both for excitatory and inhibitory actions of synapses and the results are presented.

In the second synapse model, the variable conductance of postsynaptic membrane of neuron dependence on the neurotransmitter-receptor binding activity is represented by ion-sensitive field effect transistor (ISFET). ISFET functions not only as a voltage controlled conductance but can also be converted into an enzyme modified field effect transistor (ENFET) and therefore can provide a means of measurement of specific neurotransmitters

that bind with the receptor sites of postsynaptic membrane. This analog is incorporated into the Hodgkin-Huxley (H-H) model of neuron to substitute the variable  $\text{Na}^+$  and  $\text{Cl}^-$  conductances. Simulation is performed in MATLAB environment both for excitatory and inhibitory states and results are presented.

In the third synapse model, the variable conductance of postsynaptic membrane of neuron dependence on the acetylcholine-receptor binding activity is represented by enzyme modified field effect transistor (ENFET) sensitive to acetylcholine. Acetylcholine sensitive ENFET functions not only as a voltage controlled conductance but can also provide a means of measurement of specific neurotransmitters that bind with the receptor sites of postsynaptic membrane. This analog is incorporated into the Hodgkin-Huxley (H-H) model of neuron to substitute the variable  $\text{Na}^+$  conductance. Simulation is performed in MATLAB environment both for normal (excitatory) and pathologic states and results are presented.

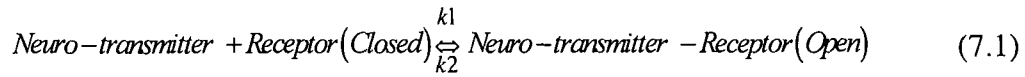
## **7.2 Biologically Motivated Circuit Model of Neuron for Simulation of Excitatory and Inhibitory Actions of Synapses:**

The communication between two neurons is one directional communication. The function of postsynaptic neuron may, therefore, be considered to be an input to the next neuron. Modeling of neuron is, therefore, performed for postsynaptic neuron.

The postsynaptic membrane consists of a lipid bilayer and transmembrane protein ion channels. Some ion channels such as sodium, chloride etc. are controlled by the neurotransmitters that bind with the receptor sites, i.e. the amount of ionic current is dependent upon the activity of the transmitter-



receptor binding. In simplest case, the binding reaction may be represented as [1]



Where  $K_1$  and  $K_2$  are the forward and backward rate constants respectively. The transmitter gated channels, therefore, have variable conductance dependence on the binding activity of transmitters. Transmitter gated ion channels can, therefore, be represented by MOSFET, because as discussed in chapter 4, MOSFET functions as a voltage controlled conductance in its linear region. Rewriting the governing equation from chapter 4 (equation 4.20):

$$G_{DS} = \beta(V_{GS} - V_t) \quad (7.2)$$

$\beta$  is the geometric sensitivity parameter given by

$$\beta = \mu C_{ox} \frac{W}{L} \quad (7.3)$$

Where  $C_{ox}$  is the oxide capacity per unit area,  $W$  and  $L$  are the width and the length of the channel respectively, and  $\mu$  is the electron mobility in the channel.  $V_{GS}$  is the gate to source voltage and  $V_t$  is the threshold voltage of the MOSFET. In MOSFET,  $\beta$  and  $V_t$  are constants and  $V_{GS}$  is the only input variable. Thus  $G_{DS}$  is dependent on gate voltage  $V_{GS}$ , analogous to the conductance of ion channels of postsynaptic membrane dependent on the binding activity. Thus, considering the transmitter-receptor binding activity, the H-H model for membrane can be modified as shown in Fig. 7.1. Here  $V_{gN}$  and  $V_{gL}$  are gate voltages applied to MOSFETs that control the conductances  $g_{Na}$  and  $g_{Cl}$  respectively.

Gate voltage is a time dependent voltage given by [1].

$$V_g(t) = V_o[(1 - \exp(-k_1 t) + \exp(-k_2 t)U(t - t_m))] \quad (7.4)$$

Where  $K_1$  and  $K_2$  are time constants analogous to the rate constants of equation (7.1),  $U(t - t_m)$  is the Heaviside function and  $V_o$  is a voltage proportional to the maximum attainable conductance, when all the transmitter-gated channels for a specific ion are open.

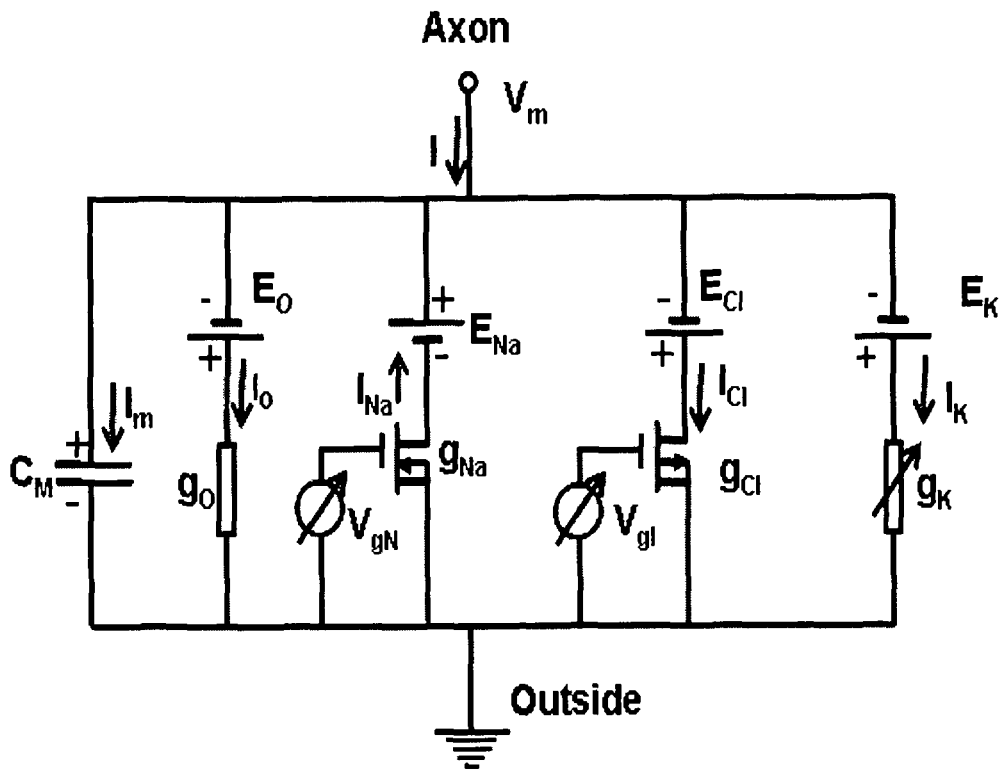


Fig. 7.1: Biologically motivated model of postsynaptic membrane

### 7.2.1 Modeling Neuron for Excitatory Synapse:

The circuit model for excitatory synapse is shown in Fig. 7.2. The leakage current  $I_o$  is considered to be small enough to be neglected. Since only sodium channels are responsible for excitatory action, the postsynaptic membrane is divided into three patches to represent spatial summation of the sodium current controlled by  $g_{Na_1}$ ,  $g_{Na_2}$ , and  $g_{Na_3}$ , where

$$I_{Na} = I_1 + I_2 + I_3 \quad (7.5)$$

So that,  $I = I_m - I_{Na} + I_K$

$$= C_m \frac{dV_m}{dt} - g_{Na}(V_m - E_{Na}) + g_K(V_m - E_K) \quad (7.6)$$

Where  $g_{Na}$  is the total Sodium conductance and  $g_K$  is the total Potassium conductance.

The membrane potential  $V_m$  is obtained by spatially and temporally varying  $g_{Na}$  of transmitter-gated sodium channels.

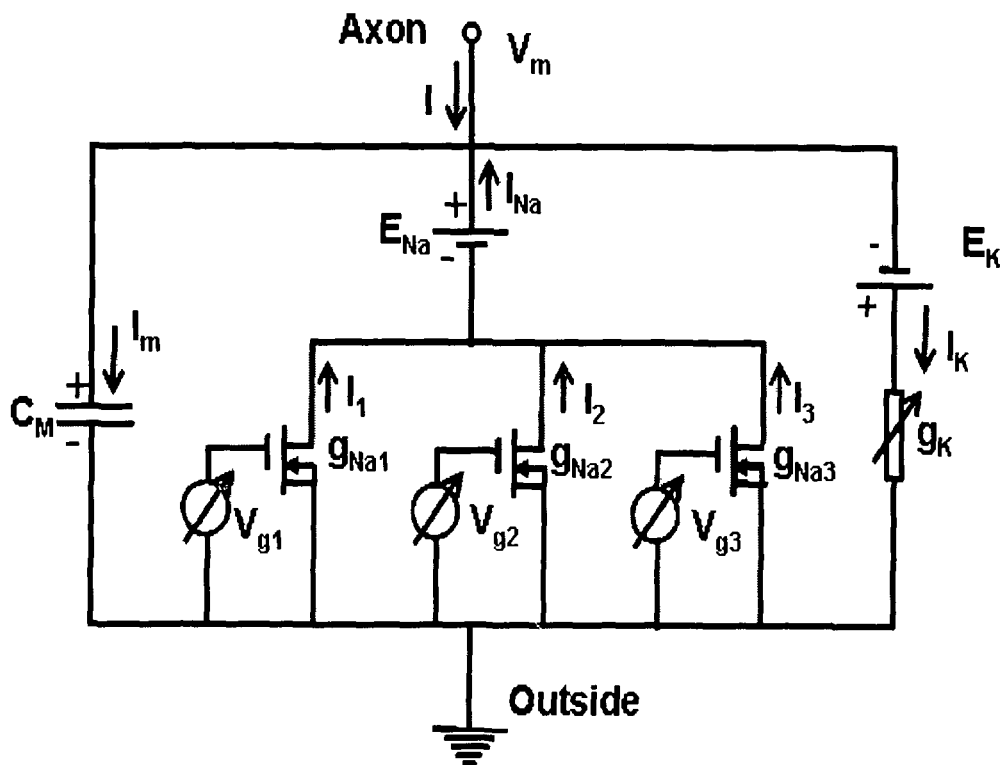


Fig. 7.2: Circuit model for excitatory action of synapse

The component values assigned in the model for MATLAB simulation are taken from literature [1] and are given in Table 7.1. The specifications for three n-channel MOSFETS, the parameters for exponential function in equation (7.4), applied to each MOSFET inputs are also given in Table 7.1.

TABLE 7.1  
DIFFERENT COMPONENTS USED IN THE PROPOSED MODEL OF EXCITATORY SYNAPSE

Sl. No.	Parameter	Parameter Details	Unit	Value
01	$C_M$	Membrane Capacitance	Farad	1 $\mu\text{F}$ per $\text{cm}^2$
02	$g_K$	Potassium Conductance	Mho	1 mS per $\text{cm}^2$
03	$E_{Na}$	Sodium Potential	Volt	60mV
04	$E_K$	Potassium Potential	Volt	-90mV
05	L	Channel Length	Meter	15 $\mu\text{m}$
06	W	Channel Width	Meter	2 $\mu\text{m}$
07	$t_{ox}$	Oxide Thickness	Meter	100 nm
08	$\mu$	Electron mobility	$\text{cm}^2/\text{V-sec}$	600 $\text{cm}^2/\text{V-sec}$
09	$V_o$	Voltage proportional to the maximum attainable conductance	Volt	2 Volts
10	$t_m$	Time	Second	600 $\mu\text{sec}$
11	$k_1 = k_2$	Time Constant	Second	0.8 msec

### 7.2.2 Modeling Neuron for Inhibitory Synapse:

The modeling for inhibitory synapse is shown in Fig. 7.3. Considering only  $\text{Cl}^-$  channels to be responsible for inhibitory action, the post synaptic membrane is divided into three patches to represent spatial summation of the Chloride current controlled by  $g_{Cl1}$ ,  $g_{Cl2}$  and  $g_{Cl3}$ , where

$$I_{Cl} = I_1 + I_2 + I_3 \quad (7.7)$$

So, that,  $I = I_m + I_{Cl} + I_K$

$$= C_m \frac{dV_m}{dt} + g_{Cl}(V_m - E_{Cl}) + g_K(V_m - E_K) \quad (7.8)$$

Where  $g_{Cl}$  is the total Chlorine conductance and  $g_K$  is the total Potassium conductance.

The membrane potential  $V_m$  is obtained by spatially and temporally varying  $g_{Cl}$  of transmitter-gated Chlorine channels.

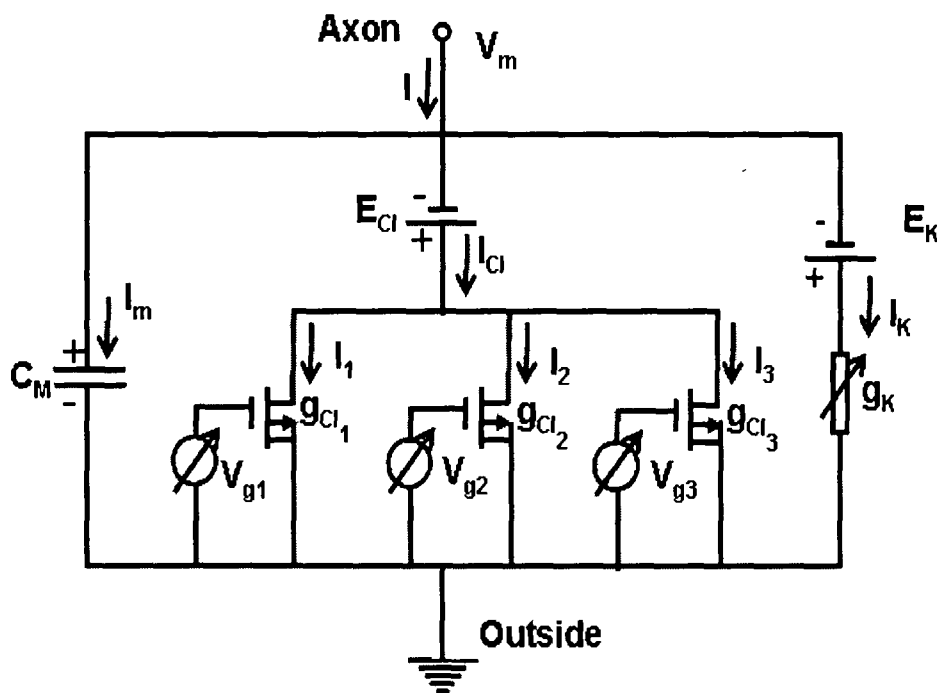


Fig. 7.3: Circuit model for inhibitory action of synapse

The component values assigned in the model for MATLAB simulation, the specifications for three p-channel MOSFETS, and the parameters for exponential function in equation (7.4), applied to each MOSFET inputs are given in Table 7.2.

**TABLE 7.2**  
DIFFERENT COMPONENTS USED IN THE PROPOSED MODEL OF INHIBITORY SYNAPSE

Sl. No.	Parameter	Parameter Details	Unit	Value
01	$C_M$	Membrane Capacitance	Farad	1 $\mu\text{F}$ per $\text{cm}^2$
02	$g_K$	Potassium Conductance	Mho	1 mS per $\text{cm}^2$
03	$E_{Cl}$	Chloride Potential	Volt	-100mV
04	$E_K$	Potassium Potential	Volt	-90mV
05	$L$	Channel Length	Meter	15 $\mu\text{m}$
06	$W$	Channel Width	Meter	2 $\mu\text{m}$
07	$t_{ox}$	Oxide Thickness	Meter	100 nm
08	$\mu$	Electron mobility	$\text{cm}^2/\text{V-sec}$	600 $\text{cm}^2/\text{V-sec}$
09	$V_o$	Voltage proportional to the maximum attainable conductance	Volt	-5 Volts
10	$t_m$	Time	Second	850 $\mu\text{sec}$
11	$k_1 = k_2$	Time Constant	Second	0.8 msec

### 7.2.3 Results:

The MATLAB simulation outputs are shown in Fig. 7.4. The top waveform represents the normal postsynaptic membrane potential. Here  $V_m$  is established by spatial summation and temporal integration of the transmitter gated sodium current and non-gated potassium current. Simulation results indicate that when  $V_m$  exceeds a threshold in the range of -60 to -40mV, an action potential initiates which illustrates an EPSP. The bottom waveform represents the inhibitory action. It illustrates an IPSP with sufficient amplitude for triggering an action potential in negative direction.

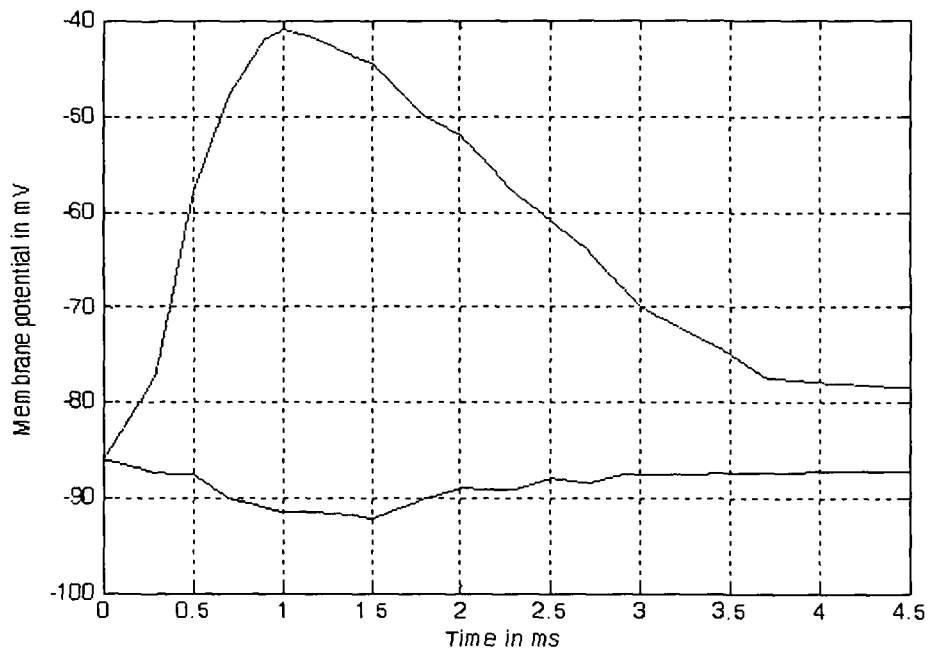


Fig. 7.4: Simulation results of excitatory and inhibitory actions of postsynaptic membrane .  
Top waveform represents the EPSP and bottom waveform represents the IPSP.

Here, MOSFET based electrical models both for excitatory and inhibitory actions of neurons have been developed. Postsynaptic membrane is divided into three patches to represent spatial summation of gated currents. Temporal integration of the currents is achieved by modeling exponentially varying time dependent gate voltage applied to MOSFET. This model can be used in neurobioengineering area for simulation of neurotransmitter-receptor binding activity and electrical activity of the postsynaptic neuron.

The results obtained from simulation of proposed circuit models of synapse for excitatory and inhibitory actions using MOSFET are compared with those



of the other proposed models and models reported by previous researchers and are given in Table 7.8.

### **7.3 Modeling Neuron for Simulation of Transmitter Gated Ion Channels of Postsynaptic Membrane at Synaptic Cleft:**

In this work, the variable conductance of postsynaptic membrane of neuron dependence on the neurotransmitter-receptor binding activity is represented by Ion Sensitive Field-Effect Transistor (ISFET). This work starts with thorough study on ISFET.

#### **7.3.1 Ion Sensitive Field-Effect Transistor (ISFET):**

The exploitation of field effect concept for measurement of ions in aqueous solution has given the birth of a new class of chemical sensors known as Ion Sensitive Field Effect Transistors (ISFET). This device was first reported by Bergveld in 1970, who used it for the measurement of ionic in and effluxes around a nerve [2]. This work was described in detail in 1972 [3] which is now cited by most authors as a pioneering publication in the field of ISFET development. Bergveld demonstrated that if the metal gate of ordinary Metal Oxide Semiconductor Field Effect Transistor (MOSFET) is omitted and the silicon dioxide layer is exposed to an electrolyte, the characteristics of the device are then affected by the ionic activity of the electrolyte and hence this device functions as an ion-sensitive transducer. At the same time Matsuo and Wise developed a similar device using silicon nitride as a sensitive sub gate layer, which greatly improved the sensor performance [4]. These pioneering works prompted further research in the field of ISFETOLOGY resulting into a large number of publications devoted to various aspects of ISFET development [5]. Due to their small dimensions, these devices were initially

meant for biomedical applications and almost all papers at that time, described ISFETs as future tools for electrophysiological measurements and were therefore published in biomedical journals [5]. Nevertheless, with the new possibilities for electrophysiology measurements, research on ISFETs went in the direction of ion sensing in general, not specifically biomedical. Since 1970, led by Bergveld, more than 600 papers, devoted on ISFETs and another 170 on related biosensors , such as Enzyme FETs (ENFETs) [6] –[11], ImmunoFETs (IMFETs) [12], DNA biosensor [13]etc. appeared in many world's leading journals on biomedical, electron devices, sensors and actuators, biosensors and bioelectronics, biotechnology advances etc. These devices exhibit several advantages over conventional ion-selective electrodes. The advantages of these devices are given below [14] - [15]:

1. The history of silicon usage for developing a wide range of sensors is well reviewed by Middelhock [16].
2. ISFETs are very robust and durable. Unlike many conventional sensors, ISFET probes withstand cleaning with a toothbrush.
3. The ISFETs are mass-produced by integrated circuit(IC) group technology, which make them very small and cost effective.
4. ISFETs can be stored dry and require little routine maintenance.
5. ISFETs can be used over an extremely wide temperature range and are sterilizable.
6. ISFETs have potential for on-chip circuit integration leading to the development of micrototal analysis system ( $\mu$ -TAS) [17] or lab-on-chip system [18].

7. Both computation and detection can be performed on the same chip with a buffer electronic system of information processing and storage.
8. ISFETs can be made multifunctional by a combination of membranes.
9. The insulating surface of ISFET contains reactive groups, which can be used for covalent attachment of organic molecules and polymers. ISFETs can, therefore, be converted into biosensors and bioelectronic devices [19] which are now regarded as promising tools in medicine, biotechnology, environmental control, agriculture, food industry and defense.

### 7.3.1.1 Theory of ISFET:

Ion Sensitive Field Effect Transistor (ISFET) is in fact a Metal Oxide Semiconductor Field Effect Transistor (MOSFET) in which metal gate is replaced by a complex structure sensitive to hydrogen ion concentration. The schematic representation of a MOSFET and an ISFET is given in Fig. 7.5, as well as their common electronic diagram.

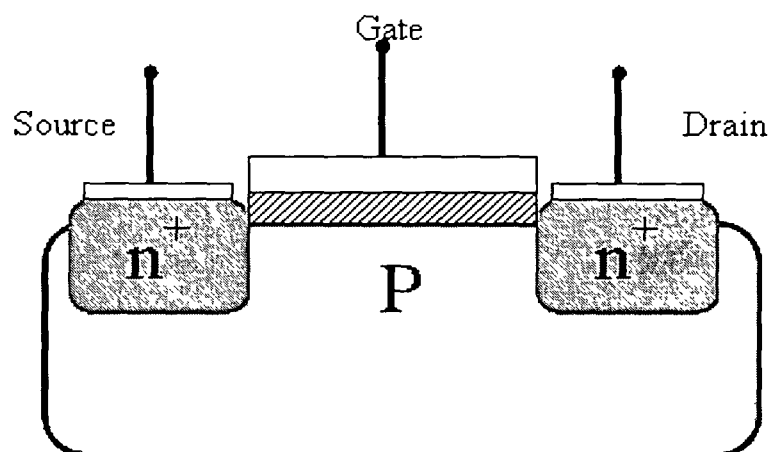


Fig. 7.5(a): Structure of MOSFET

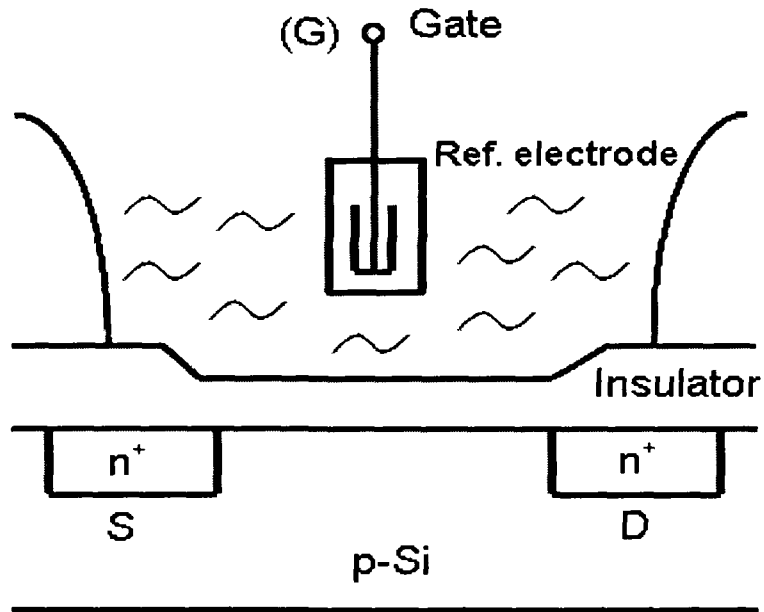


Fig. 7.5(b): Schematic of ISFET

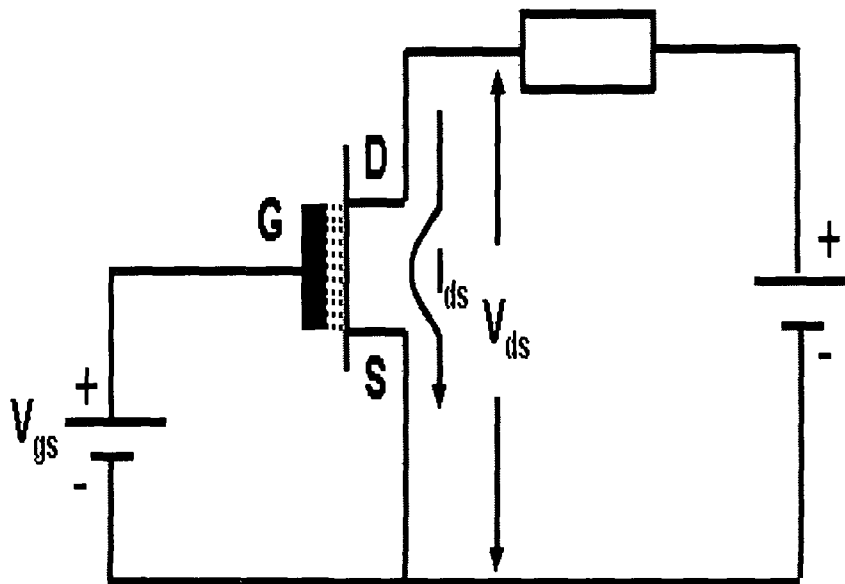


Fig. 7.5(c): Electronic Diagram of ISFET

It is obvious that ISFET is obtained by replacing the standard metal gate of a MOSFET with a reference electrode, a chemically sensitive insulator between which presents a measured electrolyte. The gate voltage is applied to the reference electrode and the electrolyte closes the electric Gate-Source circuit. ISFET is therefore fundamentally a MOSFET and hence the theoretical description of MOSFET is essential to describe ISFET's theory. The most important equation of MOSFET is the threshold voltage,  $V_{TH(MOS)}$ , which is defined as the value of gate voltage ( $V_G$ ) that is necessary to cause surface inversion and is given by [20]

$$V_{TH(MOS)} = \phi_M - \phi_{si} - \frac{Q_{ox} + Q_{ss} + Q_B}{C_{ox}} + 2\phi_f \quad (7.9)$$

where,

$2\phi_f$  = semiconductor surface inversion potential,

$\phi_f$  = Fermi potential of the semiconductor,

$Q_B$  = semiconductor depletion charge per unit area,

$\phi_M$  = work function of the gate metal in volts,

$\phi_{si}$  = work function of bulk semiconductor i.e. extrinsic semiconductor (in volts),

$Q_{ss}$  = the fixed surface-state charge per unit area at the insulator-semiconductor interface,

$C_{ox}$  = capacitance per unit area of the oxide, and

$Q_{ox}$  = accumulated charge in the oxide

Here all terms are purely physical in nature. In case of the ISFET, the same fabrication process is used, resulting in the same constant physical part of the threshold voltage. But the introduction of electrolyte between the reference electrode and the insulator, produces two more potentials: the constant potential of the reference electrode,  $E_{ref}$  and the interfacial potential  $\Psi_0 + \chi^{sol}$  at the solution / oxide interface, where  $\Psi_0$  is the surface potential, shown to be a function of the solution pH and  $\chi^{sol}$  is the surface dipole potential of the solvent having a constant value. Therefore, the equation for the ISFET threshold voltage is as follows [15]:

$$V_{TH(IS)} = E_{ref} - \Psi_0 + \chi^{sol} - \varphi_{Si} - \frac{Q_{ox} + Q_{ss} + Q_B}{C_{ox}} + 2\varphi_f \quad (7.10)$$

The general expressions for the drain current of the MOSFET in the non-saturated and saturated mode are respectively [21]:

$$I_{DS} = \beta \left[ \left( V_{GS} - V_{TH(MOS)} \right) V_{DS} - \frac{1}{2} V_{DS}^2 \right] \quad (7.11a)$$

$$I_{DS} = \frac{1}{2} \beta \left( V_{GS} - V_{TH(MOS)} \right)^2 \quad (7.11b)$$

$$\text{where } \beta = C_{ox} \mu \frac{w}{l} \quad (7.11c)$$

where

$\mu$  = electron mobility,

$w$  = width of the channel,

$l$  = length of the channel,

$V_{GS}$  = Gate-Source voltage in volts, and

$V_{DS}$  = Drain-Source voltage in volts.

In MOSFET, the parameter  $\beta$  is a design constant and  $V_{DS}$  is kept constant by the applied electronic circuit. Moreover, the fabrication processes for MOSFET devices are so well controlled that  $V_{TH(MOS)}$  is also a constant. Thus,  $V_{GS}$  is the only input parameter. In conventional MOSFET, therefore,  $I_{DS} / V_{DS}$  curves are drawn as a function of  $V_{GS}$  as shown in Fig. 7.6 (a).

If proceeded like MOSFET then the general expressions for the drain current of ISFET in the non-saturated and saturated mode can be directly written respectively as:

$$I_{DS} = \beta \left[ \left( V_{GS} - V_{TH(IS)} \right) V_{DS} - \frac{1}{2} V_{DS}^2 \right] \quad (7.12a)$$

$$I_{DS} = \frac{1}{2} \beta \left( V_{GS} - V_{TH(IS)} \right)^2 \quad (7.12b)$$

$$\text{where } \beta = C_{ox} \mu \frac{w}{l} \quad (7.12c)$$

Since ISFET is a sensing device i.e., an ion sensor, the input parameter should be  $V_{TH}$ . And since  $V_{TH}$  can be chemically modified via the interfacial potential at the electrolyte/oxide interface,  $\Psi_0$ , the  $I_{DS} / V_{DS}$  curves are recorded as a function of pH of the solution as shown in Fig. 7.6(b). This effect is due to the relation  $\Psi_0 = f(\text{pH})$ . This analysis clearly indicates that an ISFET is electronically identical to a MOSFET and can be seen as an electronic device, with one additional feature: its threshold voltage can be chemically modified via the interfacial potential at the electrolyte/oxide interface.

This analysis also gives the answer of debates regarding the need of reference electrode. Since field effect concept is explored in ISFET, to charge the

electrolyte–insulator– semiconductor (EIS) structure, which is analogous to metal–oxide–semiconductor (MOS) structure, with the gate oxide as insulator, needs two connections – one in silicon and the other in the electrolyte. In order that the electrolyte terminal can be connected to one terminal of the voltage source, a reference electrode is required so that the reference electrode and electrolyte together can substitute the metal gate of MOSFET which is connected to one terminal of voltage source, i.e.  $V_{GS}$  [21].

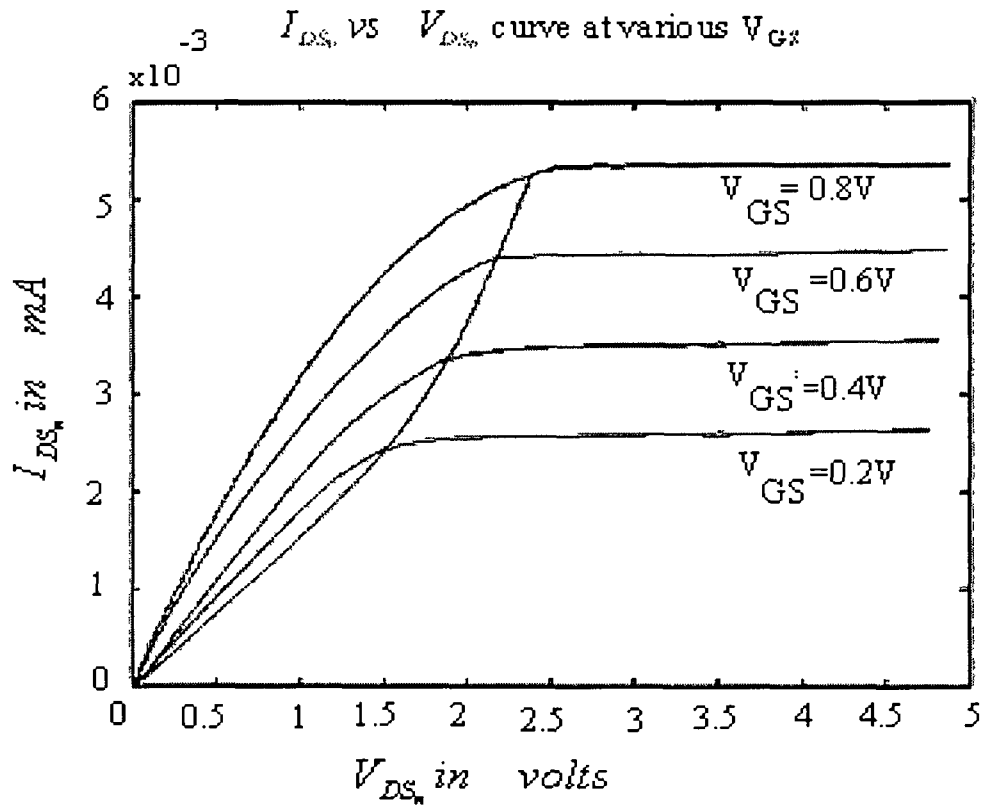


Fig. 7.6(a): Drain current vs. drain to source voltage at various Gate voltage of a MOSFET



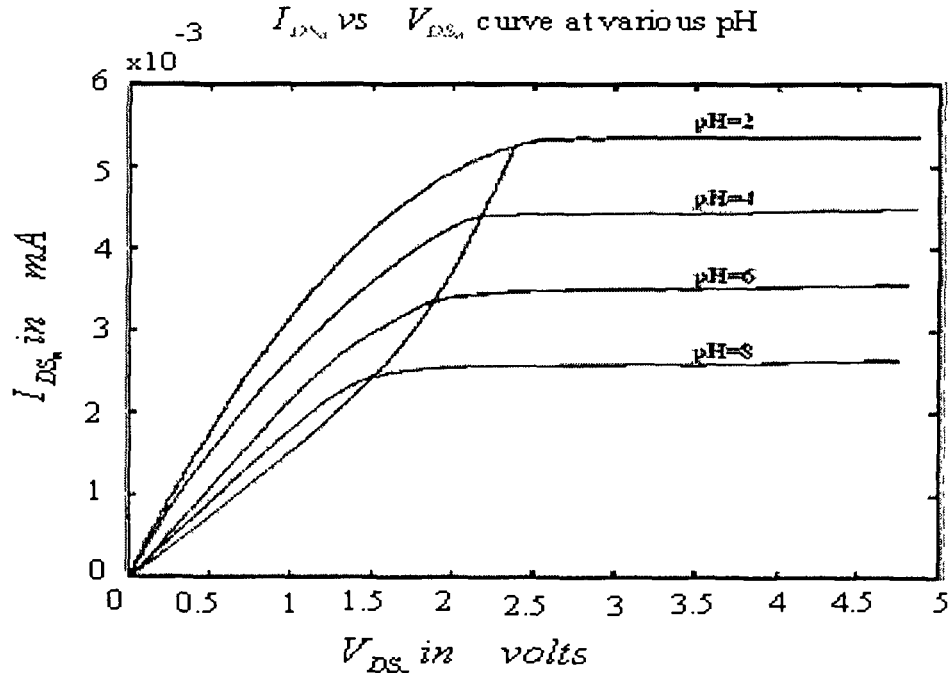
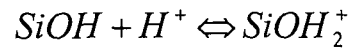
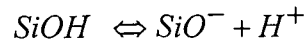


Fig. 7.6(b): Drain current vs. drain to source voltage at various pH of an ISFET

### 7.3.1.2 ISFET Operational Principle:

The mechanism responsible for the change in surface charge can be explained by well known site-binding theory introduced in 1973 by Yates et al. [22] to describe the properties of an oxide aqueous electrolyte interface and was generalized in 1986 by Fung et al [23] to characterize ISFETs with oxide insulators. According to this theory, the insulating surface contains hydroxyl groups (OH) which can be protonated (thus positively charged) or deprotonated (thus negatively charged) depending on the concentration of the hydrogen ions in the electrolyte. The surface hydroxyl groups which can bind hydrogen ions are called binding sites. In case of  $\text{SiO}_2$  insulator, it is assumed

that it has only one kind of  $H^+$ -specific binding site represented by  $SiOH$ ,  $SiO^-$  and  $SiOH^+$ . The ionization reactions are:



with  $H^+$  representing the protons in the vicinity of the surface. It is thus clear that the originally neutral surface may become a positive site or negative site by accepting or donating protons from or to the electrolyte solution respectively. As a result of these chemical reactions at the interface, the originally neutral oxide surface containing only neutral sites is converted into a charged surface having positive and negative charge sites. The resulting surface charge depends on an excess of one type of charged site over the other and is a function of the solution pH. For this reason  $H^+$  and  $OH^-$  are referred to as potential determining ions for this interface. Besides the potential determining ions, electrolyte has other anions and cations called electrolyte ions. These electrolyte ions form ion pairs with oppositely charged surface sites or groups - a process known as surface complexation. The formation of surface complexes also readjusts the acid - base equilibrium and affects the surface charge by partly compensating the charged sites. Of course, the distribution of ions in the electrolyte solution can be well explained by using Gouy - Chapman - Stern theory [24]. According to this theory, two layers are formed in the electrolyte solution. Double layer consists of Stern inner layer and a diffuse layer. Inner layer consists of two planes namely inner Helmholtz plane (IHP) and outer Helmholtz plane (OHP). IHP is the locus of centers of adsorbed ions which form pairs with the charged surface sites as already discussed in surface complexation. The OHP is the locus of the centers of the

hydrated ions with the closest approach to the surface. The diffuse layer extends from the OHP to the bulk of solution and contains the nonspecifically adsorbed ions that behave as an ionic cloud and balanced by the uncompensated surface sites. With this model, the electrical double layer behaves as two capacitors  $C_H$  and  $C_D$  in series where  $C_H$  is the Helmholtz capacitance and  $C_D$  is the diffused layer capacitance as shown in Fig. 7.7.

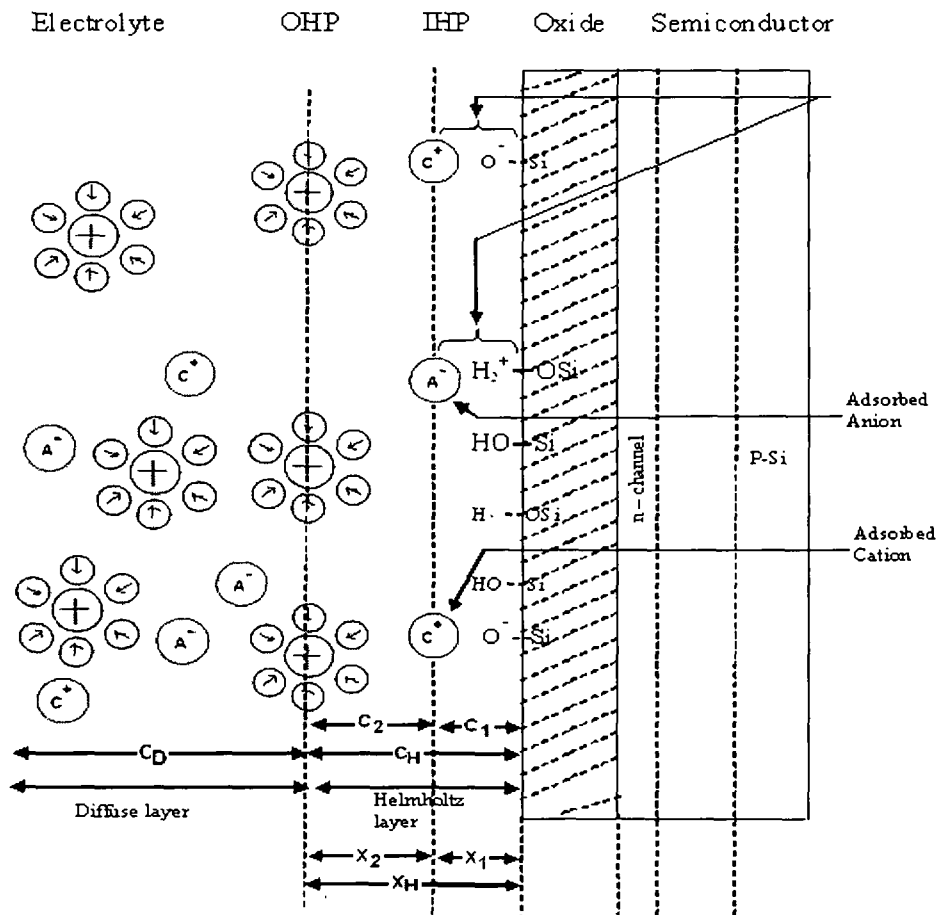


Fig. 7.7(a): Site binding theory of electrical double layer

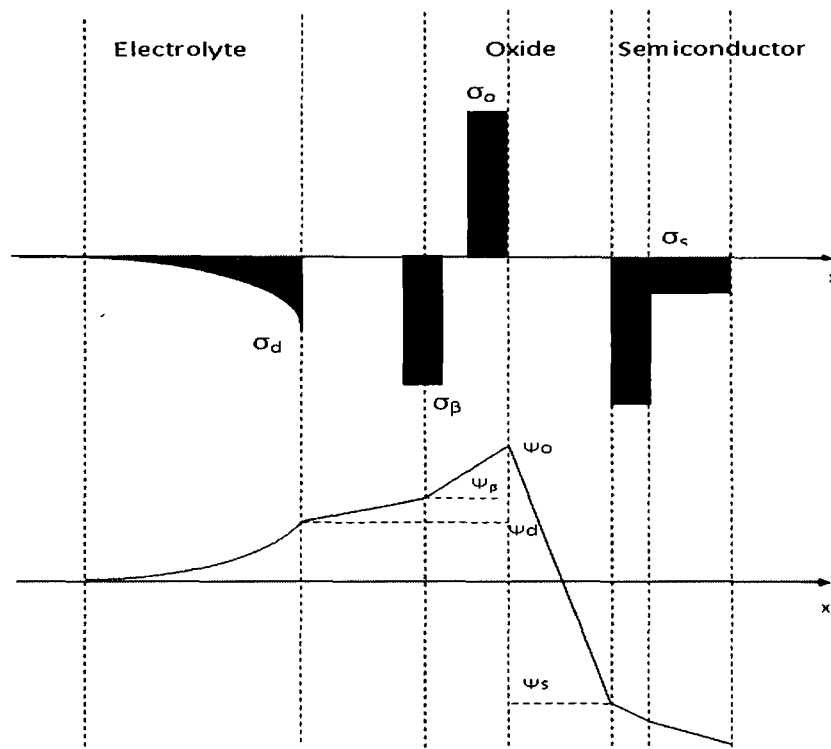


Fig. 7.7(b) Charge and potential distribution of an ISFET for  $\text{pH} < \text{pHzc}$

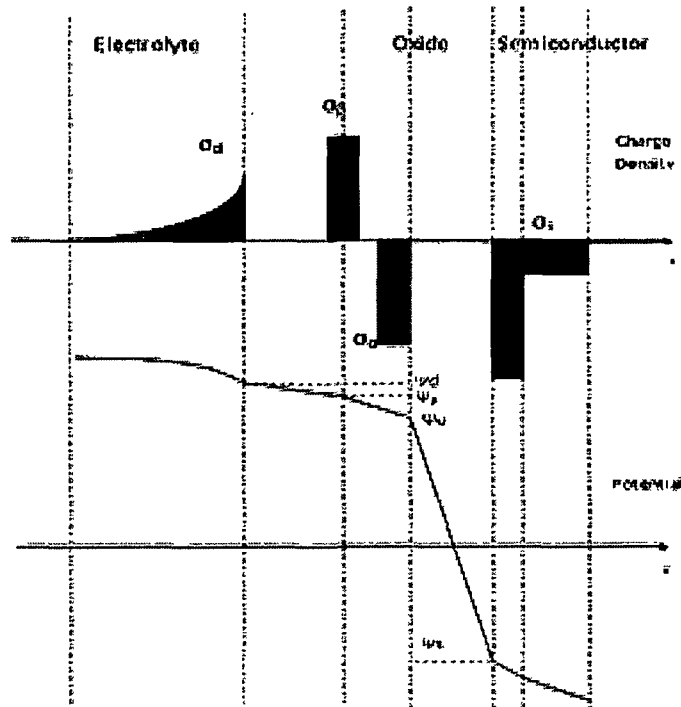


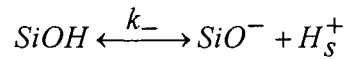
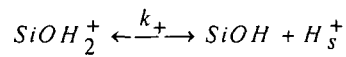
Fig. 7.7(c): Charge and potential distribution of an ISFET for  $pH > pH_{pzc}$

### 7.3.1.3 ISFET Modeling:

Modeling of ISFET provides important tools for prediction of function of the device for different new sensing materials that can be used to make devices with enhanced sensitivity. Since the introduction of site-binding model, many models have been developed- some are physico-chemical and some are based on SPICE (Simulation Program with Integrated Circuit Emphasis). But irrespective of different approaches, basic objective of ISFET modeling is to obtain a relationship of the form  $\Psi_0 = f(pH)$  and almost all models have considered the condition of charge neutrality of an electrolyte-insulator-semiconductor (EIS) system in conjunction with the site binding theory and

electrical double layer theory. The aim of this section is to describe some mathematical quantities used for many ISFET models.

Considering site-binding theory, let us denote  $\text{SiOH}_2^+$ ,  $\text{SiOH}$ ,  $\text{SiO}^-$  positive, neutral and negative surface sites of insulating surface. Exchange of the potential determining ions with these sites can be described as follows:



Under equilibrium conditions, the amphoteric dissociation constants are given by:

$$K_+ = \frac{[\text{SiOH}][\text{H}^+]_s}{[\text{SiOH}_2^+]} \quad (7.13)$$

$$K_- = \frac{[\text{SiO}^-][\text{H}^+]_s}{[\text{SiOH}]} \quad (7.14)$$

The subscript in  $[\text{H}^+]_s$  means that the concentration of protons is near the surface of the insulator, and  $[\text{SiOH}_s^+]$ ,  $[\text{SiOH}]$ , and  $[\text{SiO}^-]$  are the concentration of the proton binding sites present in the oxide surface.

Now according to the Boltzmann distribution, the relation between the concentration of an ion species  $X$  at a location  $i$  in the electrolyte double layer,  $[X]_i$ , and the concentration of the same species at the bulk electrolyte,  $[X]_b$ , is

$$[X]_i = [X]_b \exp\left(\frac{-q\psi_i}{kT}\right)$$

Therefore, equations (7.13) and (7.14) may be rewritten respectively as

$$K_+ = \frac{[SiOH][H^+]_b}{[SiOH_2^+]} \exp\left(-q\psi_0/kT\right) \quad (7.15)$$

$$K_- = \frac{[SiO^-][H^+]_b}{[SiOH]} \exp\left(-q\psi_0/kT\right) \quad (7.16)$$

Using this basic site binding model, Bousse et al. [25] develops a simple model and proven to be applicable for an ISFET surface of  $SiO_2$  and  $Al_2O_3$ . According to this model, the resulting equation for the surface potential is

$$\Psi_0 = 2.3 \frac{kT}{q} (pH_{pzc} - pH) \frac{\beta}{\beta + 1} \quad (7.17)$$

Where,  $pH_{pzc}$  is the value of the pH for which the oxide surface is electrically neutral and  $\beta$  determines the final sensitivity.

In 1996, based on the same site binding theory, a new model was developed by R.E.G. Van Hal et al [26]. This model explores the well known equation for capacitance  $Q = CV$ , where  $Q$  is the surface charge,  $C$  is the double layer capacitance at the interface and  $V$  is the surface potential denoted by  $\psi_0$ . According to this model,  $\psi_0$  can be expressed as

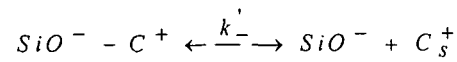
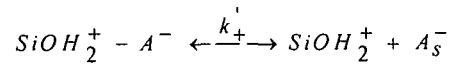
$$\Delta\Psi_0 = -2.3\alpha \frac{kT}{q} \Delta pH_{bulk} \quad (7.18)$$

With

$$\alpha = \frac{1}{\left(2.3kTC_{diff}/q^2\beta\right) + 1} \quad (7.19)$$

Where  $\beta$  symbolizes the ability of the oxide surface to deliver or take up protons called buffer capacity of the surface and  $C_{diff}$  is the differential double layer capacitance,  $\alpha$  is a dimension less sensitivity parameter varying between 0 and 1, depending on the intrinsic buffer capacity.

Considering electrolyte ions, the surface complexation due to anions and cations of electrolyte solution can be represented by the following chemical reactions:



Here the left hand sides represent the bindings with the surface charge groups.

The dissociation constants at equilibrium can again be written as:

$$K'_+ = \frac{[SiOH_2^+][A^-]_s}{[SiOH_2^+ - A^-]} \quad (7.20)$$

$$K'_- = \frac{[SiO^-][C^+]_s}{[SiO^- - C^+]} \quad (7.21)$$

Using Boltzmann distribution, we have

$$[C^+]_s = [C^+]_b \exp\left(\frac{-q\psi\beta}{kT}\right) \text{ and } [A^-]_s = [A^-]_b \exp\left(\frac{q\psi\beta}{kT}\right)$$

Therefore, the equations (7.20) and (7.21) may be rewritten as

$$K'_+ = \frac{[SiOH_2^+]}{[SiOH_2^+ - A^-]} C^0 \exp\left(\frac{q\psi\beta}{kT}\right) \quad (7.22)$$



$$K'_- = \frac{[SiO^-]}{[SiO^- - C^+]} C^0 \exp\left(\frac{-q\psi_\beta}{kT}\right) \quad (7.23)$$

where  $C^0$  is the electrolyte bulk concentration such that  $[C^+] = [A^-] = C^0$ .

On the oxide surface, there is a fixed number of surface sites per unit area,  $N_s$ :

$$N_s = [SiOH] + [SiOH_2^+] + [SiO^-] + [SiO^- - C^+] + [SiOH_2^+ - A^-] \quad (7.24)$$

Depending on the chemical equilibrium of the surface sites, a surface charge density  $\sigma_0 [C/m^2]$  exists:

$$\sigma_0 = q\left([SiOH_2^+] - [SiO^-] + [SiOH_2^+ - A^-] - [SiO^- - C^+]\right) \quad (7.25)$$

The combination of equations (7.13) to (7.16) and (7.21) to (7.22) yields [27]:

$$\sigma_0 = qN_s \frac{[H^+]_s^2 - K_+K_-}{\left([H^+]_s K_- + (1 + K'_-[A^-]_s)[H^+]_s^2 + K_+K_- + K_1K_2K'_+[C^+]_s\right)} \quad (7.26)$$

The charge density at IHP,  $\sigma_\beta [C/m^2]$  is:

$$\sigma_\beta = q\left([SiOH_2^+ - A^-] - [SiO^- - C^+]\right) \quad (7.27)$$

The diffuse layer charge density,  $\sigma_d [C/m^2]$  is [20]:

$$\sigma_d = -\sqrt{8kT\varepsilon_0\varepsilon_r C^0} \sinh\left(\frac{q\psi_d}{2kT}\right) \quad (7.28)$$

where  $\varepsilon_r$  is the dielectric constant of the solution,  $\varepsilon_0$  is the permittivity of the free space and  $C^0$  is the ion concentration in the bulk electrolyte.  $k$  is the Boltzmann constant and  $T$  is the absolute temperature.

The charge neutrality of the system requires that

$$\sigma_d + \sigma_\beta + \sigma_0 + \sigma_s = 0 \quad (7.29)$$

where semiconductor surface charge density  $\sigma_s$  is given by [28]:

$$\sigma_s = \sqrt{2\varepsilon_s\varepsilon_0kT \left[ p_0 \left( \exp\left(\frac{-q\psi_s}{kT}\right) + \frac{-q\psi_s}{kT} + 1 \right) + n_0 \left( \exp\left(\frac{q\psi_s}{kT}\right) - \frac{q\psi_s}{kT} - 1 \right) \right]} \quad (7.30)$$

where  $\varepsilon_s$  is the silicon relative permittivity and  $p_0$  and  $n_0$  are the equilibrium hole and electron concentration.

The charges and the potentials at the interfaces are related by the following equations:

$$\psi_0 - \psi_\beta = \frac{\sigma_0 + \sigma_s}{C_1} \quad (7.31a)$$

$$\psi_\beta - \psi_d = -\frac{\sigma_d}{C_2} \quad (7.31b)$$

$$\psi_s - \psi_0 = \frac{\sigma_s}{C_0} \quad (7.31c)$$

where  $C_1$  and  $C_2$  are the unit area capacitances of the inner and outer Helmholtz layers respectively and  $C_0$  is the unit area capacitance of the insulator film.

The system of equations that can describe an ideal electrolyte-insulator-semiconductor (EIS) structure can now be described as follows: equations (7.13) through (7.16) and (7.20) through (7.28) represent the reaction at the electrolyte –insulator interface and the charge potential relationships in the electrolyte diffused layer and oxide surface. The condition for charge neutrality is given by equation (7.29). The charge potential relationship on the semiconductor surface is given by the equation (7.30). The link between the different regions such as OHP, IHP, oxide surface and semiconductor surface

of the system is contained in equations (7.31). It is obvious from the equations (7.31a) and (7.31c) that the semiconductor surface potential is dependent on the oxide surface potential  $\Psi_0$  and hence the measurement of  $\sigma_s$  will provide a means of obtaining the surface potential  $\Psi_0$  at the electrolyte-oxide interface. The dependence of the oxide surface potential  $\Psi_0$  on the pH can be verified by solving the set of equations mentioned above. Some values required for simulation purpose, collected from various papers have been presented in Table 7.3.

Table 7.3: Some values required for simulation

Materials	Values of $K_+$ $K_-$	Values in $\mu\text{F} / \text{cm}^2$ $C_1$ $C_2$	Values of $K_+ /$ $K_- /$	Number of binding sites	Types of binding sites	$\text{pH}_{\text{PZC}}$
$\text{SiO}_2$	$63.1 \times 10^{-9}$ 15.8	120 20	0.317 0.9	-	Nsil	3
$\text{Si}_3\text{N}_4$	$63.1 \times 10^{-9}$ 15.8	120 20	0.317 0.9	$1.0 \times 10^{-10}$	Nsil & Nnit	6.8
$\text{Al}_2\text{O}_3$	$79.9 \times 10^{-10}$ $12.6 \times 10^{-9}$	120 20	0.317 0.9	-	Nsil	8.5

### 7.3.1.4 ISFET Technology:

As mentioned above, ISFETs are fundamentally MOSFETs, therefore, the classic microelectronic technology of integrated circuits (IC) is also the basic technology used in ISFET development. The fabrication step is similar to the process of the p-channel or n-channel metal gate MOSFETs. ISFETs are fabricated with silicon films on sapphire wafers (SOS). The gate  $\text{SiO}_2$  film is thermally grown on the surface of the substrate at about  $1000^\circ\text{C}$ . But unlike the MOSFETs, the selection of gate dielectric coating of ISFETs is important

as protonation/deprotonation of this material is influenced by the pH of the electrolyte. The various methods used for fabrication of these coatings are plasma enhanced chemical vapor deposition (PECVD), plasma anodic oxidation, evaporation by electron beam, sputtering etc. [29]. The pH response of different types of oxide coatings is presented in Table 7.4. As far as physical shape is concerned, most ISFETs have source, drain and gate on the same side of the chip but there are also those in which drain-source and gate are placed on the opposite sides of the substrate [30]. The specifications of various ISFETs fabricated at different institutes, laboratories, groups etc. are given in Table 7.5 [31] – [33]. The review by Sergei V. Dzyadevych et al., describe the development of ISFETs including the technology in details [15]. The latest investigations concern the miniaturization of reference electrodes for field effect sensors compatible with silicon chip technology [34], the integration of biosensors based on ISFETs into a flow-injection analysis system and the development of nanoscale ISFETs.

Table 7.4 Specifications of pH sensors having different sensitive layer

Sensitive layer	pH range	Sensitivity (mV / pH)
SiO <sub>2</sub>	2-5	25-48
Al <sub>2</sub> O <sub>3</sub>	2-12	53-57
Si <sub>3</sub> N <sub>4</sub>	2-12	46-56
Ta <sub>2</sub> O <sub>5</sub>	2-12	56-57

Table 7.5: Specifications of ISFET-based pH sensors manufactured by different institutes, laboratories, groups

Institutes/ laboratories/ groups	Sensitive layer	$I_D / V_D$ ( $\mu\text{A}$ / $\text{V}$ )	pH range	Sensitivity (mV /pH)
RIMD (Ukraine)	$\text{Si}_3\text{N}_4$	200 / 1	2-12	30-40
LASS (France)	$\text{SiO}_2$ / $\text{Si}_3\text{N}_4$	100 / 1	3-9	40-50
ESIEE (France)	$\text{Si}_3\text{N}_4$	200/1	7-12	15
ITIMS (Vietnam)	$\text{SiO}_2$	200-500 / 0.2-1	2.5-8	11-13

ISFET are microelectronic/nanoelectronic devices and have been found to be growing interest in the rapidly developing field of bioelectronics encompassing a very wide spectrum of applications. Many ISFET based pH electrodes have been reported in recent years, most of which are in the state of commercialization. A good number of companies, including giants in this field are involved in their manufacturing and marketing. They have even been presenting the advantages of ISFET based pH electrodes via various media to promote the development of ISFET based sensors such as CHEMFET, ENFET, BIOFET, and DNAFET etc. The advantages that they have highlighted are unbreakable, portable, fast response, easy to store and clean for repeated use. They can also be used for direct measurement in complex aqueous and semisolid samples like cheese, meat, etc and have potential for on-chip circuit integration leading to the development of micrototal analysis system and can also be mass-produced by existing integrated circuit(IC) batch production technology. Due to these advantages, extensive research is being carried out in a number of Universities/laboratories across the globe to develop various ISFET based biosensors mainly for biomedical, bio-

analytical, food processing, defense applications. Though, a series of reliable and promising results have been obtained, no successful commercial version of ISFET based biosensor is available so far. Keeping these factors in view, it is expected that like the ISFET based pH electrode, attempts to commercialize the biosensors will also be made in near future. In view of the future perspective of nano technology, efforts have also been made by the Bioelectronics Division of Tezpur University with special emphasis on modeling of different geometries of ISFET devices at very small dimensions such as the Cylindrical ISFET, Conical ISFET etc.

### 7.3.2 ISFET Based Modified H-H Model:

Referring to the equation (7.12a), for very small value of drain to source voltage,  $V_{DS}$ , the conductance of ISFET in its linear region can be written as

$$\frac{I_{DS}}{V_{DS}} = \beta (V_{GS} - V_{TH(IS)})$$

or,  $G_{DS} = \beta (V_{GS} - V_{TH(IS)})$  (7.32)

where,  $\beta = \mu C_{ox} \frac{W}{l}$  (7.33)

In equation (7.32),  $\beta$  and  $V_{GS}$  are constants and  $V_{TH (IS)}$  is the only input variable. Thus  $G_{DS}$  is dependent on the threshold voltage,  $V_{TH(IS)}$ , analogous to the conductance of ion channels of postsynaptic membrane dependent on the binding activity. Thus, considering the transmitter-receptor binding activity, the H-H model for membrane can be modified as shown in Fig. 7.8. Here  $V_{gN}$  and  $V_{gL}$  are fixed gate voltages applied to the reference electrodes of ISFETs

and  $V_{TH1}$  and  $V_{TH2}$  are the respective threshold voltages of ISFETs that control the conductances  $g_{Na}$  and  $g_{Cl}$  respectively.

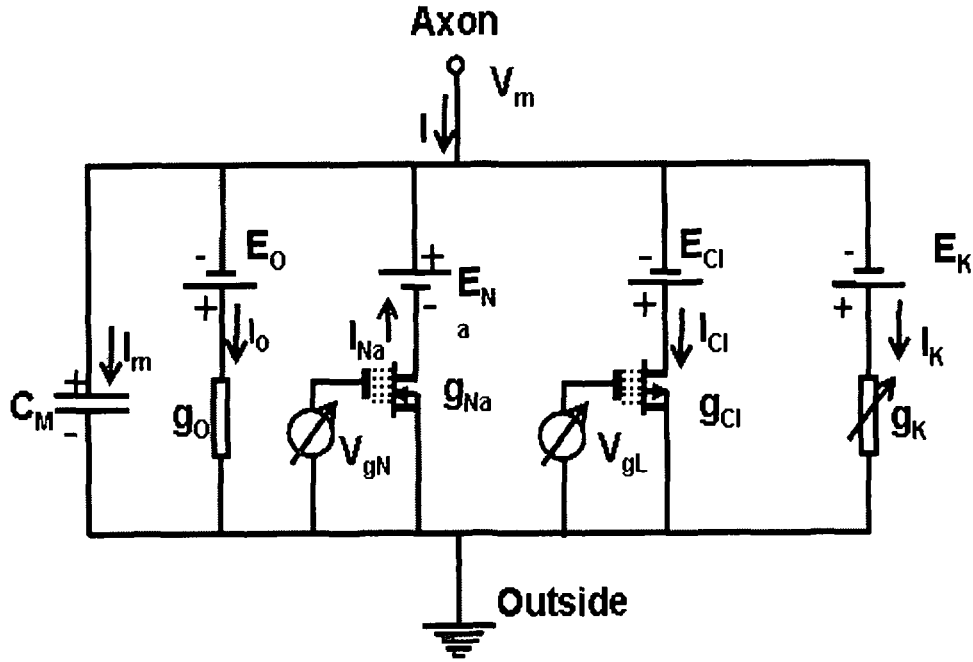


Fig. 7.8: Modified H-H model of Postsynaptic membrane

Neurotransmitter-receptor binding activity is a time dependent phenomenon and therefore number of opening of transmitter gated ion channels will be varying with respect to time.  $V_{TH(IS)}$  in equation (7.32) can, therefore, be modeled as given in equation (7.4):

$$V_{TH(IS)}(t) = V_{THO} \left[ \left( 1 - \exp(-k_1 t) + \exp(-k_2 t) U(t - t_m) \right) \right] \quad (7.34)$$

Where  $K_1$  and  $K_2$  are time constants analogous to the rate constants of equation (7.9),  $U(t - t_m)$  is the Heaviside function and  $V_{THO}$  is the threshold voltage proportional to the maximum attainable conductance, when all the transmitter-gated channels for specific ions are open.

### 7.3.2.1 Modeling Neuron for Excitatory Synapse:

The modeling for excitatory synapse is shown in Fig. 7.9. The leakage current  $I_o$  is considered to be small enough to be neglected. Since only sodium channels are responsible for excitatory action, the postsynaptic membrane is divided into three patches to represent spatial summation of the sodium current controlled by  $g_{Na_1}$ ,  $g_{Na_2}$ , and  $g_{Na_3}$ , where

$$I_{Na} = I_1 + I_2 + I_3 \quad (7.35)$$

So that,  $I = I_m - I_{Na} + I_K$

$$= C_m \frac{dV_m}{dt} - g_{Na}(V_m - E_{Na}) + g_K(V_m - E_K) \quad (7.36)$$

Where  $g_{Na} = g_{Na_1} + g_{Na_2} + g_{Na_3}$  and  $g_K$  is the total Potassium conductance.

The membrane potential  $V_m$  is obtained by spatially and temporally varying  $g_{Na}$  of transmitter-gated sodium channels.



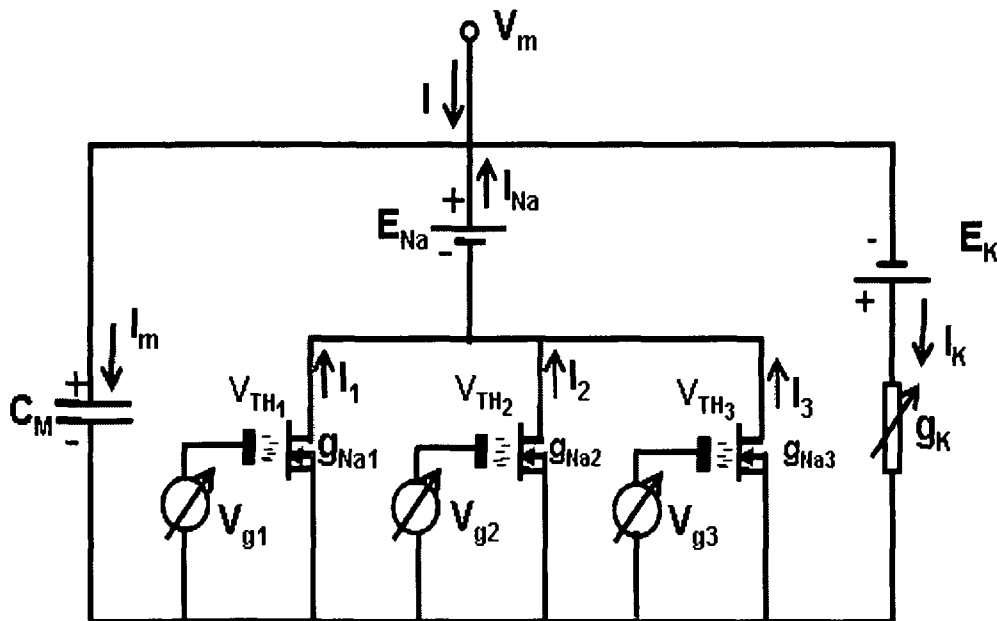


Fig. 7.9: ISFET based Circuit model for excitatory action of synapse

The component values assigned in the model for MATLAB simulation are taken from reference [35] and are given in Table 7.6. The specifications for three n-channel ISFETs as well as the parameters for exponential function in equation (7.34), applied to each ISFET inputs are also given in Table 7.6. The three gate to source voltages of three ISFETs i.e.,  $V_{g1}$ ,  $V_{g2}$  and  $V_{g3}$  are kept constants at 1 Volt each. The three input parameters of ISFETs namely  $V_{TH1}$ ,  $V_{TH2}$  and  $V_{TH3}$  are applied in a staggered sequence at 1.5 msec intervals. This is done to simulate the time variation in neurotransmitter-receptor binding with respect to different patches of postsynaptic membrane in accordance with reference [35].

TABLE 7.6  
DIFFERENT COMPONENTS USED IN THE PROPOSED MODEL OF EXCITATORY SYNAPSE

Sl. No.	Parameter	Parameter Details	Unit	Value
01	$C_M$	Membrane Capacitance	Farad	1 $\mu\text{F}$ per $\text{cm}^2$
02	$g_K$	Potassium Conductance	Mho	1 $\text{mS}$ per $\text{cm}^2$
03	$E_{\text{Na}}$	Sodium Potential	Volt	60mV
04	$E_K$	Potassium Potential	Volt	-90mV
05	$I$	Membrane Current	Ampere	0 A
06	$L$	Channel Length	Meter	15 $\mu\text{m}$
07	$W$	Channel Width	Meter	2 $\mu\text{m}$
08	$t_{\text{ox}}$	Oxide Thickness	Meter	100 nm
09	$\mu$	Electron mobility	$\text{cm}^2/\text{V-sec}$	600 $\text{cm}^2/\text{V-sec}$
10	$V_{\text{THO}}$	Threshold Voltage	Volt	- 2 Volts
11	$t_m$	Time	Second	600 $\mu\text{sec}$
12	$k_1 = k_2$	Time Constant	Second	0.8 msec

### 7.3.2.2 Modeling Neuron for Inhibitory Synapse:

The modeling for inhibitory synapse is shown in Fig. 7.10. Considering only  $\text{Cl}^-$  channels to be responsible for inhibitory action, the post synaptic membrane is divided into three patches to represent spatial summation of the Chloride current controlled by  $g_{\text{Cl}1}$ ,  $g_{\text{Cl}2}$  and  $g_{\text{Cl}3}$ , where

$$I_{\text{Cl}} = I_1 + I_2 + I_3 \quad (7.37)$$

So, that,  $I = I_m + I_{\text{Cl}} + I_K$

$$= C_m \frac{dV_m}{dt} + g_{\text{Cl}}(V_m - E_{\text{Cl}}) + g_K(V_m - E_K) \quad (7.38)$$

Where  $g_{Cl} = g_{Cl1} + g_{Cl2} + g_{Cl3}$  and  $g_K$  is the total Potassium conductance.

The membrane potential  $V_m$  is obtained by spatially and temporally varying  $g_{Cl}$  of transmitter-gated Chlorine channels.

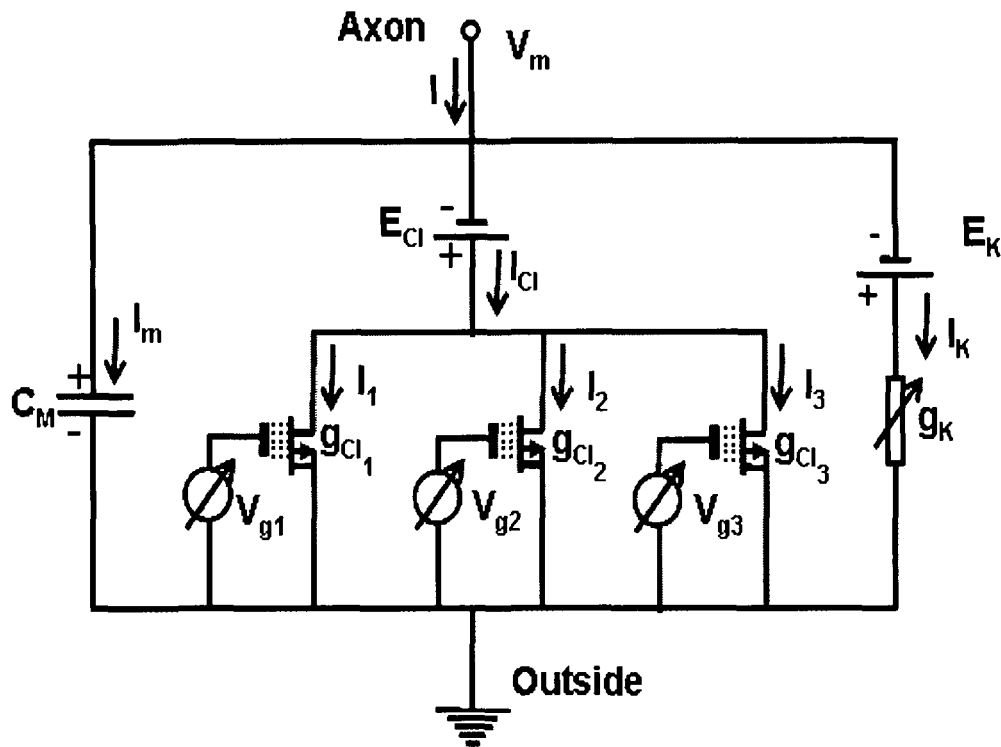


Fig. 7.10: ISFET based Circuit model for inhibitory action of synapse

Table 7.7 summarizes the component values assigned in the model for MATLAB simulation for inhibitory action of synapse. The specifications for three p-channel ISFETs as well as the parameters for exponential function in equation (7.34), applied to each ISFET inputs are also given in Table 7.7. The three gate to source voltages of three ISFETs i.e  $V_{g1}$ ,  $V_{g2}$  and  $V_{g3}$  are kept

constants at 1Volt each. The three input parameters of ISFETs namely  $V_{TH1}$ ,  $V_{TH2}$  and  $V_{TH3}$  are applied in a staggered sequence at 1.5 msec intervals. This is done to simulate the time variation in neurotransmitter –receptor binding with respect to different patches of postsynaptic membrane.

**TABLE 7.7**  
**DIFFERENT COMPONENTS USED IN THE PROPOSED MODEL OF INHIBITORY SYNAPSE**

Sl. No.	Parameter	Parameter Details	Unit	Value
01	Parameter	Parameter Details	Unit	Value
02	$C_M$	Membrane Capacitance	Farad	1 $\mu$ F per $cm^2$
03	$g_K$	Potassium Conductance	Mho	1 mS per $cm^2$
04	$E_{Cl}$	Chloride Potential	Volt	-100mV
05	$E_K$	Potassium Potential	Volt	-90mV
06	I	Membrane Current	Ampere	0 A
07	L	Channel Length	Meter	15 $\mu$ m
08	W	Channel Width	Meter	2 $\mu$ m
09	$t_{ox}$	Oxide Thickness	Meter	100 nm
10	$\mu$	Electron mobility	$cm^2/V$ -sec	600 $cm^2/V$ -sec
11	$V_{THO}$	Threshold Voltage	Volt	5 Volts
12	$t_m$	Time	Second	850 $\mu$ sec

### 7.3.2.3 Results:

The MATLAB simulation outputs are shown in Fig. 7.11. The top waveform represents the normal postsynaptic membrane potential. Here  $V_m$  is established by spatial summation and temporal integration of the transmitter gated sodium current and non-gated potassium current. Simulation results indicate that when  $V_m$  exceeds a threshold in the range of -60 to -40mV, an action potential initiates which illustrates an EPSP. The bottom waveform represents the

inhibitory action. It illustrates an IPSP with sufficient amplitude for triggering an action potential in negative direction. The simulated EPSP and IPSP are very similar to the experimentally recorded ones, i.e., with real excitatory and inhibitory actions of postsynaptic membrane.

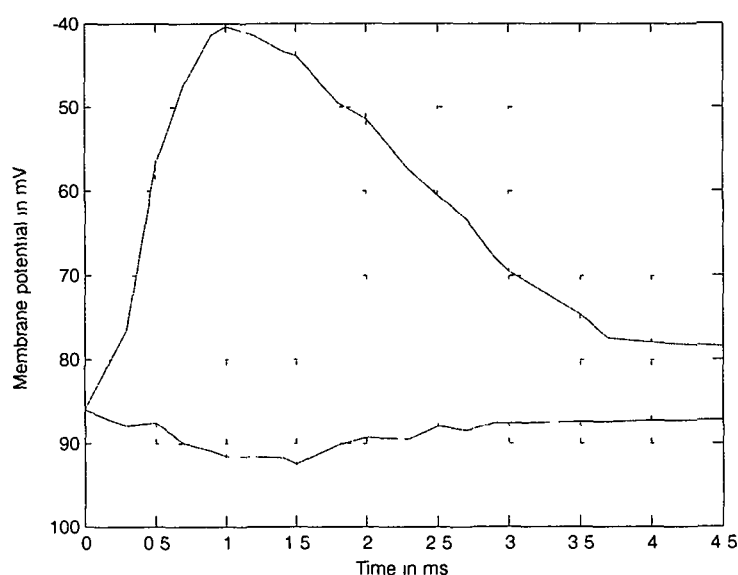


Fig 7.11 Simulation results of excitatory and inhibitory actions of postsynaptic membrane. Top waveform represents the EPSP and bottom waveform represents the IPSP.

ISFET based electrical models both for excitatory and inhibitory actions of neurons have been developed. Postsynaptic membrane is divided into three patches to represent spatial summation of gated currents. Temporal integration of the currents is achieved by modeling exponentially varying time dependent threshold voltage of ISFET. The main aim of this work is to show that ISFET can be used as circuit analog to simulate the excitatory and inhibitory postsynaptic potentials with an additional advantage possibility of measurement of neurotransmitters diffused through the synaptic cleft by

converting the ISFET into neurotransmitter sensitive ENFET [8]. This biologically motivated model may become a useful research and teaching unit both in neurology and bioelectronics areas.

The results obtained from simulation using ISFET are also compared with those reported by previous researchers and with the other proposed models and are given in Table 7.8.

TABLE 7.8  
COMPARISON OF SIMULATION RESULTS

Excitatory				Inhibitory			
Sl. No.	Threshold limit to initiate action potential	Time to attain peak value	Total duration of EPSP	Sl. No.	Threshold limit to initiate action potential	Time to attain peak value	Total duration of IPSP
[1]	- 65 mV to - 50 mV	1 ms	3.5 ms	[1]	No Action Potential	1.2 ms	3.5 ms
[35]	- 60 mV to - 40 mV	3 ms	6 ms	[35]	Simulation performed only for excitatory synapse		
Present Work of 7.2	- 60 mV to - 40 mV	1 ms	3.5 ms	Present Work of 7.2	No Action Potential	1.5 ms	3 ms
Present Work of 7.3	- 60 mV to - 40 mV	1 ms	3.5 ms	Present Work of 7.3	No Action Potential	1.5 ms	3 ms

## **7.4 Biologically Inspired Circuit Model for Simulation of Acetylcholine Gated Ion Channels of the Postsynaptic Membrane at Synaptic Cleft:**

The purpose of this work is to develop a simple analog circuit model that can simulate the function of neurotransmitter acetylcholine gated ion channels of postsynaptic membrane at the synaptic cleft. Simulation is performed in MATLAB environment for excitatory actions of synapses both for normal and pathologic states.

It has been mentioned in the previous section that ISFET can be converted into Enzyme Modified Field Effect Transistor (ENFET) by immobilizing specific enzyme on its gate surface. Acetylcholine sensitive ENFET devices have practical applications, specially in the analysis of phosphorous pesticides or nerve gases. In view of its practical implications a description of such devices are discussed below.

### **7.4.1 Acetylcholine (ACh):**

The acetylcholine (ACh) is a chemical compound which acts as a neurotransmitter in both the peripheral nervous system (PNS) and central nervous system (CNS). ACh is the only neurotransmitter used in the motor division of the somatic nervous system (Sensory neurons use glutamate and various peptides at their synapses). ACh is also the principal neurotransmitter in all autonomic ganglia. ACh basically acts as excitatory neurotransmitter, but can work as inhibitory neurotransmitter. ACh behaves as an excitatory neurotransmitter at neuromuscular junctions. But, it slows down the heart rate

when functioning as an inhibitory neurotransmitter. Acetylcholine is considered to be the first neurotransmitter which was identified.

Acetylcholine functions both in the PNS and in the CNS as a neuromodulator. In the PNS, acetylcholine activates muscles, and is a major neurotransmitter in the autonomic nervous system. In the CNS, acetylcholine and the associated neurons form a neurotransmitter system, the cholinergic system, which tends to cause anti-excitatory actions.

In the PNS, when acetylcholine binds to acetylcholine receptors on skeletal muscle fibers, it opens ligand-gated sodium channels in the cell membrane. Sodium ions then enter the muscle cell, initiating a sequence of steps that finally produce muscle contraction. Although acetylcholine induces contraction of skeletal muscle, it acts via a different type of receptor (muscarinic) to inhibit contraction of cardiac muscle fibers.

In the CNS, ACh has a variety of effects as a neuromodulator upon plasticity, arousal and reward. ACh has an important role in the enhancement of sensory perceptions when we wake up and in sustaining attention. Damage to the cholinergic (acetylcholine-producing) system in the brain has been shown to be plausibly associated with the memory deficits associated with Alzheimer's disease.

Acetylcholine and the associated neurons form a neurotransmitter system, the cholinergic system from the brainstem and basal forebrain that projects axons to many areas of the brain. In the brainstem it originates from the Pedunclopontine nucleus and dorsolateral tegmental nuclei collectively known as the mesopontine tegmentum area or pontomesencephalotegmental complex. In the basal forebrain, it originates from the basal optic nucleus of



Meynert and medial septal nucleus. In addition, ACh acts as an important internal transmitter in the striatum, which is part of the basal ganglia. It is released by a large set of interneurons with smooth dendrites, known as tonically active neurons or TANs.

Acetylcholine is synthesized in certain neurons by the enzyme choline acetyltransferase from the compounds choline and acetyl-CoA. The enzyme acetylcholinesterase converts acetylcholine into the inactive metabolites choline and acetate. This enzyme is abundant in the synaptic cleft, and its role in rapidly clearing free acetylcholine from the synapse is essential for proper muscle function. Certain neurotoxins work by inhibiting acetylcholinesterase, thus leading to excess acetylcholine at the neuromuscular junction, thus causing paralysis of the muscles needed for breathing and stopping the beating of the heart.

There are two main classes of acetylcholine receptor (AChR), nicotinic acetylcholine receptors (nAChR) and muscarinic acetylcholine receptors (mAChR). They are named for the ligands used to activate the receptors.

Nicotinic AChRs are ionotropic receptors permeable to sodium, potassium, and chloride ions. They are stimulated by nicotine and acetylcholine. They are of two main types, muscle type and neuronal type. The former can be selectively blocked by curare and the latter by hexamethonium. The main location of nicotinic AChRs is on muscle end plates, autonomic ganglia (both sympathetic and parasympathetic), and in the CNS. The disease myasthenia gravis, characterized by muscle weakness and fatigue, occurs when the body inappropriately produces antibodies against acetylcholine nicotinic receptors,

and thus inhibits proper acetylcholine signal transmission. Over time, the motor end plate is destroyed.

Muscarinic receptors are metabotropic, and affect neurons over a longer time frame. They are stimulated by muscarine and acetylcholine, and blocked by atropine. Muscarinic receptors are found in both the CNS and the PNS, in heart, lungs, upper GI tract and sweat glands [36].

#### **7.4.2 Acetylcholine-sensitive ENFET:**

The application of enzymes as bioactive matrices for tailoring of biosensors and bioelectronic devices is of substantial basic and practical importance. The organization of biosensor and bioelectronic devices requires the integration of the biomaterial, e.g. enzyme, with a transducer to generate an electronically contacted assembly that enables the electronic transduction of biorecognition or biocatalytic events occurring on the transducer.

Electrical contacting of redox-proteins and electrode supports can be accomplished by the application of diffusional electron-transfer mediators, by tethering of redox-relay on the enzyme and by the immobilization of redox biocatalysts in redox-polymer systems.

The assembly of monolayers and multilayers of biomaterials on electronic supports can be used as a general method to organize biosensing systems. The thin sensing interfaces of monolayer/multilayer assemblies provide matrices that lack diffusion barriers for the analyte penetration. Redox-relay-tethered enzyme layers assembled on electrodes, surface-reconstitution of apo-proteins on redox-relay/cofactor composite layers, and crosslinking of complex composite layers consisting of redox-enzyme / cofactor / redox-relay units were reported as electrically contacted enzyme-electrodes for electrochemical

sensing. Similarly, antigen monolayers associated with electrodes or oligonucleotide-functionalized electrodes can be used for the electrochemical detection of antibodies and DNA, respectively.

The application of silicon-based microelectronics, and particularly ion-sensitive field-effect transistors (ISFETs) as transduction elements for biocatalytic transformations and biological recognition events, is a challenging subject in bioelectronics and analytical chemistry. Enzyme-based field-effect transistors, ENFETs, are based on biocatalytic reactions affecting the charge at the gate surface, and producing an electronic signal dependent on the enzyme substrate concentration. The sensing performance of the ENFET is affected by the integration method of the enzymes and the ISFET device. The immobilization of enzymes in thick polymer films (such as polyvinylchloride, polyacrylamide hydrogels or polyurethane) on ISFET devices, or the construction of membrane- (e.g. Nafion or polyvinylpyridine) covered crosslinked enzyme matrices on the ISFET, yield active ENFET sensing devices. These bioelectronic systems, however, suffer from basic limitations associated with diffusion barriers of the substrates through the polymer membranes, leading to slow response times and moderate sensitivities. The organization of monolayer/multilayer enzyme-based ISFET could substantially improve the response-times and analytical performance of the ENFET devices. ENFETs can be fabricated by the nano-engineering of the electronic device with a nanoporous thin film that is functionalized with a biocatalytic enzyme-monolayer. The Acetylcholine-Sensitive ENFET is in fact an ISFET whose gate surface is immobilized with enzyme, acetylcholine-esterase.

Fig. 7.12 outlines the configuration of this ENFET device. Field-effect transistors with an  $\text{Al}_2\text{O}_3$  gate is used as the transducer of the ENFET. An Ag / AgCl-electrode is used as a reference electrode. The differential output signal between the source of the ENFET device and the reference electrode is recorded with a semiconductor parameter analyzer keeping the drain current ( $I_d$ ) and source-drain voltage ( $V_{ds}$ ) constant. The schematic diagram as well as its electronic diagram is shown in Fig. 7.13. The equation 7.39 summarizes the biocatalytic transformation stimulated by the acetylcholine-esterase enzyme that is used to generate ENFET sensor sensitive to acetylcholine.

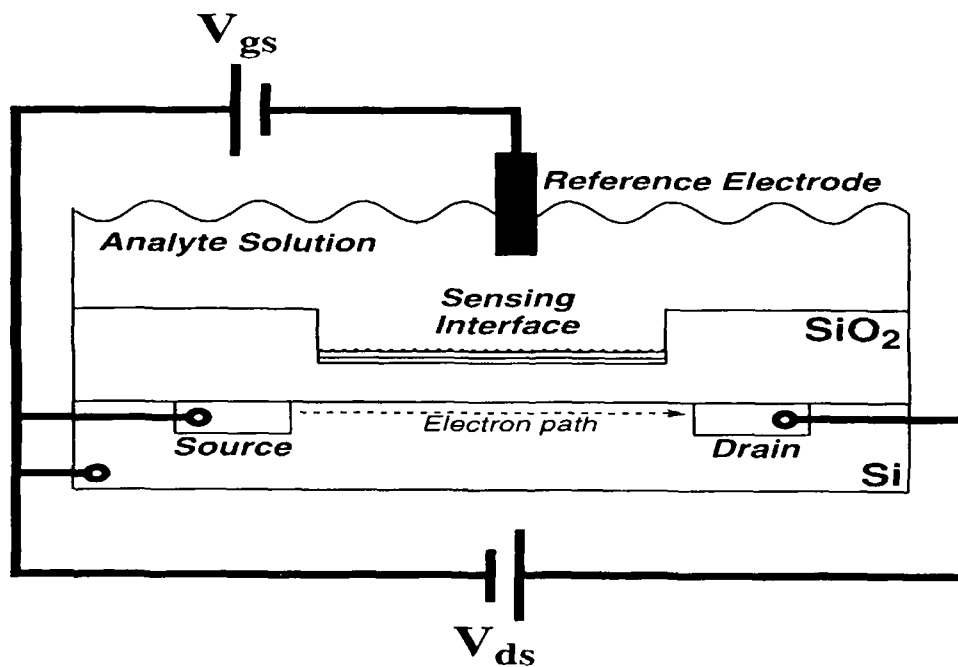
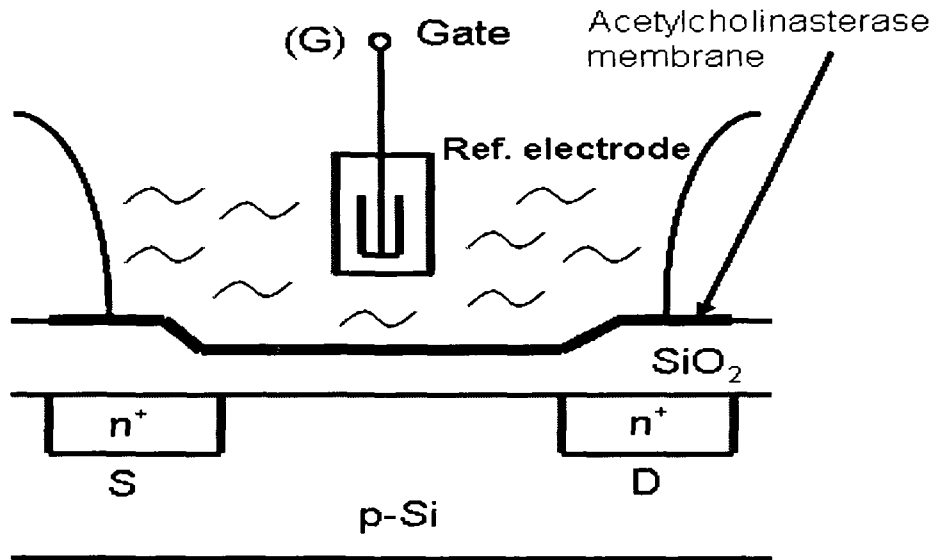
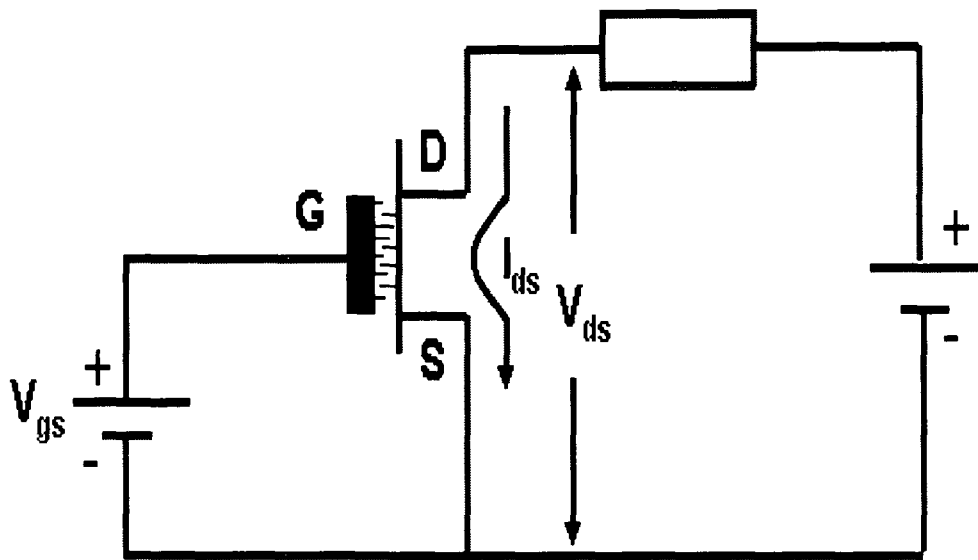


Fig. 7.12: General configuration of ENFET.

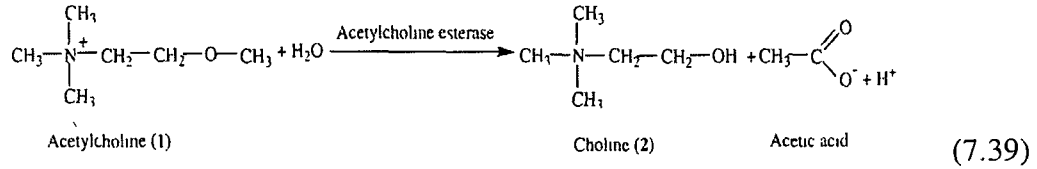


(a)



(b)

Fig. 7.13: Acetylcholine ENFET (a) Schematic diagram (b) Electronic diagram



The proton generated in this reaction alters the pH at the gate surface which is registered by the underlying ISFET. These changes in the pH affect the potential of the gate interface and consequently affect the potential difference between the gate and the source electrode ( $V_{GS}$ ) when  $I_D$  and  $V_{DS}$  are kept constant.

Since it is essentially an ISFET, the governing equation with reference to the equation (7.32) can therefore be written as-

$$G_{DS} = \beta (V_{GS} - V_{TH(ENFET)}) \quad (7.40)$$

$$\text{Where, as previous } \beta = \mu C_{ox} \frac{W}{L} \quad (7.41)$$

Here  $V_{TH(ENFET)}$  is a function of pH of solution dependent on the concentration of acetylcholine. Response of such a particular device with respect to  $V_{GS}$  is shown in Fig. 7.14 [8].

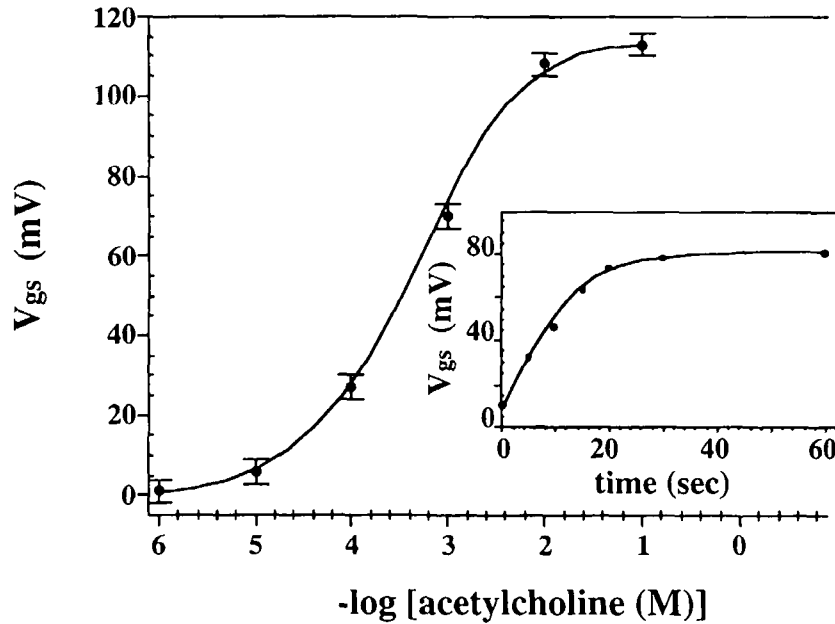


Fig 7.14 Calibration plot of the AChE-modified ENFET in the presence of different concentrations of acetylcholine. Inset: time-dependent response of the AChE-modified ENFET upon interaction with an acetylcholine solution [8].

### 7.4.3 Circuit Model based on Acetylcholine Sensitive ENFET:

Referring to equation (7.40) i.e.

$$G_{DS} = \beta (V_{GS} - V_{TH(ENFET)})$$

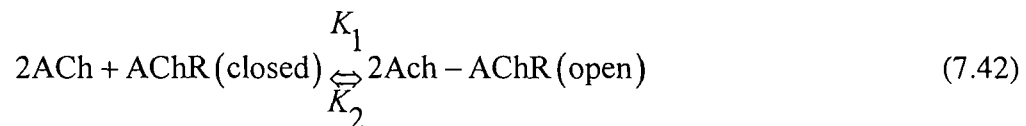
In ENFET,  $\beta$  and  $V_{GS}$  are constants and  $V_{TH(ENFET)}$  is the only input variable. Thus  $G_{DS}$  is dependent on the threshold voltage,  $V_{TH(ENFET)}$ , analogous to the conductance of ion channels of postsynaptic membrane dependent on the

binding activity. The acetylcholine gated ion channels can therefore be represented by acetylcholine sensitive ENFET due to its variable nature of conductance with respect to voltage.

In case of excitatory action, acetylcholines (Ach) are released by the presynaptic terminals into the synaptic cleft. Acetylcholines diffuse through the cleft and bind with specific receptor sites of post synaptic membrane. These receptors are called nicotinic acetylcholine receptors (AChR). The acetylcholine – receptor binding activity initiates the opening of sodium channels causing the flow of sodium ions into the cell. If a sufficient number of channels open, then the membrane potential exceeds the threshold for initiating an action potential.

In the case of pathologic state, the number of functional receptor sites in the post synaptic membrane is reduced. This is caused by an autoimmune disease, called myasthenia gravis, where the host manufactures antibodies. These antibodies destroy acetylcholine receptors in the post synaptic membrane at the synaptic cleft causing the reduction of functional receptors and hence the neurotransmitter – receptor binding activity at the postsynaptic membrane. In this condition, sufficient numbers of channels are not open to initiate an action potential and as a result the patient suffers from muscle weakness [35].

In simplest case the acetylcholine – receptor binding activity is governed by the chemical reaction [35]-



Where  $K_1$  and  $K_2$  are the forward and backward rate constants respectively.



Acetylcholine-receptor binding activity is a time dependent phenomenon and therefore number of opening of transmitter gated ion channels will be varying with respect to time.  $V_{TH(ENFET)}$  in equation (7.40) can, therefore, be modeled as [35]:

$$V_{TH(ENFET)}(t) = V_{THO} \left[ \left( 1 - \exp(-k_1 t) + \exp(-k_2 t) U(t - t_m) \right) \right] \quad (7.43)$$

Where  $K_1$  and  $K_2$  are time constants analogous to the rate constants of equation (7.42),  $U(t - t_m)$  is the Heaviside function and  $V_{THO}$  is the threshold voltage proportional to the maximum attainable conductance, when all the transmitter-gated channels for  $Na^+$  ions are open.

The circuit model for post synaptic membrane is shown in Fig. 7.15. Since only sodium channels are responsible for excitatory action, the postsynaptic membrane is divided into three patches to represent spatial summation of the sodium current controlled by  $g_{Na1}$ ,  $g_{Na2}$ , and  $g_{Na3}$ , where

$$I_{Na} = I_1 + I_2 + I_3 \quad (7.44)$$

So that,  $I = I_m - I_{Na} + I_K$

$$= C_m \frac{dV_m}{dt} - g_{Na}(V_m - E_{Na}) + g_K(V_m - E_K) \quad (7.45)$$

Where  $g_{Na}$  is the total sodium conductance and  $g_K$  is the non-gated potassium conductance.  $V_{g1}$ ,  $V_{g2}$  and  $V_{g3}$  are the voltages applied to the reference electrodes of the ENFETs.

The membrane potential  $V_m$  is obtained by spatially and temporally varying  $g_{Na}$  of acetylcholine-gated sodium channels.

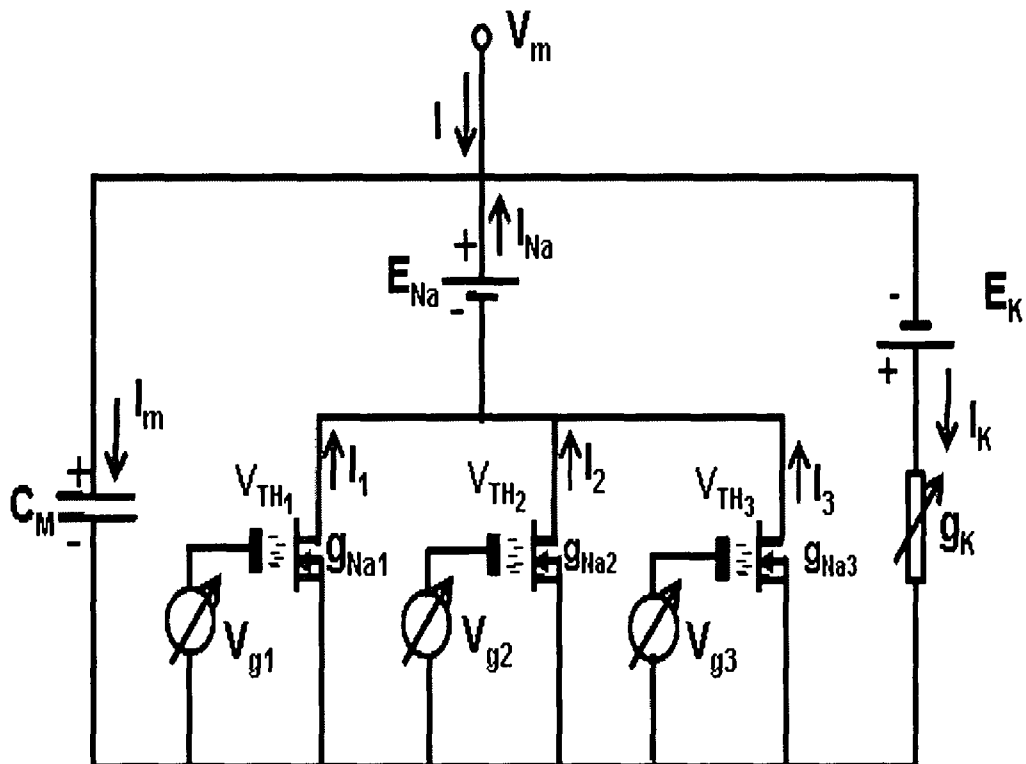


Fig. 7.15: Circuit model for Postsynaptic membrane

The component values assigned in the model for MATLAB simulation are taken from reference [35] and are given in Table 7.9. The specifications for three n-channel ENFETs and the parameters for exponential function in equation (7.21), applied to each ENFET inputs are also given Table 7.9. The three gate to source voltage of three ENFETs i.e  $V_{g1}$ ,  $V_{g2}$  and  $V_{g3}$  are kept constants at 1Volt each. The three input parameters of ENFET namely  $V_{TH1}$ ,

$V_{TH2}$  and  $V_{TH3}$  dependence on concentration of acetylcholine are applied in a staggered sequence at 1.5 msec intervals. This is done to simulate the time variation in acetylcholine transmitter –receptor binding with respect to different patches of postsynaptic membrane [35].

In order to reduce the number of functional receptors caused by autoimmune disease,  $V_{TH0}$  is considered as -1 volt. The time constants  $k_1$  and  $k_2$  are considered as 1.5msec to prolong the rate of acetylcholine-receptor binding activity.

TABLE 7.9  
DIFFERENT COMPONENTS USED IN THE PROPOSED MODEL OF SYNAPSE

Sl. No.	Parameter	Parameter Details	Unit	Value
01	$C_m$	Membrane Capacitance	Farad	1 $\mu$ F per $cm^2$
02	$g_K$	Potassium Conductance	Mho	1 mS per $cm^2$
03	$E_{Na}$	Sodium Potential	Volt	60mV
04	$E_K$	Potassium Potential	Volt	-90mV
05	I	Membrane Current	Ampere	0 A
05	L	Channel Length	Meter	15 $\mu$ m
06	W	Channel Width	Meter	2 $\mu$ m
07	$t_{OX}$	Oxide Thickness	Meter	100 nm
08	$\mu$	Electron mobility	$cm^2/V$ -sec	600 $cm^2/V$ -sec
09	$V_{TH0}$	Threshold Voltage	Volt	-2 Volts
10	$t_m$	Time	Second	600 $\mu$ sec
11	$k_1 = k_2$	Time Constant	Second	0.8 msec

#### 7.4.4 The Result:

The MATLAB simulation outputs are shown in Fig 7 16 The top waveform represents the normal postsynaptic membrane potential and the bottom waveform represents the postsynaptic membrane potential in the case of pathologic state. It is seen that when  $V_m$  exceeds the threshold in the range of -60mV to -45mV, more or less all the sodium channels open and initiates an action potential. But during pathologic state, the membrane potential degrades due to reduction of functional receptors and hence no action potential is developed.

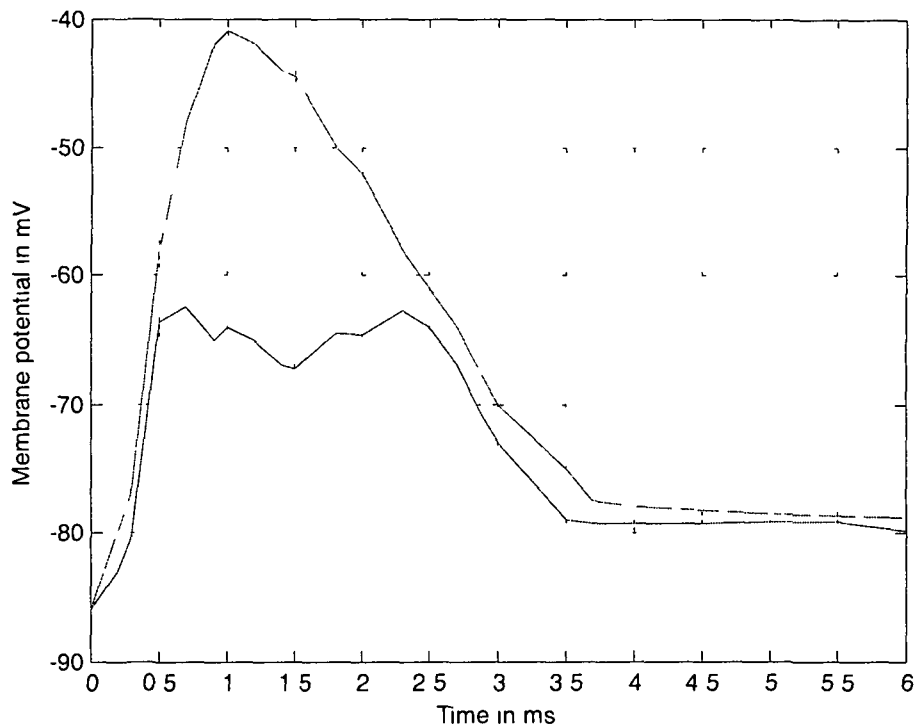


Fig 7 16 Simulated result of postsynaptic membrane potential

The aim of this work is to show that acetylcholine-sensitive ENFET can be used as circuit analog to simulate the excitatory postsynaptic potential with an additional advantage: measurement of concentration of acetylcholine diffused through the synaptic cleft. This biologically motivated model may become a useful research and teaching unit both in neurology and bioelectronics areas. The basic idea of the model can be used for other types of neurotransmitter-gated channels and can reproduce a wide variety of electrical responses.

The results obtained from simulation of the proposed model are compared with those reported by previous researchers and with the other proposed models and are given in Table 7.10.

TABLE 7.10  
COMPARISON OF SIMULATION RESULTS

Sl. No.	Threshold limit to initiate action potential	Time to attain peak value	Total duration of EPSP
[1]	- 65 mV to - 50 mV	1 ms	3.5 ms
[35]	- 60 mV to - 40 mV	3 ms	6 ms
Present Work of 7.2	- 60 mV to - 40 mV	1 ms	3.5 ms
Present Work of 7.3	- 60 mV to - 40 mV	1 ms	3.5 ms
Present Work of 7.4	- 60 mV to - 45 mV	1 ms	3.5 ms

## 7.5 References:

- [1] Levine, M. D. Fare, T. L. Eisenberg, M. F. A Physiologic Based Circuit Model of Excitation & Inhibition in the postsynaptic region, *IEEE*

- Proceedings of the 35<sup>th</sup> Midwest Symposium on Circuits & Systems.*, pp. 268-269, Vol-I, ISBN : 0-7803-0510-8.
- [2] Bergveld, P. Development of an ion-sensitive solid-state device for neurophysiological measurements, *IEEE Trans. Biomed. Eng. BME – 17 (1970) 70-71*.
- [3] Bergveld, P. Development, operation and application of the ion-sensitive field effect transistor as a tool for electrophysiology, *IEEE Trans. Biomed. Eng. BME –19 (1972) 342-351*.
- [4] Matsuo, T. Wise, K. D. An integrated field effect electrode for biopotential recording, *IEEE Trans. Biomed. Eng. BME – 21 (1974) 485-487*.
- [5] Bergveld, P. Thirty years of ISFETOLOGY what happened in the past thirty years and what may happen in the next thirty years, *Sensors and Actuators B*, 88 (2003),1-20.
- [6] Vianello, F. Stefani, A. et al. Potentiometric detection of formaldehyde in air by an aldehyde dehydrogenase FET, *Sensors and Actuators, B 1996;37:49-54*.
- [7] Senillou, A. Jaffrezic-Renault, N. Martelet, C. Cosnier, S. Aminiaturized urea sensor based on the integration of both ammonium based urea ENFET and a reference FET in a single chip. *Talanta 1999; 50(1):219-26*.
- [8] Kharitonov, A. B. Zayats, M. Lichtenstein, A. Katz, E. Willner, I. Enzyme monolayer-functionalized field-effect transistors for biosensor applications. *Sensors and Actuators, B 2000; 70:222-231*

- [9] Park, K. Choi, S. Lee, M. Sohn, B. ISFET glucose sensor system with fast recovery characteristics by employing electrolysis. *Sensors and Actuators, B* 2002; 83 (1-3): 90-97
- [10] Dzyadevych, S. V. Korpan, Y. I. Arkhipova, V. N. Alesina, M. Y. et al. Application of enzyme field effect transistors for determination of glucose concentrations in blood serum. *Biosensors and bioelectronics*, 1999;14:183-187
- [11] Sergei, V. D. Alexey, P. S. Yaroslav, I. K. et al. Biosensors based on enzyme field –effect transistors for determination of some substrates and inhibitors. *Anal Bioanal Chem*, 2003, 377:496-506
- [12] Starodub, V. M. Starodub, N. F. Electrochemical immune sensors based on the ion-sensitive field effect transistor for the development of the level of myoglobin. *The 13<sup>th</sup> European Conference on Solid-State Transducers*, September 12-15,1999
- [13] Landheer, D. Aers, G. Mckinnon, W.R. et al. Model for the field effect from layers of biological macromolecules on the gates of metal-oxide-semiconductor transistors. *Journal of applied physics* 98, 044701 (2005)
- [14] Yuqing, Miao. Jianguo, Guan. Jianrong, Chen. Ion sensitive field effect transducer based biosensors. *Biotechnology advances*,Vol.- 21,Issue-6,September-2003.
- [15] Dzyadvych, S. V. et al. Enzyme biosensors based on ion-selective field effect transistors. *Analytica Chimica Acta* 568 (2006) 248-258

- [16] Middlehoek, G. S. Celebration of the tenth transducers conference: the past, present and future of transducer research and development, *Sens. Actuators* 82 (2000) 2-23.
- [17] Sprenkels, A. Pijannowska, D. et al. The comprehensive integration of microdialysis membranes with silicon sensors, <http://www.bios.el.utwente.nl>, 2003
- [18] Poghossian, A. Luth, H. Schultze, J. W. Schoning, M. J. Bio-chemical and physical microsensor arrays using a identical transducer principle. *Electrochimica* 2001; 47:243-249
- [19] Gopel, W. Heiduschka, P. Introduction to bioelectronics: interfacing biology with electronics. *Biosensors and Bioelectronics*, 9 (1994)
- [20] Grattarola, M. et al. Modeling H<sup>+</sup>-Sensitive FETs with SPICE. *IEEE trans. Elect. Devices*, Vol.39, No.4, April, 1992
- [21] Bergveld, P. Sibbald, A. Analytical and Biomedical Applications of Ion selective Field Effect Transistors. *Elsevier Science Publishers, Amsterdam, 1988*
- [22] Yates, D. E. Levine, S. Healy, T. W. Site binding model of the electrical double layer at the oxide/water interface. *J. Chem.Soc. Faraday Trans.,(70): 1807 – 1819, 1974.*
- [23] Fung, C. D. Cheung, P. W. Ko, W. H. A generalized theory of an electrolyte-insulator – semiconductor field effect transistor. *IEEE, ED – 33(1) (1986) 8.*
- [24] Bard, A. J. Faulkner, L. R. Electrochemical methods, fundamentals and applications. *New York: Wiley; 1980*



- [25] Bousse, L. Rooij, N. F. De. Bergveld, P. Operation of Chemically sensitive field effect sensors as a function of the properties of the insulator/ electrolyte interface, *IEEE Trans. Electron Devices ED-30* (1983) 1263 – 1270.
- [26] Van Hal, R.E.G. et al. A general model to describe the electrostatic potential at electrolyte/oxide interfaces, *Adv.Coll. Interf. Science*,69 (1996) 31-62
- [27] Janicki, M. et al. Ion sensitive field effect transistor modeling for multidomain simulation purposes, *Microelectronics journal* 35 (2004) 831-840
- [28] Grattarola, M. Massobrio, G. *Bioelectronics Handbook: MOSFETs, Biosensors, and Neurons*, McGraw Hill,1998, 2<sup>nd</sup> Ed.
- [29] Akiyama, T. Ujihira, Y. et al. Ion- Sensitive Field-Effect Transistors with Inorganic gate Oxide for pH Sensing, *IEEE Trans. On Electron Devices, Vol, ED-29, No.12, December 1982, p.1936-1941.*
- [30] Cane, C. Gracia, I. Merlos, A. Microtechnologies for pH ISFET Chemical Sensors, *Microelectronics Journal-28* (1997) 389.
- [31] Shul'ga, A. A. Netchiporuk, L. I.; et al. Operation of an ISFET with non-insulating substrate directly exposed to the solution, *Sensors and Actuators B* 30 (1996) 101.
- [32] Temple-Boyer, P. Launay, J. et al. Study of front side connected chemical field effect transistors for water analysis, *Microelectron, Reliab*,44 (2004) 44

- 
- [33] Dzyadevych, S.V. Anh, T. M. et al. Book of XVI International Symposium on Bioelectro chemistry and Bioenergetics 2001, Bratislava, Slovakia, June 1-6, 2001,p.124.
- [34] Simonis, A. Dawgul, M. Luth, H. Schoning, M. Miniaturised reference electrode for field effect sensor compatible to Silicon Chip Technology, *Electrochimica Acta* 51 (2005) 930–937, doi:10.1016/j.electacta.2005.04.06
- [35] Levine, Michael D. Fare, T. L. A Physiologic-Based Circuit Model of the Postsynaptic region at the Neuromuscular Junction, *IEEE Proceedings*, pp. 1602 - 1603, ISBN : 0-7803-0785-2.
- [36] <http://en.wikipedia.org/wiki/Acetylcholine>

# **Chapter 8**

## **Conclusion and Future Research**

## **Conclusion and Future Research**

### **8.1 Conclusion and Future Research:**

In this dissertation, simple analog circuit models of neuron based on Integrate-&-Fire model is developed and simulated. The dissertation also includes some biologically motivated circuit models of post synaptic membrane for simulation of excitatory and inhibitory actions of synapses. The models are designed and simulated using ORCAD and MATLAB software. The basic purpose of this research work is to develop simple analog circuit models that can simulate the function of ion channels of postsynaptic membrane dependent on the neurotransmitters diffused through the synaptic cleft.

The first chapter is the introduction chapter that includes research problems, research objectives, and scope of the work. This chapter also highlights the thesis outline of all the remaining chapters.

The second chapter describes the physiological structure of nerve membrane and the principle of generation & conduction of nerve impulses. It includes biological overview of neuron, neuron morphology. It discusses in details the different types of neurons available. It also highlights the generation of action potential and different aspects of action potential. The second part of this chapter includes synapse in details and different aspects of synapse.

The third chapter presents the literature review of neuron modeling. It includes the conductance based model starting with Hodgkin-Huxley models to different conductance based models proposed by different neuroscientist.

Then it discusses different integrate-&-fire (I-F) models proposed by different neuroscientists.

The fourth chapter describes the general overview of synapse starting with the literature review of different models of synapse proposed by different neurologists. This chapter also includes the basic operation principle of MOSFET, which is used in the design of synapse models. This chapter describes in details the different synapse models considering excitation and inhibition actions.

In chapter five, two simple silicon neuron models have been proposed based on Lapicque's philosophy. The first model is developed for excitation and resting actions. The second model is the model comprising of dendritic regions and the soma. The input to the dendritic regions are integrated and brought to a single point, and that single point value is applied to the soma to generate action potential. The simulation results indicate that this I&F model can reproduce the neural dynamics as close as to H-H type models.

In Chapter six, simple integrate-&-fire based model both for excitatory and inhibitory synapses has been developed by considering each biological synapses as a two state device. Simulation of the model yields an output representing the overall membrane potential of the postsynaptic region. Results obtained from simulation are compared with the results of previous researchers and a good agreement is obtained. This model can be used to demonstrate the basic mechanism of neuron namely the effects of excitation and inhibition.

In chapter seven, some biologically motivated circuit models have been proposed to predict the behaviour of postsynaptic membrane dependence on

neurotransmitter receptor binding activity i.e. a synaptic action. In the first part of this chapter, an electronic circuit analog of postsynaptic membrane has been proposed using MOSFET as circuit analog. MOSFET functions as a voltage controlled conductance in its linear region and therefore analogous to the variable conductance of the ion channels of postsynaptic membrane. This model can be used in neurobiology area for simulation of neurotransmitter-receptor binding activity and electrical activity of the postsynaptic neuron.

In the mid part of this chapter, an Ion Sensitive Field Effect Transistor (ISFET) is used as the circuit analog to simulate a group of excitatory and inhibitory transmitter-gated ion channels. This analog is incorporated into a circuit model of the postsynaptic membrane at the synaptic cleft. Simulation of the circuit yields an output representing the membrane potential of the input region. Simulation shows the effects of excitation and inhibition on a single neuron.

In the last part of this chapter, Enzyme Modified Field Effect Transistor (ENFET) sensitive to acetylcholine is used to simulate a group of excitatory acetylcholine-gated ion channels. This analog is incorporated into a circuit model of the postsynaptic membrane at the neuromuscular junction. Simulation of the model yields an output representing the overall membrane potential of the postsynaptic region. Simulation is performed both for the normal and the pathologic states. This model has general applicability in the field of neurology for understanding receptor function and electrical activity of the postsynaptic cell.

Finally, simulation results of all the biologically motivated models have been analyzed and compared. From this analysis, it can be concluded that the ISFET based circuit model is more advantageous because it can be modified

into specific neurotransmitter sensitive ENFET leading to the simultaneous measurement of neurotransmitters that bind with the receptor sites of the postsynaptic membrane. The techniques can be extended to simulate the other ion channels mediated by other neurotransmitters using different ENFETS sensitive to specific transmitters. Measurement of neurotransmitter plays an important role in the field of neurology.

It has been already stated that  $g_{Na}$  and  $g_K$  have very low values in their resting state and both conductances are increased with applied potential and reached a saturation value when applied voltage is sufficiently large. Moreover both conductances have slow time dependence. In future, these characteristics may be directly explored by introducing feed back circuit in the gate of ISFET/ENFET. The time dependence of conductances can be simulated by introducing RC circuit in the feed back path. Such circuit, that can accurately simulate the action of the chemical transmitters, will have importance in building complex neuron networks.